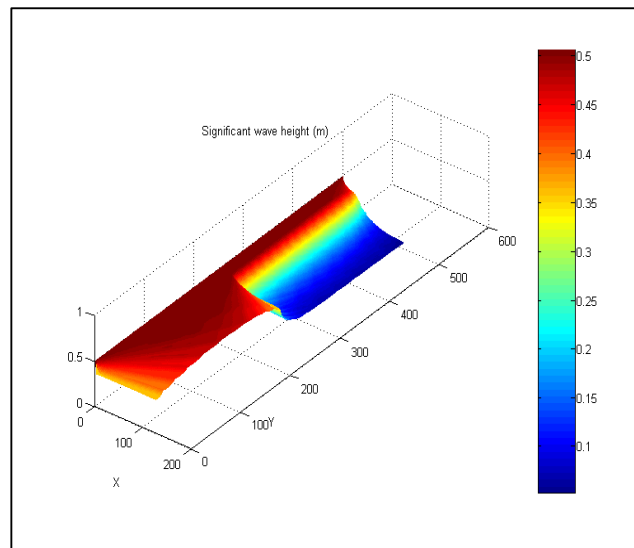
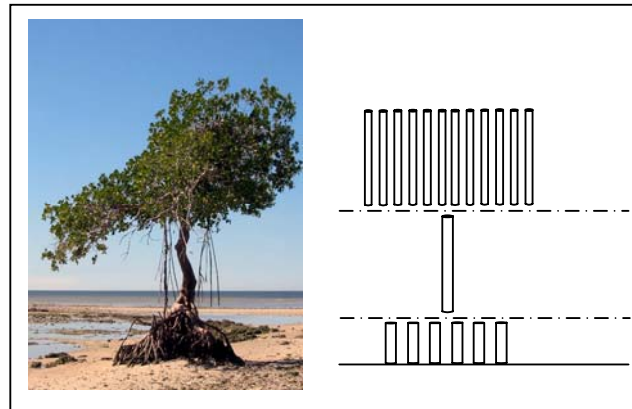


# Wave Attenuation in Mangrove Forests

Numerical modelling of wave attenuation by implementation of a physical description of vegetation in SWAN



M.Sc. Thesis

B. Burger, September 2005

TU Delft

Faculty of Civil Engineering and Geosciences

Section of Hydraulic Engineering



Delft University of Technology

Thesis committee:

Prof. dr. ir. M.J.F. Stive

Ir. H.J. Verhagen

Drs. M. de Vries

Dr. ir. M. Zijlema

H.J. Opdam

## Preface

The M.Sc. thesis study resulting in this report has been carried out at Delft University of Technology, Faculty of Civil Engineering and Geosciences, Section Hydraulic Engineering, in cooperation with Royal Haskoning and WL | Delft Hydraulics. The area of interest in this thesis is wave attenuation in vegetation and in particular in mangrove forests. The involvement of Royal Haskoning arises from their interest in mangrove areas in Guyana, South America. In Guyana, Royal Haskoning participates as a consultant in an Integrated Coastal Zone Management project, executed by the government of Guyana. Mangrove areas are part of the sea defence system of Guyana.

As research institute and consultant, WL | Delft Hydraulics has performed much research on wave attenuation by vegetation. Because of the close relation between TUDelft and WL | Delft Hydraulics, especially concerning the exchange of knowledge and numerical models, WL | Delft Hydraulics was involved in this thesis study as well.

Furthermore this study has partly been done in cooperation with Martijn Meijer who is performing his M.Sc. study on wave attenuation by salt marsh vegetation, because of the analogy in the subjects.

First of all I would like to thank the members of my thesis committee for the contribution to my thesis, Professor M.J.F. Stive (TU Delft), Ir. H.J. Verhagen (TU Delft), Drs. M. de Vries (TU Delft and WL | Delft Hydraulics), Dr. ir. M. Zijlema (RIKZ and TU Delft) and H.J. Opdam (Royal Haskoning).

Next I would like to thank Martijn Meijer for a superb cooperation on this thesis subject and the interesting discussions on the subject.

Last I would like to thank Arjan Luijendijk and Reimer de Graaff for their contribution in the early stages of my thesis, Mark Voorendt for his great computer and software related help, Hendrik Burger, Gerrit Burger and Pieter Dierx for their effort to revise my thesis report, Marjolijn Burger for her mental support and finally my parents all for their support during my study.

Bastiaan Burger

Delft, September 2005

## Abstract

Mangrove forests cover large parts of the tropical and subtropical shorelines. These trees are tolerant to saline environments, which enable them to grow in the inter-tidal zone. Very diverse flora and fauna can be found in mangrove areas. Often, these coastlines are sheltered or are subject to a moderate wave climate. Mangrove forests act as a natural coastal protection. The most important features of this protection are the prevention of erosion by the collecting of sediment and the reduction of the wave climate.

Understanding these key processes is important to the preservation of the mangrove forest themselves, but also of the often highly populated areas behind it. Nevertheless there is a lack of both quantitative and qualitative knowledge on hydraulic processes in mangrove forests. Therefore there is a need to quantify and model hydraulic and morphologic processes, wave attenuation in particular, in order to predict and simulate the natural hydraulic behaviour and evaluate the consequences of any artificial measure in mangrove forests.

In this study it is found, that the best numerical approximation to model wave attenuation in vegetation with SWAN (a numerical wave model), was a formulation described by Dalrymple (1984). The formulation expresses the amount of dissipated wave energy in terms of vegetation characteristics and wave parameters. Vegetation characteristics are the drag coefficient, vegetation diameter, density and relative vegetation height. Wave parameters are amplitude and water height. After adaptation of the formulation to suit for the spectral energy density used in SWAN, it has been implemented in SWAN.

The drag coefficient ( $C_d$ ) is the only calibration parameter in the Dalrymple (1984) formulation. It has been studied in order to assess the most important relations with vegetation characteristics and wave parameters. For the vegetation characteristics it turned out that the drag coefficient depends mainly on the relative spacing.

The dependency of the drag coefficient on the wave parameters is determined by the horizontal orbital velocity and the peak period, and could be best described by the relation between the drag coefficient and the Keulegan-Carpenter number.

What has to be kept in mind is that some non-drag related and initially neglected processes such as bed friction, vegetation motion and inertia (added mass) are discounted in the drag coefficient. Therefore it is not physically correct to refer to the parameter  $C_d$  as a drag coefficient.

From a first analysis of the Dalrymple (1984) formulation it was found valid to divide the vegetation into segments vertically, and add up the energy dissipation per segment to form the total amount of energy dissipation over the plant height. Next the method was implemented this in the SWAN model, resulting in an adapted SWAN model in which wave attenuation can be modelled due to homogenous, horizontally variable or vertically variable vegetation. Subsequently the implementation was validated on the results of physical model tests from Mendez and Losada (2004). This validation was successful and gave evidence the implementation was done correctly.

As a next step, a sensitivity analysis was performed which resulted in the expected relations between the wave attenuation and the vegetation characteristics, respectively the hydraulic conditions.

From literature Battjes (2001) it is known that wave energy dissipation leads to wave induced setup of the averaged water level. For wave dissipation vegetation areas this is also the case. This setup can induce currents which are thought to be responsible for important morphologic processes such as pioneering of a vegetation field. In a test simulation with patchy vegetation it was found to be possible to model this phenomenon, however the potential flow itself can not be modelled by SWAN, because the model cannot simulate flow.

Two measurement campaigns in Vietnam on wave attenuation in mangrove forests were modelled as test cases in the adapted SWAN model. In these cases hydraulic conditions and vegetation characteristics were known from measurements and thus the drag coefficient could be calibrated. This resulted in values for the drag coefficient between 0.01 and 0.1 for both cases.

Finally it is concluded that the implementation in SWAN was successful for different types of vegetation. Nevertheless the dependency of the drag coefficient on both wave parameters and vegetation characteristics implies that the model can only be used when vegetation characteristics and wave parameters have been measured and related to the drag coefficient.

## Table of contents

|   |     |
|---|-----|
| Preface.....  | ii  |
| Abstract .....  | iii |
| List of coefficients .....  | vii |
| 1 Introduction.....   | 1   |
| 1.1 Problem analysis.....   | 1   |
| 1.1.1 Problem description .....                                   | 1   |
| 1.1.2 Problem definition.....                                     | 2   |
| 1.1.3 Research objective.....                                     | 2   |
| 2 Background on mangroves.....                                    | 3   |
| 2.1 Mangrove distribution and diversity.....                      | 3   |
| 2.2 Root structures .....   | 4   |
| 2.3 Trunks and canopies .....                                     | 5   |
| 2.4 Zonation.....   | 5   |
| 3 Waves in mangroves .....  | 6   |
| 3.1 Linear wave theory .....                                      | 6   |
| 3.1.1 Depth classification of waves .....                         | 8   |
| 3.1.2 Spectral description of waves.....                          | 9   |
| 3.2 Wave energy dissipation formulations by vegetation .....      | 10  |
| 3.2.1 Bed friction approach .....                                 | 10  |
| 3.2.2 Cylinder approach .....                                     | 12  |
| 3.2.3 Internal waves in bottom.....                               | 13  |
| 3.2.4 Conclusions .....   | 14  |
| 3.3 Physical background on the Bulk Drag Coefficient .....        | 15  |
| 3.3.1 Determination of significant energy dissipation areas ..... | 15  |
| 3.3.2 Dependence of drag on vegetation characteristics.....       | 16  |
| 3.3.3 Dependence of the drag on wave characteristics.....         | 21  |
| 3.3.4 Conclusions .....   | 22  |
| 4 Numerical wave modelling in SWAN .....                          | 23  |
| 4.1 General description of SWAN .....                             | 23  |
| 4.2 Modelling wave attenuation by vegetation .....                | 25  |
| 4.2.1 Implementation criteria .....                               | 25  |
| 4.2.2 Testing on Paulina Schor .....                              | 25  |
| 4.3 Implementation of the Dalrymple formulation in SWAN .....     | 26  |
| 4.3.1 Homogeneous vegetation .....                                | 26  |
| 4.3.2 Horizontal variation of vegetation.....                     | 28  |

|       |   |    |
|-------|---|----|
| 4.3.3 | Vertical variation of vegetation.....                         | 28 |
| 4.4   | Validation on Mendez & Losada .....                           | 32 |
| 4.5   | Sensitivity analysis on mangrove vegetation .....             | 33 |
| 4.5.1 | Bottom friction and wave breaking.....                        | 33 |
| 4.5.2 | Schematisation of mangrove vegetation .....                   | 34 |
| 4.5.3 | Vegetation Parameters .....                                   | 35 |
| 4.5.4 | Hydraulic conditions.....                                     | 40 |
| 4.5.5 | Conclusions on the sensitivity analysis.....                  | 50 |
| 4.6   | Wave setup induced currents by 'Patchy' vegetation .....      | 51 |
| 5     | Test cases .....  | 56 |
| 5.1   | Thuy Hai .....  | 57 |
| 5.1.1 | Mangrove vegetation.....                                      | 58 |
| 5.1.2 | Wave conditions .....   | 59 |
| 5.1.3 | Results of wave reduction.....                                | 59 |
| 5.1.4 | Modelling the results .....                                   | 60 |
| 5.2   | Vinh Quang .....  | 62 |
| 5.2.1 | Mangrove vegetation.....                                      | 63 |
| 5.2.2 | Wave conditions .....   | 64 |
| 5.2.3 | Results of measured wave reduction .....                      | 64 |
| 5.2.4 | Modelling the results .....                                   | 66 |
| 5.3   | Conclusions on the test cases .....                           | 68 |
| 5.4   | Discussion on drag coefficient.....                           | 68 |
| 5.5   | Predictive modelling for Guyana.....                          | 68 |
| 6     | Conclusions & Recommendations .....                           | 69 |
| 6.1   | Conclusions .....   | 69 |
| 6.2   | Recommendations.....  | 70 |
| 6.2.1 | General .....   | 70 |
| 6.2.2 | Adapted SWAN model .....                                      | 70 |
| 6.2.3 | Drag coefficient .....  | 71 |
|       | References .....  | 72 |
|       | Appendix A Results of test calculations Dalrymple formulation |    |
|       | Appendix B Implemented code                                   |    |
|       | Appendix C Validation on flume experiments                    |    |
|       | Appendix D Layout SWAN model                                  |    |
|       | Appendix E Wave setup   |    |
|       | Appendix F Calibration on Thuy Hai                            |    |

## List of coefficients

|                  |   |  |
|------------------|---|--|
| $D_v$            | Dissipation of energy per unit area of vegetation                 | $[\text{Nm}^{-1}\text{s}^{-1}]$                            |
| $f_w^*$          | friction factor   | $[-]$  |
| $D$              | stem diameter   | $[\text{m}]$   |
| $n$              | vegetation density (Collins)                                      | $[\text{m}^{-2}]$  |
| $N$              | vegetation density (Dalrymple)                                    | $[\text{m}^{-2}]$  |
| $dz$             | vegetation height   | $[\text{m}]$   |
| $\rho$           | water density   | $[\text{kgm}^{-3}]$  |
| $U_{orb}$        | horizontal orbital velocity                                       | $[\text{ms}^{-1}]$   |
| $\hat{U}_\delta$ | maximum orbital velocity near boundary                            | $[\text{ms}^{-1}]$   |
| $\mathbf{F}$     | force vector per unit volume, $\mathbf{F}=(F_x, 0, F_z)$          | $[\text{Nm}^{-3}]$   |
| $C_m$            | inertia coefficient   | $[-]$  |
| $C_d$            | drag coefficient  | $[-]$  |
| $E$              | energy density  | $[\text{Nm}^{-1}]$   |
| $c_v$            | vegetation friction factor  | $[-]$  |
| $\mathcal{E}_v$  | time-averaged rate of energy dissipation per unit horizontal area | $[\text{Nm}^{-1}\text{s}^{-1}]$                            |
| $b_v$            | plant stem diameter   | $[\text{m}]$   |
| $u$              | horizontal velocity   | $[\text{ms}^{-1}]$   |
| $\tilde{C}_D$    | drag coefficient  | $[-]$  |
| $\alpha$         | relative vegetation height  | $[-]$  |
| $k$              | wave number   | $[\text{m}^{-1}]$  |
| $\alpha h$       | vegetation height   | $[\text{m}]$   |
| $H_{\text{rms}}$ | root mean square wave height                                      | $[\text{m}]$   |
| $H_s$            | significant wave height   | $[\text{m}]$   |
| $S$              | relative spacing  | $[\text{m}]$   |
| $ad$             | population density  | $[-]$  |
| $Re$             | Reynolds number   | $[-]$  |
| $K$              | Keulegan-Carpenter number   | $[-]$  |
| $u_c$            | horizontal orbital velocity                                       | $[\text{ms}^{-1}]$   |
| $T_p$            | wave peak period  | $[\text{s}]$   |
| $\sigma$         | wave frequency  | $[\text{rads}^{-1}]$                                       |
| $\theta$         | the direction normal to the wave crest of each spectral component | $[\text{rad}]$   |
| $c_x$            | propagation velocities in x-direction                             | $[\text{ms}^{-1}]$   |
| $c_y$            | propagation velocities in y-direction                             | $[\text{ms}^{-1}]$   |
| $c_\sigma$       | propagation velocity in $\sigma$ space                            | $[\text{ms}^{-1}]$   |
| $c_\theta$       | propagation velocity in $\theta$ space                            | $[\text{ms}^{-1}]$   |
| $N$              | action density  | $[\text{N}\cdot\text{rad}\cdot\text{m}^{-1}\text{s}^{-2}]$ |
| $S$              | Energy density  | $[\text{Nm}^{-1}\text{s}^{-1}]$                            |
| $N_v$            | vegetation density  | $[-\text{m}^{-2}]$   |
| $K_T$            | Transmission coefficient  | $[-]$  |

# 1 Introduction

Mangrove forests cover large parts of the tropical and sub-tropical shores in the world. They are one of the most biologically diverse forests. The forests are the breeding grounds for sea life as fish, shrimp, prawns, crabs, shellfish and snails and also nesting sites for many shore birds as well as a home to crab eating monkeys, fishing cats, lizards, sea turtles. They are found on sheltered coastlines, river deltas and grow in brackish wetlands, in the tidal area, where other plants cannot grow. The mangrove forests are often part of a larger sea defence system and are, from a coastal and hydraulic engineering point of view, very important. They protect the coastline and prevent erosion by collecting sediment from the rivers and streams and decelerating the flow of water. More over, the roots, stems and canopies attenuate and dissipate wave energy, acting as a natural sea defence.

## 1.1 Problem analysis

### 1.1.1 Problem description

Mangrove forests act as a coastal protection, this is a fact on which most coastal engineers agree. Understanding the key processes in mangrove forests is important to the preservation of the mangrove forest and the often highly populated areas behind it. The degradation of mangrove forests is a growing problem in various mangrove areas over the world. Important causes for this degradation are human activities, as intensive shellfish farming and cutting down the mangroves for wood. Although mangrove forests serve as sea defence in many locations over the world, still limited knowledge is present to use in coastal engineering. As mentioned earlier, not only limiting the human activities, but also the understanding of morphologic processes in the mangrove forests due to waves and tidal currents is of critical importance for the preservation of these mangrove coasts. Often seen for hydraulic constructions, as well as in precarious equilibrium situations encountered in nature such as mangrove systems, extreme events are normative for the stability and preservation. The situation of high water (storm setup) in combination with storm waves is a crucial situation, in which the wave attenuation of mangrove forests is of a critical importance for the embankments behind the forests, as well as for the erosion potential in the mangroves.

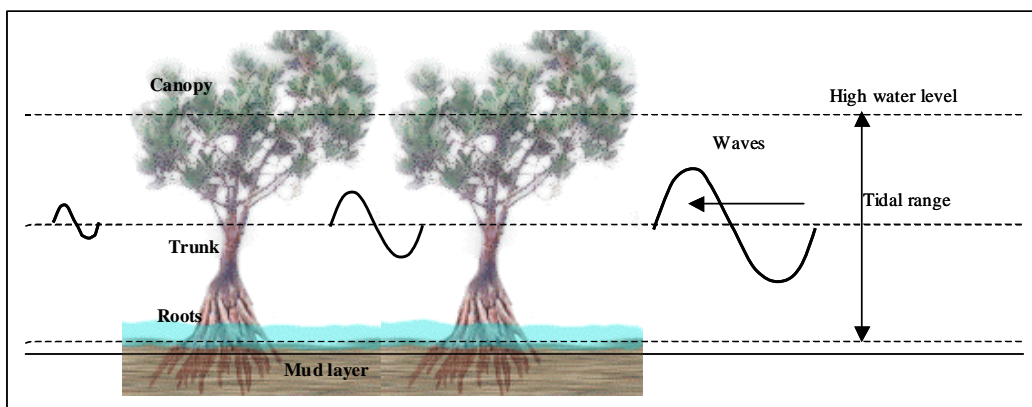


Figure 1-1 Schematisation of a mangrove system



In the general function of mangroves acting as a coastal protection, wave attenuation in particular is an important process, because it forms a boundary condition for sedimentation and erosion and for biological activities (Schiereck G.J., Booij N. (1995)). Wave attenuation in mangroves, schematised in Figure 1-1, depends on vegetation as well as on hydraulic conditions. Regarding the vegetation properties as roots, trunks and canopies, the attenuation is influenced by means of a variety of vegetation parameters. The most important are the trunk diameter, density and vegetation height. As for the hydraulic conditions the wave characteristics (amplitude and horizontal orbital velocity) and water depth are the most important parameters, (Mol (2003), Groen (1993), Mazda et al. (1997), Darymple (1984), Massel (1999)).

### **1.1.2 Problem definition**

There is a lack of both quantitative and qualitative knowledge on hydraulic processes in mangrove forests. Therefore there is a need to quantify and model hydraulic and morphologic processes, wave attenuation in particular, in order to predict and simulate the natural hydraulic behaviour and evaluate the consequences of any artificial measure in mangrove forests.

### **1.1.3 Research objective**

The main objective of the thesis is to quantify and model wave attenuation of various types of mangrove forest under various wave and tidal boundary conditions. This will be done by the physical implementation of vegetation in a numerical wave model SWAN.

## 2 Background on mangroves

### 2.1 Mangrove distribution and diversity

The distribution of mangrove is usually divided in an Eastern group and a Western group. The Eastern group includes East Africa, India, Southeast Asia, Australia and the Western Pacific. The Western group includes West Africa, Atlantic South America, the Caribbean, Florida, Central America, and Pacific North and South America. They are referred to as the Indo West Pacific (IWP) and the Atlantic East Pacific (AEP). This comes down to the eastern and the Western Hemisphere, divided by the meridian (de Vos W.J. (2004)) after (Chapman (1984)) see Figure 2-1.

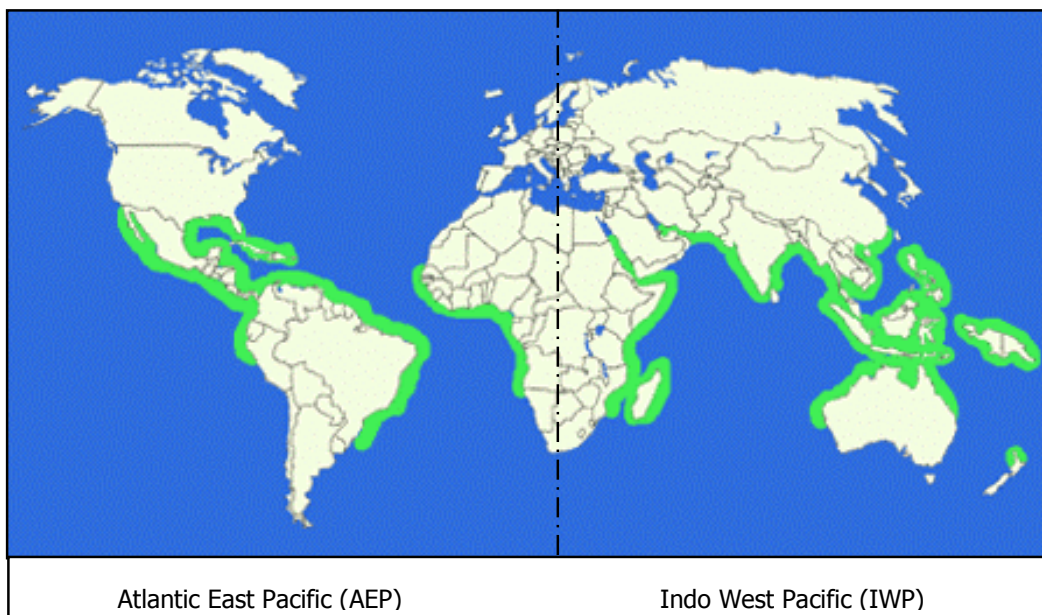


Figure 2-1 Distribution of the world's mangrove forests, modified from Spalding *et al.* (1997) and Duke *et al.* (1998).

The effects of increasing latitude are evident in reduction in species richness, forest height and maximum size of trees. There is a spectacular difference in floristic distribution between the AEP and the IWP. The ratio between the number of species in the IWP and the AEP is five to one (de Vos W.J. (2004)) after (Tomlinson (1986)). Only three genera of mangroves are common in both the AEP and the IWP. These are *Avicennia*, *Rhizophora* and *Xylocarpus*. Of these genera, the most well known and most common are *Rhizophora* and *Avicennia* see Figure 2-2. Together, the representatives of these genera in the New World constitute 80 % of the mangroves on Atlantic shores. These representatives, *Avicennia Germinans* and *Rhizophora Mangle*, are often referred to as, respectively, the 'Black mangrove' and the 'Red mangrove'. Together with the 'White mangrove', *Laguncularia Racemosa*, they are the main mangrove species in the New World (Teas, (1980)) shown.

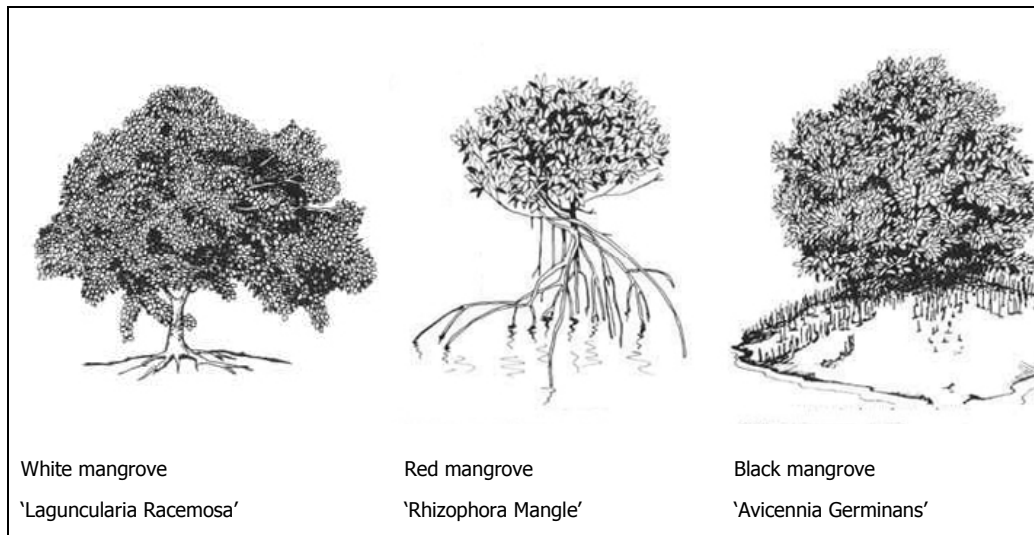


Figure 2-2 Most common mangrove species in the AEP and IWP (from Teas (1980))

## 2.2 Root structures

Like all plants, mangroves need ventilation of their root system. Since the surface on which mangroves grow is inundated for at least part of the day, the substrate is usually of anaerobic nature. In order to ventilate the root system mangroves have a third component that is exposed to the atmosphere, at least during low tide. Aerial roots diffuse oxygen throughout the root system and enable carbon dioxide to be vented out. Although the various types of aerial roots may look quite different, their function is the same and their existence is one of the features that distinguishes mangroves from other trees Tomlinson (1986).

Important from an engineering point of view are the exposed aerial root structures, because this causes the largest part of the drag forces. As shown in Figure 2-3 the various types of aerial roots clearly impose different drag forces.

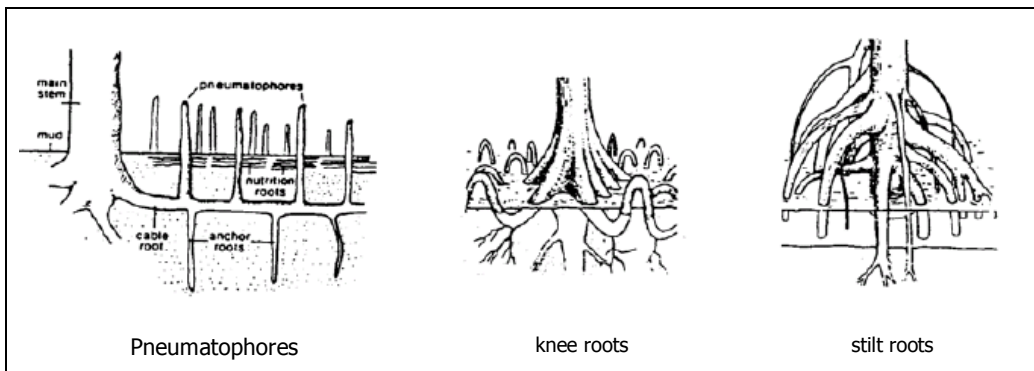


Figure 2-3 Different types of aerial roots

## 2.3 Trunks and canopies

Depending on the water depth trunks and canopies contribute to the wave attenuation. Literature shows that with low water depths the aerial roots system causes the largest part of the wave attenuation. With higher water depths trunks and canopies play of course a more significant role.

Canopies start to grow from around the high water level upwards. In case a storm occurs, there will be a set up of the mean water level. This is where canopies are said to attenuate waves efficiently because with the canopy there is an enormous increase in vegetation density. Often within the approaches to describe this attenuation in the canopies the leaves and small branches are not taken into account. However inertia forces caused these could be of significant importance.

## 2.4 Zonation

Mangrove forests usually grows in the upper tidal zone, between Mean Sea Level (MSL) and High Water Spring Level (HWSL). Seawards of mangrove often mud flats are encountered, with typical slopes of 1:1000. Behind the mangroves between HWSL and the level of occasional flooding by the ocean, salt marshes can be found with halophytic herbs and grasses (Schierck (2001)). Within the mangrove forests, communities are often zoned (see Figure 2-4) parallel to the shoreline, with series of different species dominating distinct sections from shore to the landward limits. These zones are separated by a transitional area, occupied with a mixture of mangroves from the adjacent zones.

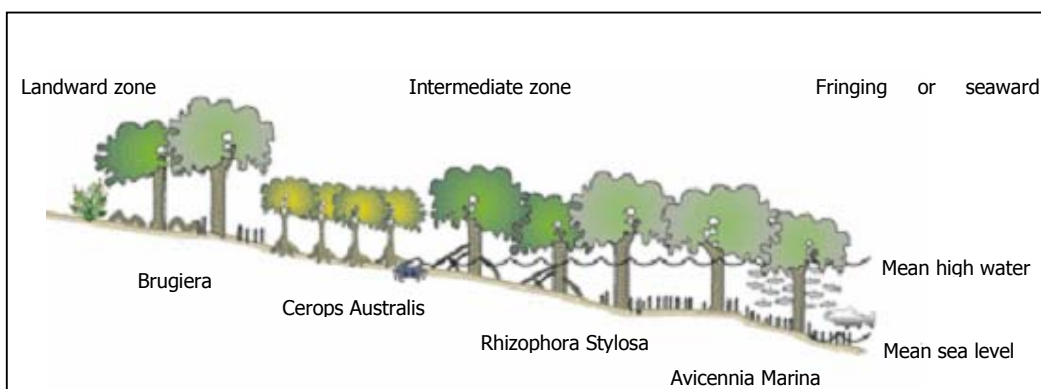


Figure 2-4 Hypothetical schematisation of zonation in a mangrove forests

### 3 Waves in mangroves

This chapter describes the most important physical processes and characteristics concerning waves penetrating mangroves. Especially the principles of wave attenuation by vegetation are elaborated.

#### 3.1 Linear wave theory

Waves are generally described by the linear wave theory or Airy wave theory (Airy, 1845). This theory presumes a number of assumptions:

- Constant water depth
- Two dimensional wave motion
- Waves are constant of form thus do not change with time,
- Incompressible fluid
- Viscosity, turbulence and surface tension are neglected,
- The wave height,  $H$  is small compared to the wave length,  $L$  and the water depth,  $d$

The equation governing the potential velocity  $\Phi$ , (Young, (1999)),

$(u, w) = \left(-\frac{\partial\phi}{\partial x}, \frac{\partial\phi}{\partial z}\right)$  in two dimensions  $(x, z)$ :

$$\frac{\partial^2\phi}{\partial x^2} + \frac{\partial^2\phi}{\partial z^2} = 0 \quad (0.1)$$

Kinematic boundary conditions on surface:

$$\begin{aligned} \frac{\partial\phi}{\partial z} &= \frac{\partial\eta}{\partial t} \\ \frac{\partial\phi}{\partial t} + g\eta &= 0 \end{aligned} \quad z = 0$$

Boundary condition bed:

$$\frac{\partial\phi}{\partial z} = 0 \quad z = -h$$

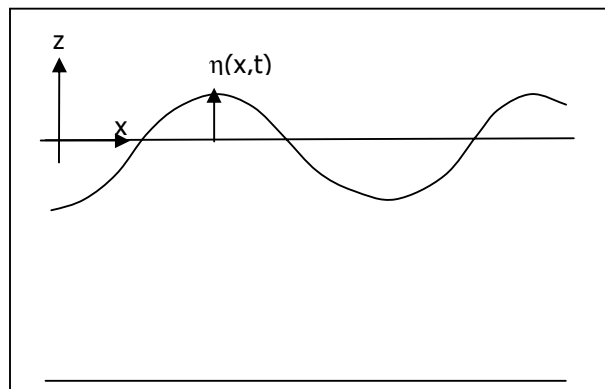


Figure 3-1 Definition sketch for the linear wave theory

Here  $\eta$  represents the water elevation,  $g$  the gravitational acceleration,  $\phi$  the velocity potential,  $u$  the velocity in the  $x$  direction,  $w$  the velocity in the  $z$  direction.

### Wave energy

Waves propagating through space contain a certain amount of potential and kinetic energy, (Battjes, (1998)). The total amount of wave energy is the sum of potential and kinetic energy (energy density) and is per unit width calculated by:

$$E = \frac{1}{8} \rho g H^2 \quad (0.2)$$

In which  $\rho$  is the specific density of water,  $g$  the gravity acceleration and  $H$  the wave height.

While waves are propagating, wave energy is transmitted in horizontal direction of the propagation. The propagating velocity of the transmitted energy is equal to the group velocity of the waves. This is determined by:

$$c_g = n \cdot c \quad (0.3)$$

In which  $c$  is the wave celerity of a single wave and  $n$  is a dimensionless factor depending on the ratio between the water depth and the wave length. The wave celerity respectively  $n$  are calculated by

$$c = \frac{\omega}{k} \quad (0.4)$$

and

$$n = \frac{1}{2} \left( 1 + \frac{2kh}{\sinh 2kh} \right) \quad (0.5)$$

$\omega$  represents the rotational speed of the waves and  $k$  is the wave number,  $h$  is the water depth,  $\omega$  and  $k$  are given by:

$$\omega = \frac{2\pi}{T} \quad (0.6)$$

and

$$k = \frac{2\pi}{L} \quad (0.7)$$

$L$  is the wave length depending of the water depth.

Via the dispersion relation:

$$\omega^2 = gk \tanh(kd) \quad (0.8)$$

the wave length,  $L$  can be found once the deep water wave length,  $L_0$  is known.

$$L = L_0 \tanh \frac{2\pi h}{L} \quad (0.9)$$

and

$$L_0 = \frac{gT^2}{2\pi} \quad (0.10)$$

The calculation of the wave length is an iterative process. Finally we can determine the energy flux  $F$ , the transmitted wave energy in the direction of the wave propagation:

$$F = E \cdot c_g \text{ or } F = E \cdot n \cdot c \quad (0.11)$$

### 3.1.1 Depth classification of waves

Waves can be classified with respect to their wavelength in relation to the water depth or similar with the wave number  $k$  multiplied by the water depth  $d$ , ( $kd$ ).

Most of the wave characteristics change when waves propagate from deep into shallow water. Important here are respectively the wave length, group velocity and the orbital motion characteristics, as shown in Figure 3-2. Table 3-1 shows the ranges of  $kd$  and  $d/L$  are presented (Young, (1999))

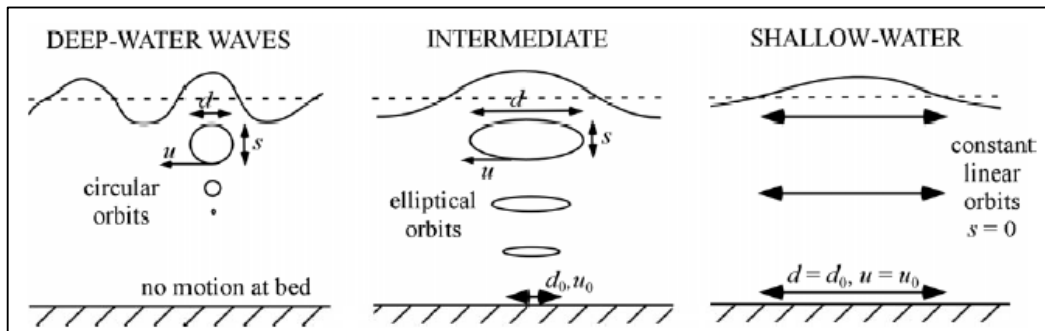


Figure 3-2 Depth classification of waves

Table 3-1 Depth classification of linear waves in terms of the relative depth parameter  $kd$

| Range of $kd$      | Range of $d/L$  | Type of waves                     |
|--------------------|-----------------|-----------------------------------|
| 0 to $\pi/10$      | 0 to 1/20       | Shallow water<br>(long waves)     |
| $\pi/10$ to $\pi$  | 1/20 to 1/2     | Intermediate depth waves          |
| $\pi$ tot $\infty$ | 1/2 to $\infty$ | Deep water waves<br>(short waves) |

### 3.1.2 Spectral description of waves

A way to order oscillatory processes is to view them as a superposition of sine waves with different amplitudes, frequencies and phases, the so-called spectral components. The functions representing the resulting distributions of amplitudes and phases over the frequencies are called frequency spectra. Spectra can be continuous as well as discrete, but wave spectra are thought to be continuous. It is very useful to focus on the energy (or variance) and to ignore the phases. This leads to the spectral distribution of variance (or energy or wave amplitude squared) as the key concept for stationary random processes (Battjes, (2001)). A typical wave energy density spectrum is shown in Figure 3-3. With horizontal axis representing the frequency and the vertical the energy density. With the spectrum it is easily seen, in which frequency domain the wave energy is located. To obtain the energy density spectrum the variance density spectrum needs to be multiplied by  $\rho g$  (density of water times the gravitational acceleration).

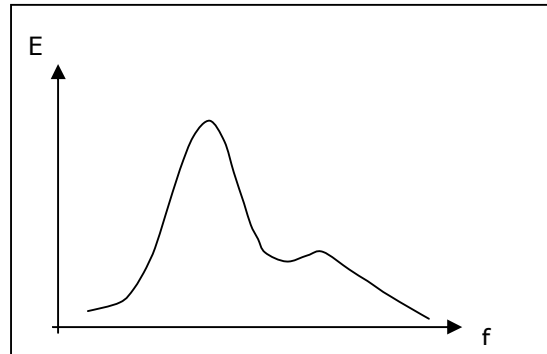


Figure 3-3 Spectral energy density distribution



## 3.2 Wave energy dissipation formulations by vegetation

A very effective way of wave energy dissipation is wave breaking, nevertheless waves propagating over, or in case of mangroves through vegetation, in most cases do not lose their energy due to breaking. An important process is wave energy dissipation due to obstacles that this vegetation forms. The vegetation imposes friction (drag) and inertia forces on the water motion, which results in energy loss and thus less wave height and lower orbital velocities.

Most of the physical descriptions are based on the energy balance, because from wave energy it is relatively simple to calculate wave heights. These wave heights can be used to calculate a wave transmission coefficient. This coefficient is described by the incoming wave height divided by the transmitted wave height.

### 3.2.1 Bed friction approach

Waves propagating in transitional or shallow water depths experience friction due to the bed. The extent of this bed friction is related to a number of parameters such as the horizontal orbital velocity, bed roughness and the water depth. In a large part of the literature on wave attenuation in mangroves, little attention is spent on the bed friction itself, although bed friction expressions are often used to describe the dissipation terms of the mangrove vegetation.

According to (Mazda et al., (1997)) the energy dissipation due to the bed friction is of an order smaller than that of drag forces due to the vegetation. This is one of the conclusions of a measuring campaign of wave attenuation on mud slope coast in the Tong King delta with and without mangrove vegetation. A theoretical explanation on this fact is that the orbital velocities near the bed decrease drastically because of the vegetation present.

A frequently used approach is to express the dissipated wave energy due to vegetation in a bottom friction parameter. Bed friction expressions like van Rijn, (1989), Collins, (1968) or Chezy are used. This parameter is dependent on the vegetation characteristics. Reliable measuring data is a necessity for this approach, to calibrate and validate this friction parameter per type of vegetation.

#### Van Rijn

The dissipation by bed friction according to van Rijn (1989), is described by  $D_f$ , which is the time averaged work done by the friction force.

$$D_f = \frac{1}{T} \int_0^T \tau_b \cdot U_b \cdot dt \quad (0.12)$$

In which  $T$  represent the duration time,  $\tau_b$  the bed shear stress,  $U_b$  the horizontal orbital velocity.

In case of wave action, substitution of

$$\tau_b = \frac{1}{2} \rho \cdot f_w \cdot \hat{U}_\delta^2 \cdot \sin^2(\omega t) \quad (0.13)$$

and

$$U_b = \hat{U}_\delta \cdot \sin^2(\omega t) \quad (0.14)$$

With  $f_w$  friction coefficient,  $\hat{U}$  the maximum of the horizontal orbital velocity,  $\rho$  the water density,  $\omega$  the absolute angular wave frequency,

yields:

$$D_f = \frac{4}{3\pi} \rho \cdot f_w \cdot \hat{U}_\delta^3 \quad (0.15)$$

This formulation shows that the dissipation due to bottom friction is related to a friction coefficient  $f_w$  and the third power of the amplitude of the horizontal orbital velocity at the bottom.

### Collins

The bottom friction model by Collins, (1972) is based on a conventional formulation for periodic waves with the appropriate parameter adapted to suit a random wave field. The dissipation rate is calculated with the conventional bottom friction formulation.

$$C_{bottom} = c_f \cdot g \cdot U_{orb} \quad (0.16)$$

where  $c_f$  the Collins friction factor of 0.015.

In recent studies (de Vries and Roelvink, (2004)) the van Rijn, (1989) formulation to prove that this Collins friction factor can in principle be used to describe wave dissipation by vegetation, which subsequently is utilized in SWAN.

This resulted in:

$$S_{ds,b}(\sigma, \theta) = -\frac{1}{2} c_f \cdot \rho \cdot U_{orb}^3 \quad (0.17)$$

Where  $S_{ds,b}$  is the wave dissipation,  $\sigma$  the angular frequency and  $\theta$  the propagation direction of a wave component.

This expression has great similarity with van Rijn (1989) and is used to make SWAN suitable for vegetation, by using an alternative vegetation friction factor,  $c_v$ .

$$c_v = f_w^* \cdot D \cdot n \cdot dz \quad (0.18)$$

which  $f_w^*$  is the vegetation friction coefficient,  $D$  the vegetation diameter,  $n$  the vegetation density and  $dz$  the vegetation height.

### 3.2.2 Cylinder approach

Another basis for a theoretical formulation for dissipation due to vegetation is to use a separate expression in which the dissipation due the most significant processes are determined. According to several authors (Dalrymple et al., (1984), Kobayashi et al., (1993)) plant or vegetation induced forces acting on the fluid are expressed in terms of a Morrison (1950) type equation, where vegetation motion (yawing or vibrating by vortices) is neglected. The energy losses are calculated as actual work carried out by the vegetation on the wave motion. In this theory the drag force is considered the most significant parameter. Surface friction and pressure gradients impose drag forces. Drag due to friction however is much smaller than the drag force as result of pressure differences. Therefore only the pressure drag is considered. Section 3.3 elaborates on the drag and bulk drag coefficient in relation to physical processes.

As for neglecting of the yawing motions we need to consider the inertia forces. In mechanics, inertia is the resistance to change acceleration. Mangrove vegetation is relatively stiff compared to for example grass, implying little relative movement of the vegetation related to the water movements. In relatively flexible vegetation fields as, reed or sea grass or canopies of mangrove trees, these processes are present however, the contribution of inertia forces to wave energy dissipation in mangrove is very little, and can therefore be neglected.

#### **Morrison**

Morrison et al., (1950) found for the force on a single slender pile in surface waves:

$$f(t) = C_m \frac{1}{4} \pi D^2 \rho \frac{dU}{dt} + C_d D \frac{1}{2} \rho U |U| \quad (0.19)$$

where  $C_m$  represent the inertia coefficient,  $D$  the pile diameter,  $C_d$  the drag coefficient and  $U$  the maximum value of the horizontal orbital velocity.

## Dalrymple

Dalrymple et al. (1984) derived an energy dissipation factor based on the Morrison equation for submerged marsh vegetation. Mendez and Losada (2004) used the method of Dalrymple et al. (1984) for their physical model to estimate the propagation of random breaking and non-breaking waves over vegetation fields. The theory assumes that the linear wave theory is valid and considers waves normally incident on a coastline with straight and parallel depth contours. It expresses the horizontal force per unit of volume dependent of depth average bulk drag coefficient dependent of vegetation characteristics, the horizontal velocity in the vegetation region due to the wave motion, the plant area and the horizontal vegetation density, Mendez and Losado (2004).

Assuming the previous assumptions, the conservation of energy is:

$$\frac{\partial(Ec_g)}{\partial x} = -\varepsilon_v \quad (0.20)$$

in which  $E$  is wave energy per unit area,  $c_g$  is wave group velocity and  $\varepsilon_v$  represents the time averaged energy dissipation per horizontal unit over the vegetation height

$$\varepsilon_v = \int_{-h}^{-h+\alpha h} F_x u dz \quad (0.21)$$

where  $F_x$  is the drag force on a plant considered in  $x$  direction,  $u$  the horizontal velocity due to wave motion,  $h$  the water depth and  $\alpha h$  the mean vegetation height. Further,

$$F_x = \frac{1}{2} \rho C_d b_v N_v u |u| \quad (0.22)$$

The vegetation characteristics used in this approach are depth averaged, with  $C_d$  the drag coefficient,  $b_v$  the stem thickness or diameter  $N_v$  and the vegetation density.

It has been assumed that the linear wave theory for waves propagating over an impermeable bottom is valid to calculate  $u$  not only for the water region but also within the vegetation area. Dalrymple et al. (1984) expressed the energy dissipation resulting from equation (0.21) and (0.22) through a vegetation field as:

$$\varepsilon_v = \frac{2}{3\pi} \rho C_d b_v N_v \left( \frac{kg}{2\sigma} \right)^3 \frac{\sinh^3 k\alpha h + 3 \sinh k\alpha h}{3k \cosh^3 kh} H^3 \quad (0.23)$$

where  $k$  is the wave number,  $\sigma$  angular wave frequency,  $\alpha h$  is the mean vegetation height. Wave reflection on vegetation is not considered in this formulation

### 3.2.3 Internal waves in bottom

Another cause of wave energy loss in mangrove forests are, believed to be the result of the composition of the soil. The composition of the bottom in mangrove areas is often one of muddy soil types, which can act as a fluid. Waves propagating over sea bed induce vertical pressure differences. As the bottom can be partly fluidized or muddy, internal waves in the interface between the water and the liquefied soil can originate, which causes damping by viscous absorption of wave energy. Through various studies on wave - mud interaction are done, (Gade, (1958)), (Liu and Mei, (1989), (1992)), on the combination on the interaction of waves, little is known about this phenomenon. One of the assumptions here, is that the contribution of this process to wave attenuation in mangroves is very little, as the muddy soil is retained by the root network.

### 3.2.4 Conclusions

The two main approaches to describe the wave energy dissipation by vegetation, as described in the previous section are the cylinder approach and an enlarged bed friction parameter.

The enlarged bed friction parameter approach based on Collins (1968) has been studied and implemented in SWAN by de Vries and Roelvink, WL Delft Hydraulics, (2004) and calibrated for sea grass (*Spartina Anglica*). However this approach seems to work when calibrated, there is no physical schematisation of the vegetation. More complex configurations of vegetation are not easily translated into this model, because the vegetation is schematised with one parameter.

As for the expanded the Dalrymple (1984) formulation by Mendez and Losada (2004) this is quite the opposite. It can handle sloping bottom conditions and breaking waves. In the flume experiments the formulation appears to provide promising results. Mendez and Losada conclude that this type of model can easily be implemented in standard wave propagation numerical models in order to incorporate dissipation induced by vegetation fields and therefore to be able to estimate wave induced circulation as well as sediment transport in a vegetation field and in its vicinity.

However what has to be realized is that the formulation contains the drag coefficient which has to be calibrated and when doing so it will certainly include a bulk of physical processes not described by the model in the first place. This is elaborated in the section 3.3.

The conclusion is drawn here is that best numerical approximation of wave attenuation in vegetation and the most suitable to implement in SWAN, was found to be the Dalrymple formulation (1984).

### 3.3 Physical background on the Bulk Drag Coefficient

The calibration parameter in the Dalrymple (1984) formulation, which is of significant importance for determining the wave dissipation due to vegetation, is the drag coefficient  $C_D$ . It is known that the drag coefficient is dependent on the Reynolds number and on the shape and orientation of the object. However there are numerous processes which also can significantly contribute to the value of the drag coefficient.

#### 3.3.1 Determination of significant energy dissipation areas

A vegetation field as a whole is an obstacle to wave motion, which is partly reflected from the field, partly attenuated and partly transmitted by interaction with the stems and leaves.

In case of a submerged vegetation field, four areas in relation to wave energy dissipation can be distinguished, respectively area 1: the bottom vegetation interface, area 2: the vegetation field, area 3: the turbulent boundary layer between the vegetation and the water layer above the vegetation and area 4: the water layer above the vegetation Figure 3-4.

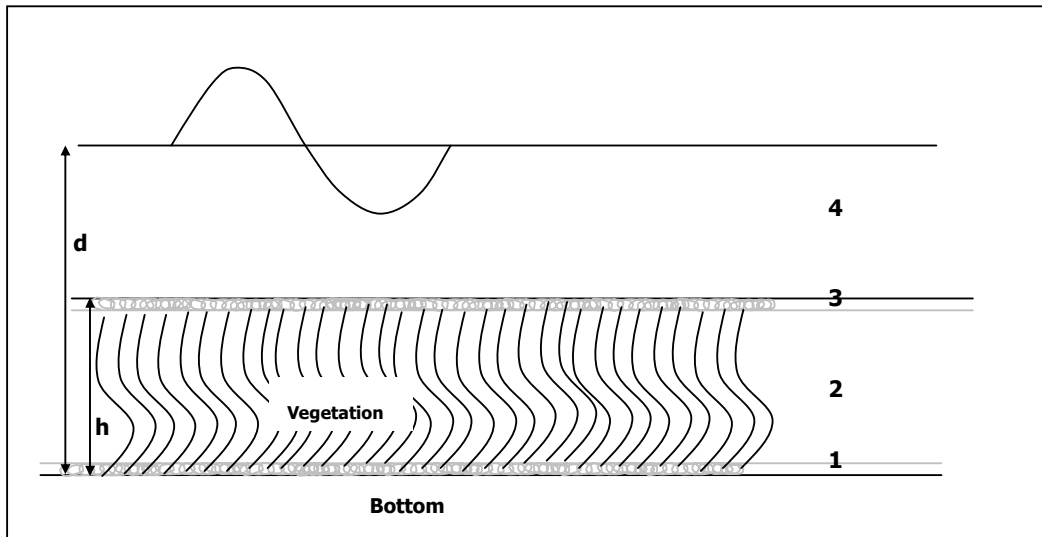


Figure 3-4 Different zones of energy dissipation in a submerged vegetation.

In layer 1, 2 and 3 energy is dissipated respectively due to the bed friction, wave-vegetation interaction and turbulence in the boundary layer. In layer 4 no energy is dissipated (no other processes that can dissipate energy are considered). In a vegetation field the dissipation due to bed friction is of an order smaller than the contribution of vegetation friction (Mendez and Losada (1997)), (Mazda et al. (1997)), even in sparse vegetation (Nepf (1999)). In Dalrymple's formulation (1984), only vegetative drag is considered and the turbulence in the boundary layer and bed friction are neglected. Therefore only dissipation in area 2 will be considered.

### 3.3.2 Dependence of drag on vegetation characteristics

On the scale of a particular trunk, the interaction of the trunk body with the (oscillating) flow induces vortices and a wake further downstream. Considering the flow around one cylinder, both surface friction and pressure gradients impose drag forces. The surface friction is dependent on the surface roughness. Considering vegetation, friction drag is much smaller than the drag force as result of pressure differences (Massel et al. (1999)). Therefore only the pressure drag will be considered in this approach. The pressure drag around a cylinder in oscillating flow induces a drag force and a lift force. The cases considered in this study assume a shallow water approximation in which vertical orbital velocities are much smaller than horizontal orbital velocities, therefore lift forces are not considered dominant here and will be disregarded.

Water flowing around a cylinder causes the streamlines to contract, resulting in an increasing water velocity and hence a decrease in pressure. Behind the point of separation a wake occurs, where the pressure is much lower than at the upstream side of the object Figure 3-5.

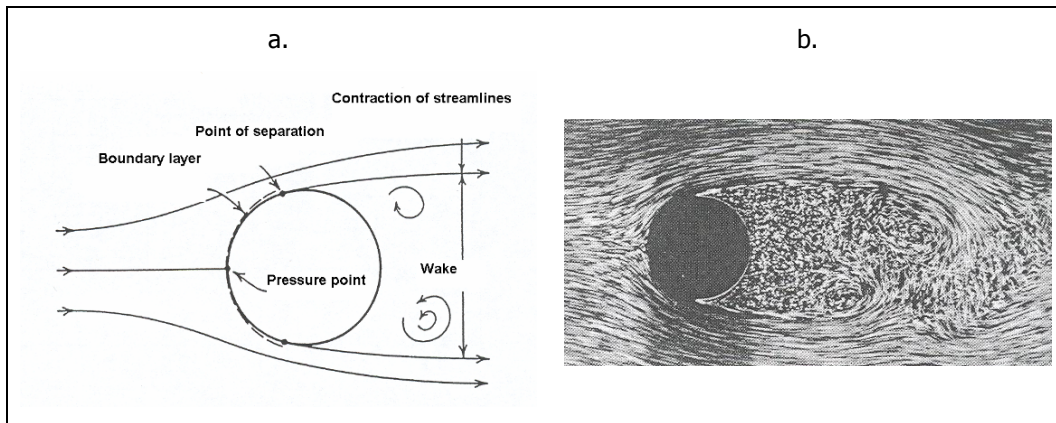


Figure 3-5 Flow around a cylinder for a. theoretical and b. experimental (for  $Re = 2300$ ) (from Battjes (1999))

The total pressure gradient in the direction of the flow forms the largest contribution to the drag force.

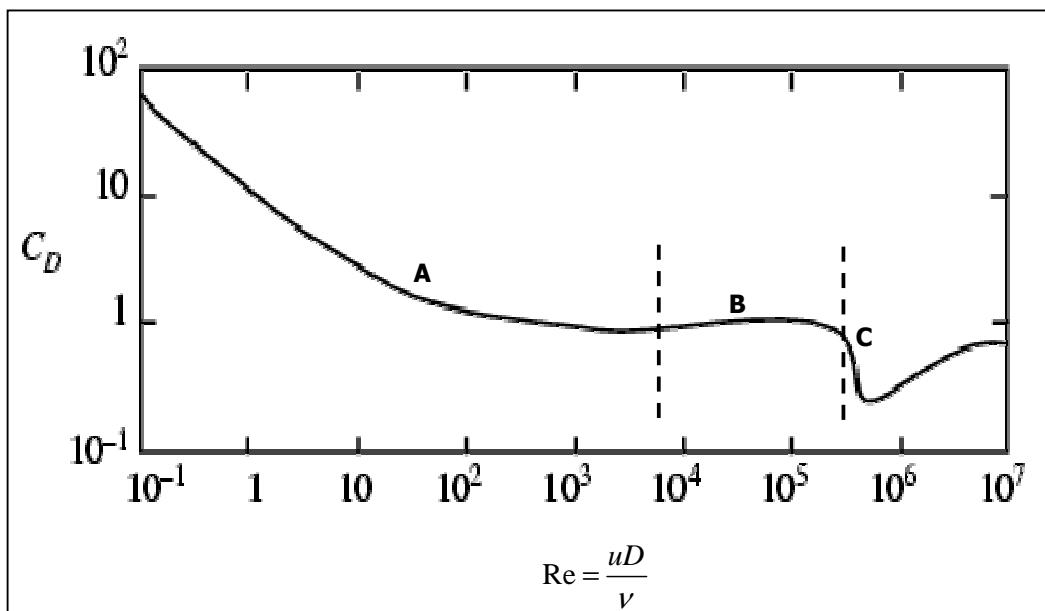


Figure 3-6 Relation between Reynolds number and drag coefficient for a single circular cylinder in flow (from Battjes (1999))

Calculations of the Reynolds number for one single stem (Figure 3-6) in case of cylinders with a diameter equal to respectively a mangrove tree and a Spartina plant (used in the SWAN model), show that the Reynolds number is in the range of area B shown in Figure 3-7. This implies that the drag coefficient for one rigid cylinder has a value of around 1.

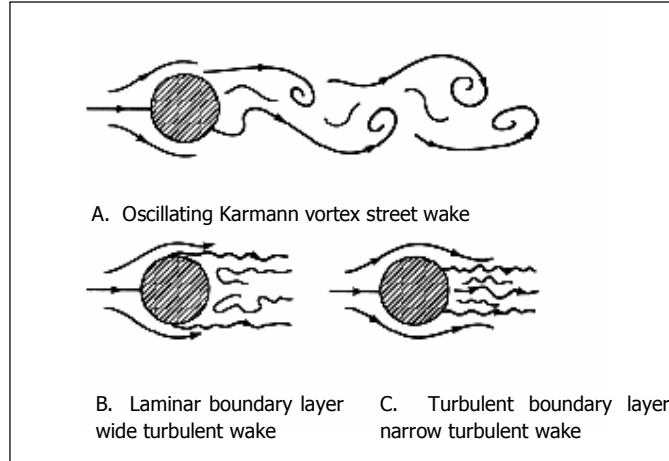


Figure 3-7 Single cylinder in a turbulent flow regime

(from [http://www.princeton.edu/~asmits/Bicycle\\_web/blunt.html](http://www.princeton.edu/~asmits/Bicycle_web/blunt.html))

Considering an array of cylinders, numerous other processes become important in respect to the drag coefficient. A convenient way to approach a multi cylinder array, is defining a relative spacing ( $S/D$ ), in which  $S$  represents the distance between the cylinders and  $D$  the

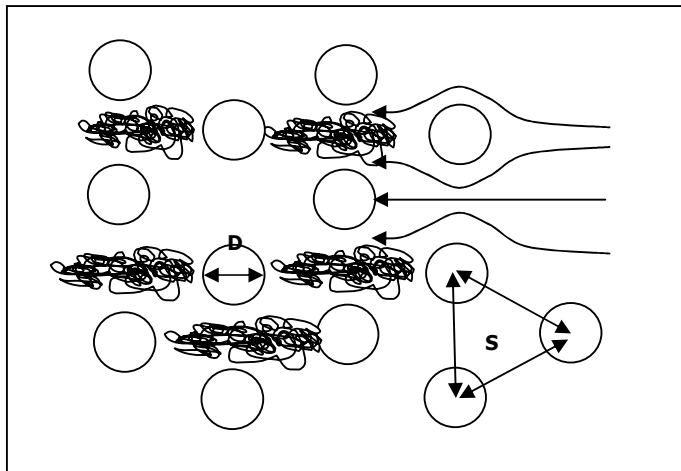


Figure 3-8 Staggered configuration of cylinders with wake interference and contraction of streamlines

diameter. In vegetation the configuration of the stems is irregular and at random, however for simplification purposes the configuration is considered staggered (Figure 3-8). For each flow regime a different drag coefficient has to be applied, as was seen in Figure 3-6. In a multi-cylinder array, the limits of these different regimes are different because of wake interference, sheltering and tortuosity, (Nepf (1999)).

For large relative spacing between the cylinders, larger than the wake length, the influence of the cylinders on each other is negligible, and a coefficient for one cylinder can be applied. This is confirmed for a uniform flow situation by Nepf (1999).



For a decrease in relative spacing, experimental studies by Heideman and Sarpkaya (1985) concluded that the bulk drag coefficient for an array of cylinders is smaller than the drag coefficient for a single cylinder in oscillatory flow. An explanation can be found in the fact that the upstream cylinders influence the flow field around the down stream cylinders as shown in Figure 3-8. Some downstream cylinders may lay in the wake of upstream cylinders and therefore be subjected to reduced flow velocities, but increased turbulence, while others may be subjected to increase fluid velocities because of fluid acceleration through spaces between upstream cylinders. (Heideman and Sarpkaya (1995)). The intensity, the length scale and diffusion of turbulence in the water body control the drag forces induced by flow on the cylinders (Massel et al. (1998)).

Another important phenomenon related to turbulence, is eddy viscosity. The turbulent transfer of momentum by eddies gives rise to an internal fluid friction, in a manner analogous to the action of molecular viscosity in laminar flow, but taking place on a much larger scale. The consequence of this is a decrease in the Reynolds number, resulting in a more viscous behavior of the water. Hence the contribution of the pressure drag decreases and friction drag could become of significance.

When the proximity of the plants increases even further, another change in the value of  $C_d$  can be seen. According to Massel (1999) after Chakrabarti (1991), the  $C_d$  values increase as the relative spacing ( $S/D$ ) approaches to 1.1, where  $S$  is the distance between the cylinder axes. This could be explained by vegetation acting as a "blunt" object, leading to an increase in drag coefficient. At some point the vegetation can be so dense, that the water prefers the way of least resistance and flows primarily over the vegetation field instead of through it. The waves might experience the vegetation as a "raised (semi) impermeable bottom". This causes the flow lines to contract and the velocity to increase. Turbulence is still induced by the interface between vegetation and the water above.

Another important factor that can attribute to this phenomenon is the relative vegetation height. If the vegetation length is small and subsurface, the water can choose the way of minimum resistance and for the larger part flow over the vegetation. On the other hand, when the relative vegetation is large or the vegetation is emerged, the water will be more or less obliged to flow through the vegetation, leading to a different value of the drag coefficient.

Nepf (1999) studied the influence of the relative spacing on the drag coefficient in flow,

$$\text{defining the vegetation density as } a = n \cdot d = \frac{d}{S^2} \quad (0.24)$$

where  $n$  is the number of cylinders per square meter,  $S$  is the relative spacing and  $d$  is the cylinder diameter. For this cylinder model  $ad$  represents the fractional volume of the flow domain occupied by the plants. Nepf combined results of several numerical and physical modelling studies in Figure 3-9.

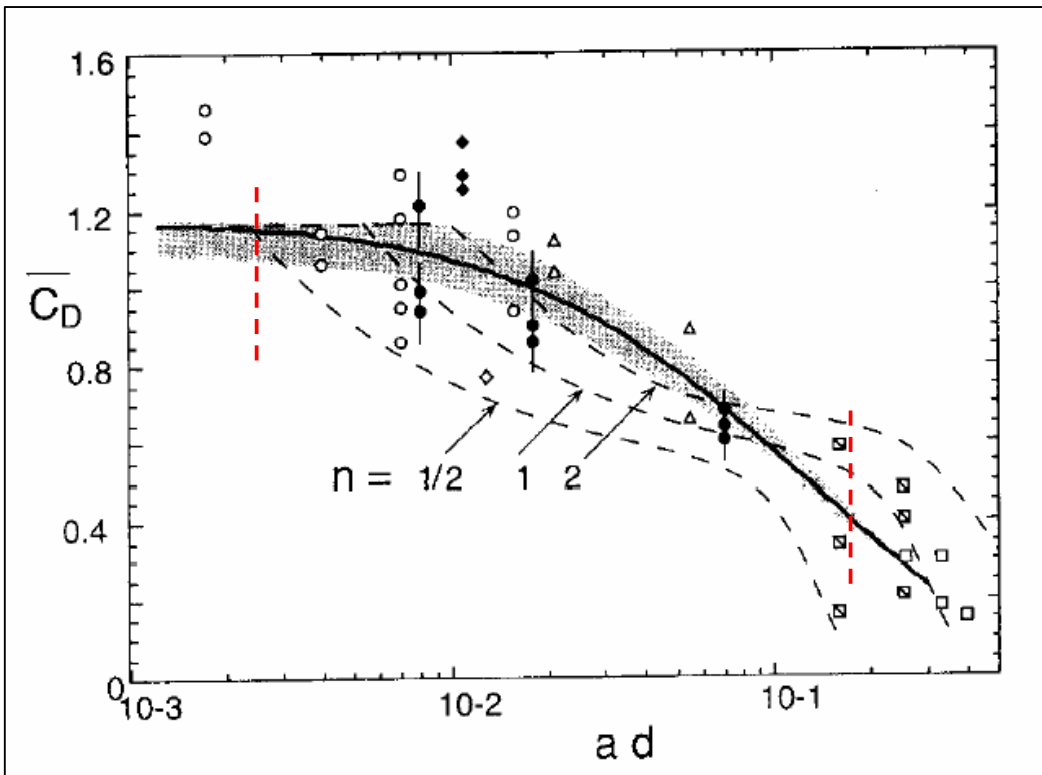


Figure 3-9 Influence of the relative spacing on the drag coefficient (from Nepf (1999))

In which  $N$  represents the ratio of longitudinal to lateral row spacing,  $N = 1$  means a square staggered array. A decrease in relative spacing (increase in population density  $ad$ ) in this case, leads to a decrease in the drag coefficient, due to an increase in wake interference. Depending on the density and diameter the range for mangrove is in between the two red dotted lines shown in Figure 3-9.

Table 3-2 Summary of Reynolds number and array configuration (Nepf (1999))

| Source                        | $Re_d$          | Configuration          | Symbol in Figure 6 |
|-------------------------------|-----------------|------------------------|--------------------|
| <i>Dunn et al.</i> [1996]     | 1,000–4,000     | staggered, $n = 1/2$   | open circle        |
| <i>Seginer et al.</i> [1976]  | 1,000           | staggered, $n = 1$     | open diamond       |
| <i>Kays and London</i> [1956] | 1,000           | staggered, $n = 1-3$   | square             |
| <i>Petryk</i> [1969]          | 10,000          | random                 | solid diamond      |
|                               |                 | staggered, $n = 1, 2$  | triangle           |
| <i>Zdravkovich</i> [1993]     | 1,000           | staggered, $n = 1^*$   | square with slash  |
| Present study                 | 4,000–10,000    | random                 | solid circle       |
| Model                         | $> \approx 200$ | random                 | solid line         |
|                               |                 | staggered, $n = 1/2-2$ | dashed lines       |

Here,  $n$  is ratio of longitudinal to lateral row spacing within staggered array.

\*One third, 2/3, and fully staggered.

### 3.3.3 Dependence of the drag on wave characteristics

The drag coefficient is dependent on the wave characteristics. In case of an oscillating flow in waves the value of the Keulegan-Carpenter number can be used to describe the relation between the drag coefficient and the wave characteristics. The Keulegan-Carpenter number is defined as:

$$K = \frac{u_c T_p}{b_v} \quad (0.25)$$

in which  $U_c$  is the maximum horizontal orbital velocity,  $T_p$  the wave period and  $b_v$  the diameter of the object.

Mendez and Losada (2004) found the following relations between the drag coefficient and the Keulegan-Carpenter number for different values of relative vegetation height  $\alpha$  (Figure 3-10). These are the results of 154 runs of a physical model in a flume with artificial vegetation, where the calibration parameter is  $C_d$  and where the vegetation density and diameter were kept constant. Details on these experiments can be found in 4.4.

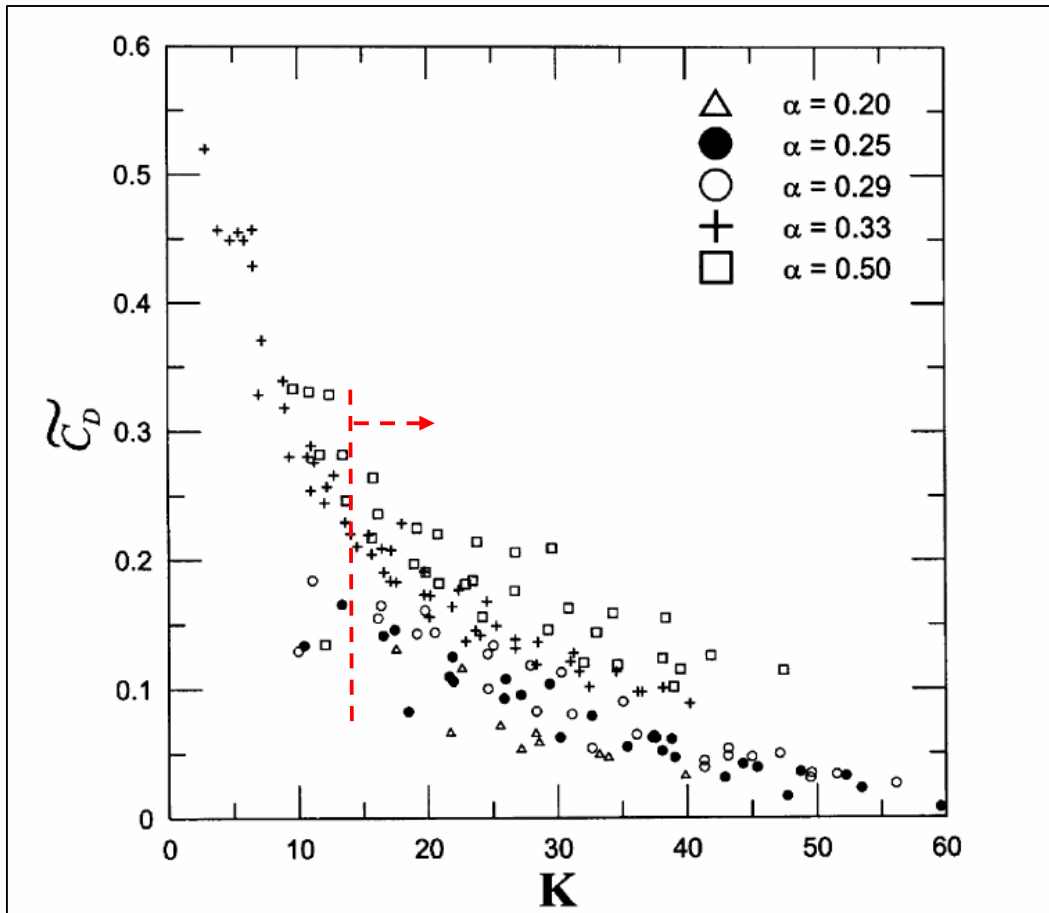


Figure 3-10 Relation between Keulegan-Carpenter number and  $C_d$  for different values (from Mendez and Losada (2004))

Mendez and Losada give little interpretation of these results. Some presumable processes are described here that could explain the relations between the drag coefficient and the Keulegan-Carpenter number.

A large peak period  $T_p$ , or a larger wave length, suggests that in a certain time frame there are less flow accelerations and decelerations than in a short wave. Because in a decelerating flow more energy (due to more turbulence (Schiereck (2001) after Booij (1992))) is dissipated than in an accelerating flow, this energy is not available for the next acceleration. This means that in a certain time frame, more short waves dissipate more energy than a longer wave. In the K-Cd relation according to Mendez and Losada a shorter period causes the K number to decrease resulting in a larger drag coefficient. For mangrove vegetation the K starts around 15 and increases with increasing wave conditions (Figure 3-10).

A wave with a high horizontal orbital velocity will induce more turbulence behind the vegetation stem, resulting in a larger wake. This results in a decrease in the bulk drag coefficient due to smaller pressure differences.

### 3.3.4 Conclusions

It has become clear that the value of the drag coefficient depends on the Reynolds number (and hence the flow regime) and the shape and orientation of the objects. The flow regime mainly depends on the wave characteristics and the relative spacing and position of the cylinders.

A relation between the drag coefficient and wave characteristics has been specified by Mendez and Losada, who express this relation, for different relative vegetation heights, by introducing the Keulegan-Carpenter number Figure 3-10.

The dependency of the drag coefficient on the relative spacing is studied by Nepf (1999). She concludes a decline in the drag coefficient when the relative spacing decreases due to wake interference (see Figure 3-9). An important additional process that arises in wake interference and that has to be taken into account is turbulent eddy viscosity.

What has to be kept in mind is that some non-drag related and initially neglected processes such as bed friction, vegetation motion and inertia (added mass) can be present in a real time situation, whereas the model does not account for these processes. This can account for a deviant value of the drag coefficient, because the contributions of these neglected processes are discounted in the drag coefficient. Therefore it is not physically correct to refer to this parameter as a drag coefficient.

## 4 Numerical wave modelling in SWAN

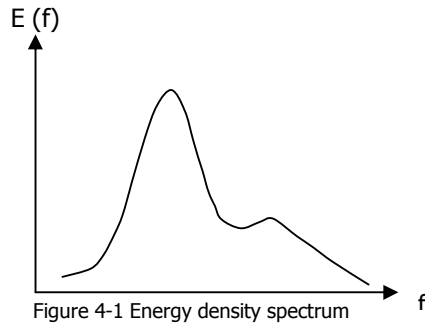
This chapter describes the numerical wave modelling done in SWAN. A general description of the working and principles of SWAN is presented. Next important considerations with regard to the implementation of Dalrymple (1984) in SWAN are discussed, followed by a description of validation of the implementation on the Mendez and Losada (2004) experimental results.

### 4.1 General description of SWAN

The SWAN (Simulating WAVes Near shore) model is a third generation spectral model developed by a team at Delft University of Technology. The SWAN model was created in an effort to extend the success of deep ocean wave models (e.g. WAM, Komen et al (1994)) into coastal areas. The SWAN model was designed to fill in the modelling gap in the dynamic area between 20-30m depth and the coastline. SWAN is an Eulerian model and is based on the action balance equation (Booij et al. (1999)). The spectrum that is considered in SWAN is the action density spectrum  $N(\sigma, \theta)$  rather than the energy density spectrum  $E(\sigma, \theta)$  since in the presence of currents, action density is conserved whereas energy density is not (e.g., Whitham (1974)). The independent variables are the relative frequency  $\sigma$  (as observed in a frame of reference moving with current velocity) and the wave direction  $\theta$  (the direction normal to the wave crest of each spectral component). The action density is equal to the energy density divided by the relative frequency:

$$N(\sigma, \theta) = \frac{E(\sigma, \theta)}{\sigma} \quad (0.26)$$

with  $E$  representing the area under the spectral curve (Figure 4-1).



This spectrum may vary in time and space. The evolution of the wave spectrum is described by the spectral action balance equation which for Cartesian coordinates is (e.g., Hasselmann et al. (1973)):

$$\frac{\partial}{\partial t} N + \frac{\partial}{\partial x} c_x N + \frac{\partial}{\partial y} c_y N + \frac{\partial}{\partial \sigma} c_\sigma N + \frac{\partial}{\partial \theta} c_\theta N = \frac{S}{\sigma} \quad (0.27)$$

The first term represents local rate of change of  $N$  in time, the second and third terms represent the propagation in  $x$  and  $y$  (geographical space) with  $c_x$  and  $c_y$  (the propagation velocities in space). The fourth term represents the shifting of relative frequency due to variations in water depth and currents while the fifth term represents depth induced refraction. The right hand term is the energy source term, which accounts for generation, dissipation and non-linear interactions between waves. Details can be found in (Booij et al., (1999)) and the User manual (2004).

The wave model accounts for the following effects:

- wave propagation in space: shoaling and refraction
- wave growth due to wind input
- transfer of energy within the spectrum by non-linear wave-wave interactions (both quadruplets and triads)
- dissipation by white capping
- dissipation by bottom friction
- dissipation by depth-induced breaking

## **4.2 Modelling wave attenuation by vegetation**

### **4.2.1 Implementation criteria**

The following three criteria are considered most important when modelling wave attenuation by vegetation.

1. Good schematization of the most important physical vegetation characteristics,
2. The applicability to all types of halophytic vegetation and
3. The extra dissipation term easily should be implemented in SWAN.

Dalrymple formulation (1984) fulfills all these criteria.

A good schematization of the most important physical vegetation characteristics is fulfilled by Dalrymple (1984) by the fact that the formulation contains input parameters as, plant height, stem thickness, number of stems per unit surface and a drag coefficient. The only parameter that cannot be determined fundamentally is the drag coefficient  $C_d$ , which has to be specified by comparison with experimental and field measurements.

Different types of vegetation species can be modelled by varying these parameters. Asano, Deguchi, Kobayashi (1993) proposed an adaptation to the formulation by Dalrymple (1984) to include the swaying motion of the plants and thereby expand the range of the application from only stiff to flexible vegetation.

The conclusions of physical modelling studies showed that varying the drag coefficient is sufficient to model flexible vegetation. Finally, the Dalrymple (1984) formulation can be expressed in terms of energy density, which makes it easy to implement in SWAN.

Both bed friction and vegetation interaction can simultaneously be utilized. Nevertheless, Mazda et al. (1997) and Nepf (1999) concludes from physical modelling tests that the contributions of bed friction to the wave dissipation is an order smaller than the vegetation interaction, thus can be neglected, as mentioned in section 3.2. SWAN is a depth averaged model, which implies a vertically uniform orbital velocity.

### **4.2.2 Testing on Paulina Schor**

In order to get a first impression, the Dalrymple (1984) formulation has been tested on the previous described measurements done at the Paulina Schor, Mol (2004). This was done using Excel, the results can be found in Appendix A *Results of test calculations Dalrymple formulation*. As input a  $C_d$  value of 0.5 was used and for the density, height and diameter average values for the Paulina Schor were applied. These first rough estimations look very promising, because the general trend in wave damping corresponds very well with the field measurement results.



### 4.3 Implementation of the Dalrymple formulation in SWAN

In the previous paragraph the action density balance equation has been discussed. Implementing dissipation due to vegetation implies adding an extra source term to this equation. The subroutine of SWAN that handles this source term is *swancom2*. Therefore the new subroutine is implemented in *swancom2*, called *SVEG*. The result will be a model that describes wave attenuation by vegetation, in which vegetation can be varied both horizontally, to account for the zonation of vegetation, and vertically, to account for different vegetation species by vertically varying vegetation characteristics. For a general description of the SWAN source code and the code implemented herein, see Appendix B *Implemented code*.

The approach of the implementation of the Dalrymple (1984) formulation will be discussed here in three sections. A distinction made to the vegetation configurations. First homogeneous vegetation was implemented, this was subsequently expanded with horizontal variation and finally vertical variation of the vegetation was implemented.

#### 4.3.1 Homogeneous vegetation

Described in 3.2.2, the formulation to be implemented reads:

$$S_{veg} = \langle \varepsilon_v \rangle = \frac{1}{2\sqrt{\pi}} \rho \tilde{C}_D b_v N_v \left( \frac{gk}{2\sigma} \right)^3 \cdot \frac{\sinh^3 k\alpha h + 3 \sinh k\alpha h}{3k \cosh^3 kh} H_{rms}^3 \quad (0.28)$$

Since the dependent variable in SWAN is the spectral energy, the formulation of Dalrymple (1984) needs to be recasted.

The quantity  $H_{rms}$  can be written in terms of spectral wave energy per spectral component as follows:

$$H_s = 4\sqrt{E} \quad (0.29)$$

so that

$$H_{rms} = \frac{H_s}{\sqrt{2}} = 2\sqrt{2}\sqrt{E} \quad (0.30)$$

Equation (0.30) substituted in equation (0.28) results in:

$$S_{veg} = \frac{8\sqrt{2}}{\sqrt{\pi}} \rho \tilde{C}_D b_v N_v \left( \frac{gk}{2\sigma} \right)^3 \cdot \frac{\sinh^3 k\alpha h + 3 \sinh k\alpha h}{3k \cosh^3 kh} E\sqrt{E} \quad (0.31)$$

Because  $S_{veg}$  is a dissipation term it needs to be treated implicitly. Since SWAN can only work with (quasi) linear terms, eq. (0.31) needs to be linearized in  $E$ . The most simple approach is a linearization by a *Picard iteration* in general:

$$S^n \cong \Phi^{n-1} E^n \quad (0.32)$$

This results for  $S_{veg}$  in:

$$S_{veg}^n \cong \gamma E^n \quad \text{with} \quad \gamma = \gamma(H_s, T_p, \dots, E^{n-1}) \quad (0.33)$$

$$\text{in this case: } \gamma = \frac{8\sqrt{2}}{\sqrt{\pi}} \rho \tilde{C}_d b_v N_v \left( \frac{kg}{2\sigma} \right)^3 \cdot \frac{\sinh^3 k\alpha h + 3 \sinh k\alpha h}{3k \cosh^3 kh} \sqrt{E^{n-1}} \quad (0.34)$$

where  $E^n$  is the energy density in the current iteration level and  $E^{n-1}$  is the energy density in the previous iteration level.

The parameters for the vegetation are the drag coefficient  $C_d$ , the vegetation density  $N_v$ , the diameter  $b_v$  and the plant height  $\alpha h$ . These parameters are constant over the entire grid, resulting in homogeneous vegetation.

This formulation (0.34) is implemented in the subroutine *swancom2*, the source code of this subroutine *SVEG* can be found in Appendix B *Implemented code*.

### 4.3.2 Horizontal variation of vegetation

In addition to the homogeneous formulation the vegetation can easily be varied horizontally in the following manner.

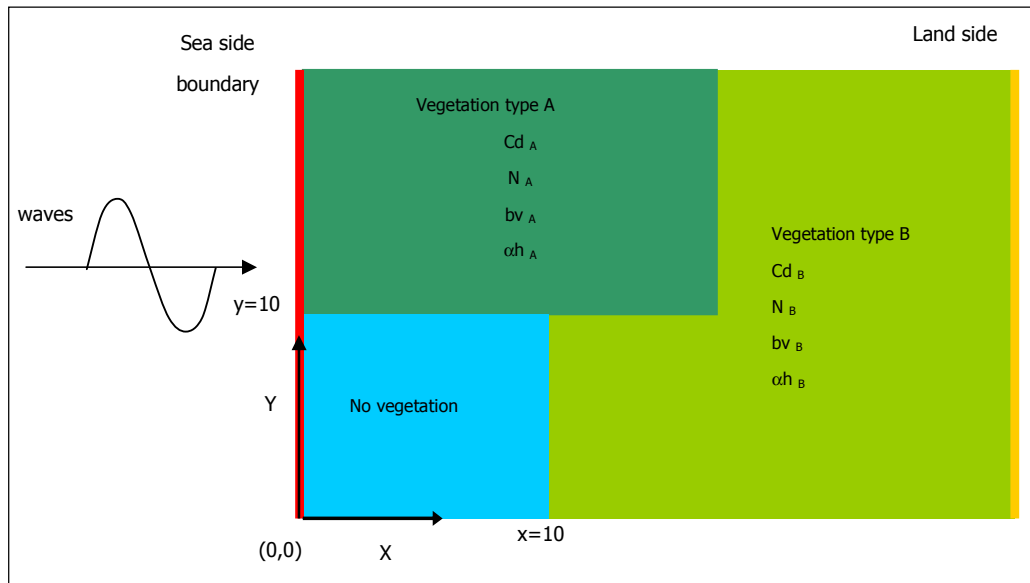


Figure 4-2 Example horizontal variation

For values of  $x \leq 10$  and  $y \leq 10$  the user defines the situation with the following vegetation characteristics:  $C_d=0$  ;  $N_V=0$  ;  $b_v=0$  ;  $\alpha h=0$ , implying that no vegetation is present. For the other areas shown in Figure 4-2 where vegetation type A and B are present this works in a similar way. (For the implemented source code of this horizontal variation procedure, see Appendix B *Implemented code*).

### 4.3.3 Vertical variation of vegetation

Next, vertical variation of vegetation is added. For the implementation of vertical variation of vegetation characteristics an important simplification on the vertical distribution of horizontal orbital velocity need to be made. Inter tidal wetlands (mangroves and salt marshes) are characterized by shallow fore shores which implies that a shallow water approximation of the waves can be assumed. In case of small wave heights a transitional situation can occur, Figure 4-3.

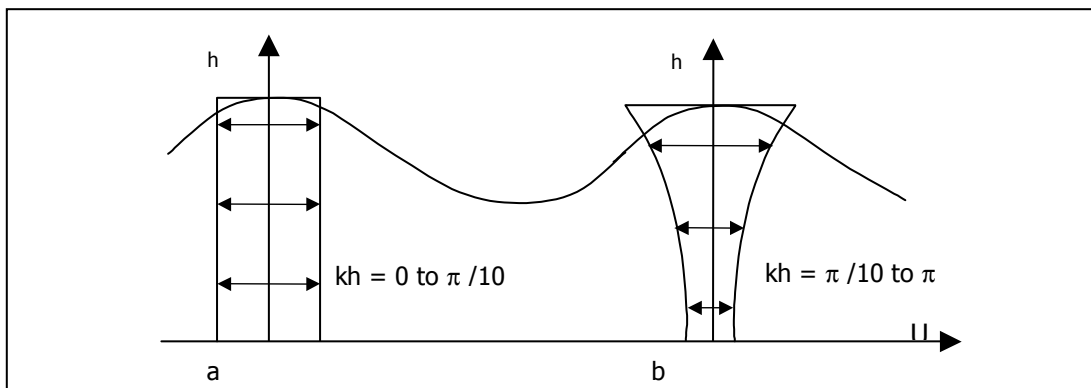


Figure 4-3 Vertical distribution of horizontal orbital velocity for a. shallow water and b. transitional water depth

Little is known about the orbital velocity profile inside the vegetation field. However, some research has been done on the interaction between flow and vegetation, Mazda and Wolanski (1995), Nepf (1999). According to Baptist (2005), the following flow pattern is found in vegetation, when only a current is present, Figure 4-4

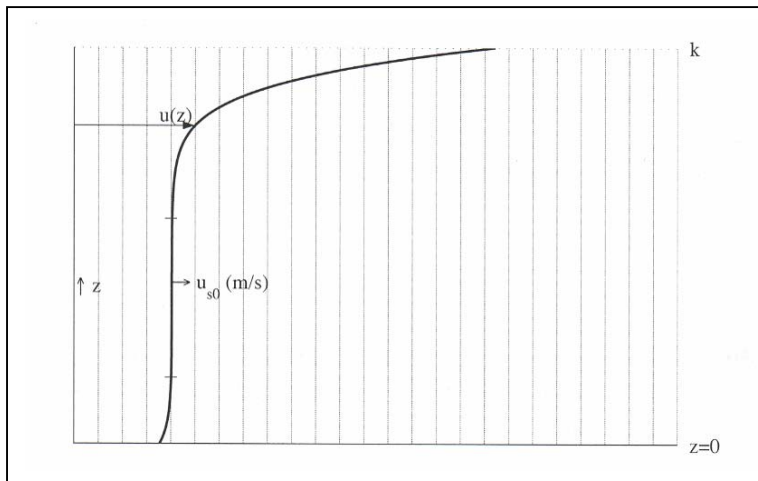


Figure 4-4 Schematized velocity profile in homogenous vegetation, where  $k$  is the vegetation height (Baptist 2005)

Especially the uniform part of the velocity profile is striking. It is assumed that the vertical distribution of horizontal orbital velocity in a homogeneous vegetation field follows a similar profile. Because of the uniformity of the velocity profile in the vegetation, it is assumed the amount of energy dissipation per unit vegetation height is uniformly distributed over the vertical as well, as the energy dissipation formula contains the orbital velocity in the third power.

SWAN is a depth averaged model; therefore the true horizontal orbital velocity distribution over the vertical is schematized as a uniform profile, shown in Figure 4-5

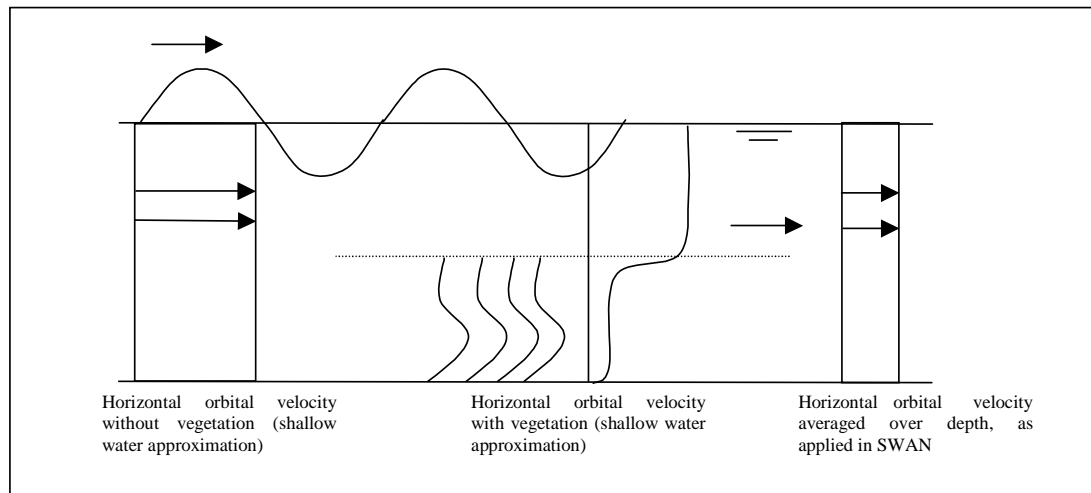


Figure 4-5 Horizontal orbital velocity profiles

Next it is verified if this assumption of the linear relation between the vegetation height and the amount of energy dissipation, can be found in Dalrymple's (1984) formulation. The results for homogenous vegetation is shown in Figure 4-6.

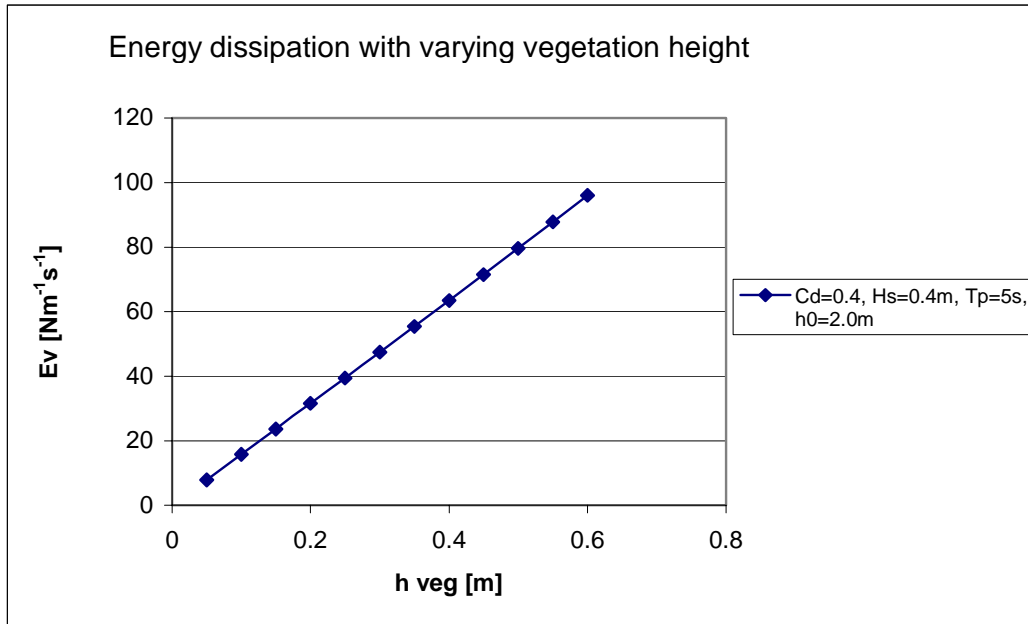


Figure 4-6 Linear relation between energy dissipation and the vegetation height

As can be seen, the relation between the amount of energy dissipation with increasing vegetation height is linear. Because in this non-breaking situation bottom friction is not considered, and no other external processes that could be responsible for wave energy dissipation are present, the dissipation is solely caused by the wave vegetation interaction. The conclusion that can be drawn is that, when the vegetation is being vertically sub divided into several segments or layers, the dissipation of each segment can be added to form the total dissipation. This conclusion makes it conveniently possible to implement vertically varying vegetation, by imposing different vegetation characteristics per layer, see Figure 4-7.

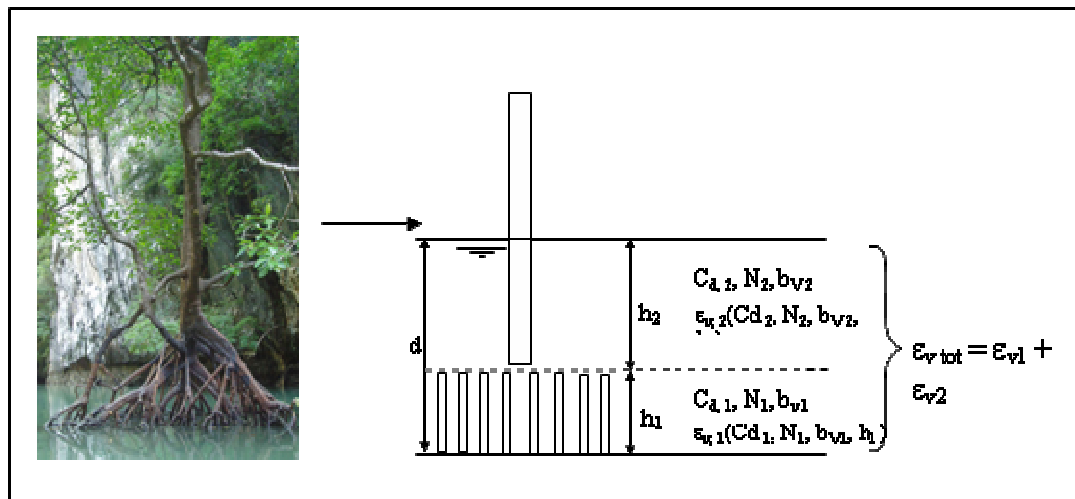


Figure 4-7 Schematisation of a mangrove tree

However, we need to realize that with applying non-homogeneous vertical vegetation characteristics, the horizontal orbital velocity profile is actually not homogeneous anymore. For instance the flow profile in a layer with 1000 stems of 5 mm diameter will be different from the profile of a layer with 3 stems of 100 mm, resulting in a different value in the energy dissipation. In SWAN as mentioned before, the total energy dissipation is a depth averaged value, therefore it can be concluded that the different contributions of each layer can be added up to form the total amount of depth averaged energy dissipation.

#### **Implementation in source code**

In the source code this summation is done in the following manner. First it is checked whether the vegetation is submerged or emerged, by comparing the water depth with the vegetation height. If the vegetation is submerged, the energy contributions of each layer are added up. If the vegetation is emerged, only the contributions of the vegetation below the water level are taken into account. For the implemented source code of this horizontal variation procedure, see Appendix B *Implemented code*.

#### 4.4 Validation on Mendez & Losada

In this section, correctness and validation of the implementation of the Dalrymple (1984) formulation is carried out. First it has to be checked if the implementation was successful. This has been done by simulating the validation case done by Mendez and Losada (2004).

Mendez and Losada (2004) used a physical model for the validation of their expanded version of the Dalrymple's (1984) formula. The experiment was carried out in a wave flume of 33 meter long, 1 meter wide and 1.6 meter high. In the flume on a horizontal bottom a 9.3m long strip of artificial kelp (*L. Hyperborea*) vegetation was present over the entire flume width. The vegetation had the following characteristics:  $b_v=0.025\text{m}$ ,  $\alpha h=0.2\text{m}$ ,  $N_v=1200\text{ m}^{-2}$  (respectively diameter, vegetation height and density). This means that the  $C_d$  value was the only calibration parameter. Mendez and Losada carried out total of 154 runs with varying water depth ( $d=0.4\text{-}1.0\text{m}$ ), wave peak periods ( $T_p=1.26\text{-}4.42\text{s}$ ), and root mean square wave heights ( $H_{rms}=0.045\text{-}0.17\text{m}$ ). The input for irregular waves was the JONSWAP spectrum, with the default shape parameter ( $\gamma_j = 3.3$ ).

In this study the exact same line up was used as input in the SWAN version with vegetation and the results were compared with the measurements. As can be seen in Figure 4-8 and in appendix C *Validation on flume experiments*, the results of the model correspond very well with the physical model tests. Thus it can be concluded that the implementation was successful. Next, a sensitivity analyses was applied on the SWAN implementation, this is elaborated in the next section.

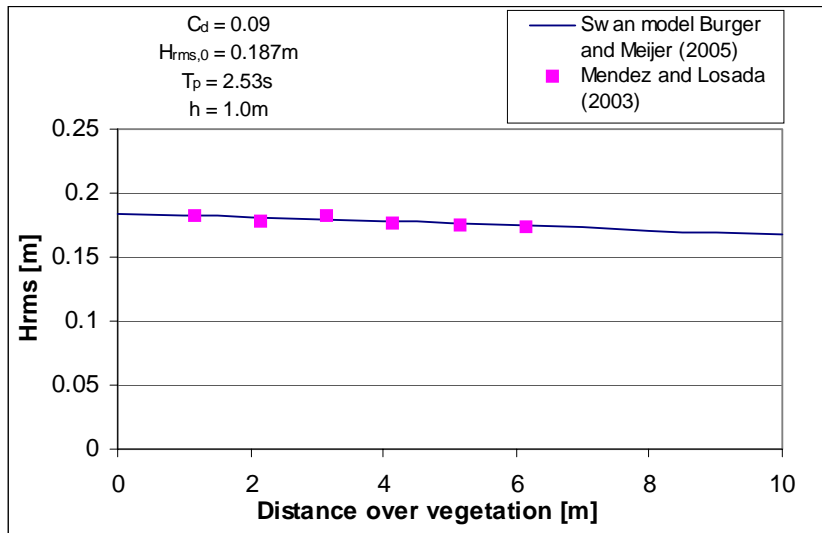


Figure 4-8 SWAN implementation validation

## **4.5 Sensitivity analysis on mangrove vegetation**

The general setup of this sensitivity analyses is to obtain insight on the influence of the vegetation parameters and hydraulic conditions on the wave attenuation. The setup and layout of the SWAN model used in the sensitivity analysis can be found in appendix D *Layout SWAN model*.

First the handling and the influence of bottom friction and wave breaking in the model is discussed in this section. After this the applied schematisation of mangrove vegetation is presented. Here a layered system is used. Next the sensitivity of the vegetation parameters is tested. In order to obtain insight in these sensitivities, the non importance of the layer order is described. From here the vegetation characteristics are varied to verify the sensitivity on the amount of wave attenuation. Increasing densities and diameter implies increasing wave damping. Also an increase in drag coefficient shows the right tendency for the wave attenuation.

Subsequently the sensitivity of the wave conditions is studied. The following parameters are varied: water level, wave height wave period. The varying of these wave parameters results in the expected tendencies on the amount of wave attenuation. Furthermore the influence of the wave attenuation on the near bottom orbital velocity is studied. Noted here is that SWAN is a depth averaged model, and therefore the results of these near orbital velocities (in the vegetation model) are overestimated by SWAN.

### **4.5.1 Bottom friction and wave breaking**

Bottom friction and wave breaking are processes besides the vegetation interacting with the waves, which dissipate wave energy. To be able to clearly study the effect of dissipation of the vegetation on the wave attenuation it is comfortable that the wave breaking and bottom friction processes are not present in the model.

The bottom friction in the adapted SWAN model was not utilized so no energy was lost to this process. What has to be noted here is that bottom friction in general, but also in a spectral wave model as SWAN has a significant effect when very mild slopes, shallow water conditions and long distances for the waves (in the order of kilometers) to travel over, are present. In the setup of the model used in this study, the transect length of the model was 125 m. Bottom friction applied here had no effect on the wave attenuation.

As for wave breaking two triggers of breaking have to be considered. First the wave breaking induced by the water becoming shallower, normal breaking occurs in this situation. Second, because of the vegetation present the waves can experience the vegetation as a shallower bottom and can break in an earlier stage, on the vegetation field edge. As for the first type of breaking in all runs no breaking conditions were used. A rule of thumb in shallow water, waves will start breaking if the wave height relatively to water depth is in the order of 0.5. This condition has been accounted for in the settings of the wave conditions and water depth.

The second process in which the waves experience the vegetation as a shallow bed, is thought to be present when very dense vegetation is present. Here fairly average densities are applied and therefore this phenomenon is absent.



### 4.5.2 Schematisation of mangrove vegetation

The vertical composition of a mangrove tree is easily divided in layers relating to the roots, trunk and a canopy as mentioned in 4.3.3. Vegetation data collected in measurement campaigns on mangroves is often classified in this way; therefore it is a convenient arrangement to use a similar layer division in the numerical model. Depending on the species and how easily difference can be made between the roots, trunk and canopy characteristics, two or three layer schematisations are used, as shown in Figure 4-9.

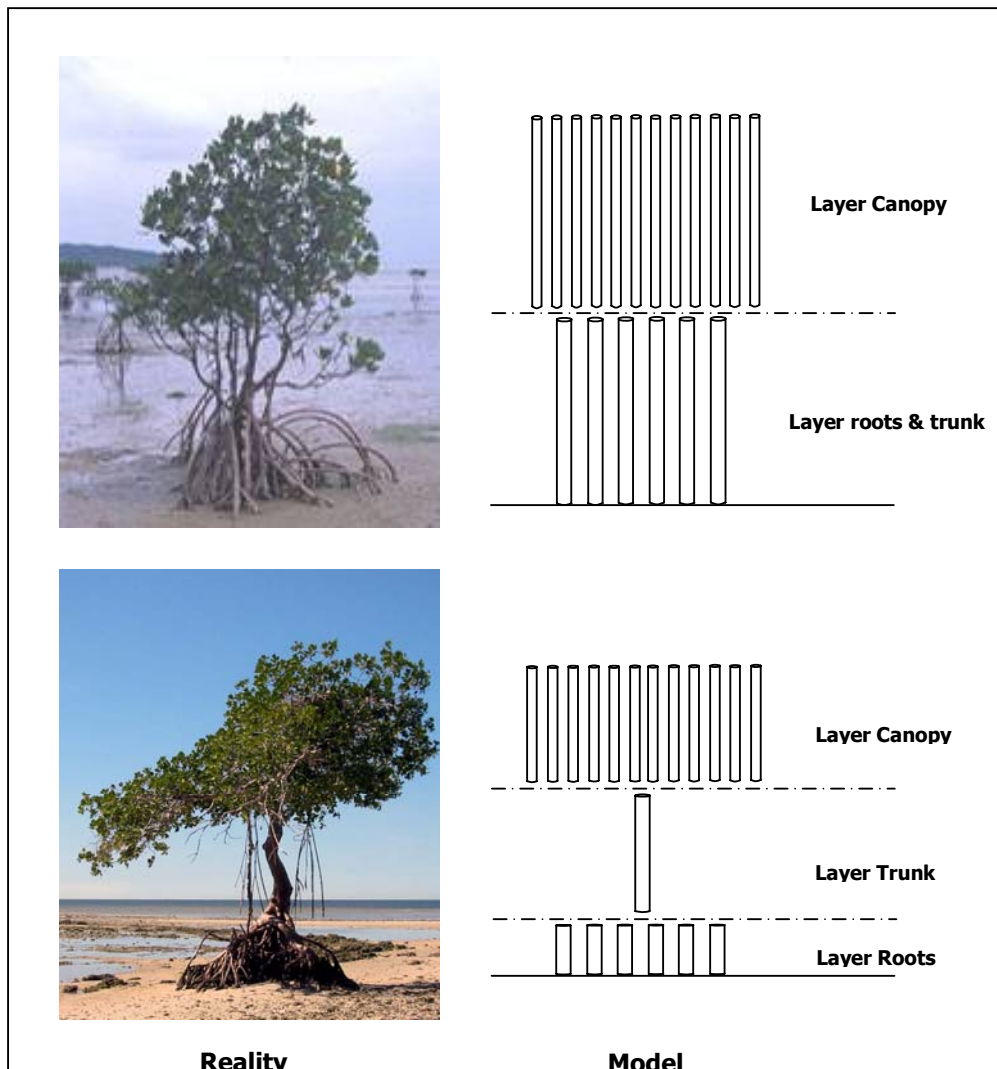


Figure 4-9 Visualisation of schematisation mangroves in model

### 4.5.3 Vegetation Parameters

In this section the behaviour of the model is tested by varying the vegetation parameters is described. First the non-importance of the layer order is shown, next the density and diameter sensitivities on the wave attenuation are shown. Last the increasing effect on wave attenuation by increasing the drag coefficient is presented.

#### Layer order

Because SWAN is a depth averaged model, vertical varying vegetation input is translated into a depth averaged contribution to the energy dissipation. When different configurations with same layers of vegetation are considered, these different configurations contribute to the same attenuation results. To illustrate this, two cases in with three layers of vegetation are modelled. One case comprising two layers with low density and one with high density and a reference case with only layers of low vegetation densities. Three different configurations of the first case are possible, shown in Figure 4-10, which should result in same wave attenuation. For this analysis the model layout configuration (shown in appendix D *Layout SWAN model*) is used. The hydraulic conditions are the same for both cases and there not elaborated here. Figure 4-11 is shows that layer order is not relevant in the model.

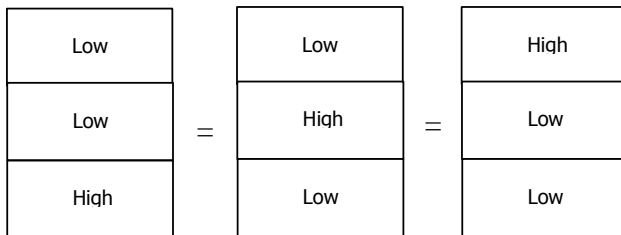


Figure 4-10 Possible configurations of one layer with high density

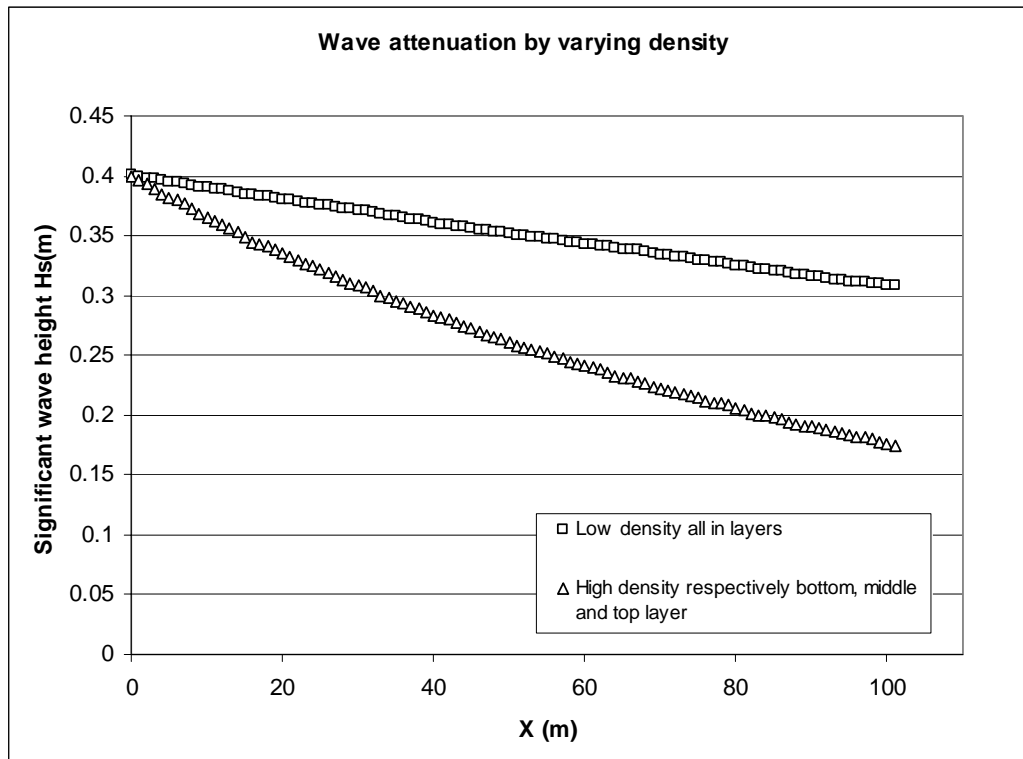


Figure 4-11 Wave attenuation by varying density

### Mangrove density and diameter

The density and diameter is of significant influence on the wave attenuation, because for a large part the drag coefficient is determined by these parameters. However in this part of the sensitivity analysis the drag coefficient has been considered constant and only the density and diameter have been varied. For this a three layer system is applied in which layer 3 the density and diameter have been varied according to Table 4-1. For vegetation characteristics besides the density and diameter and hydraulic parameters used in this case, see Table 4-2 and Table 4-3.

Table 4-1 Vaying density and diameter

|              | Density( $-/m^2$ ) |        |       |       |       |        |        |        |
|--------------|--------------------|--------|-------|-------|-------|--------|--------|--------|
| Diameter (m) | Surface ( $m^2$ )  | 1      | 10    | 25    | 100   | 500    | 2000   | 10000  |
|              | 0.001              |        |       |       |       | 0.0004 | 0.0016 | 0.0079 |
|              | 0.05               |        |       | 0.049 | 0.196 | 0.982  |        |        |
|              | 0.1                | 0.0079 | 0.079 | 0.196 | 0.785 |        |        |        |

Table 4-2 Vegetation parameters

| Vegetation parameters | Layer 1 | Layer 2 | Layer 3      |
|-----------------------|---------|---------|--------------|
| Density ( $-/m^2$ )   | 1       | 1       | See table xx |
| Diameter (m)          | 0.1     | 0.1     | See table xx |
| Drag coefficient (m)  | 0.25    | 0.25    | 0.25         |
| Vegetation height (m) | 0.4     | 0.4     | 0.4          |

Table 4-3 Hydraulic conditions

| Hydraulic conditions              |     |
|-----------------------------------|-----|
| Water level (m)                   | 2.0 |
| Bed slope                         | -   |
| Significant wave height $H_s$ (m) | 0.4 |
| Peak period $T_p$ (s)             | 6   |

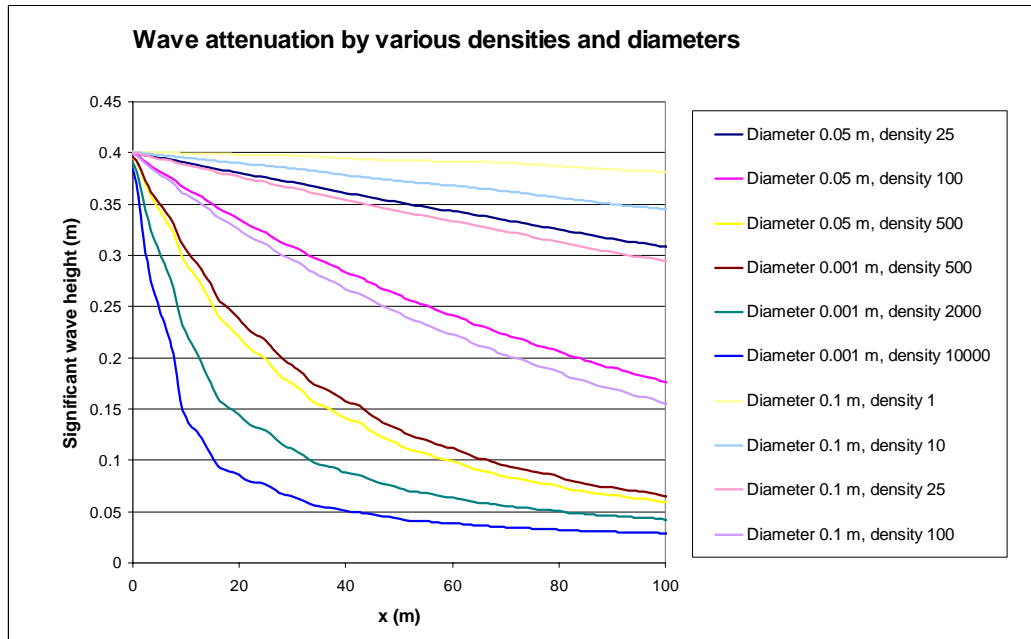


Figure 4-12 The influence of the diameter and the density wave attenuation

Figure 4-12 shows, that high densities result in larger attenuation. It may seem that the influence of the density is dominant over that of the diameter; however the range of the diameter is smaller than that of the density. In different cases where the diameter multiplied with the density is of the same order e.g. (dia 0.05 m, den 100  $-/m^2$  and dia 0.1 m, den 100  $-/m^2$ ), the attenuation is found to be in the same order as well. This is because in the energy dissipation formulation the vegetation parameters are multiplied with each other see equation(0.28).

### Drag coefficient

The drag coefficient is besides the most important parameter, also the most difficult-to-determine parameter of the wave-vegetation interaction system. As mentioned in section 3.3, different physical processes related to the vegetation parameters and wave parameters play an important role for the determination of the drag coefficient. However when using the model to simulate wave attenuation in certain case, the drag coefficient just needs to be calibrated, with keeping the previous in mind.

Here, a hypothetical layered mangrove vegetation is used in which only the drag coefficient is varied, with all other parameters constant. What is to be expected is that by an increasing drag coefficient the wave attenuation will increase. This is shown in Figure 4-13, these results however are only indicative for this type of wave conditions and vegetation parameters (Table 4-4 and Table 4-5).

Table 4-4 Vegetation parameters

| <b>Vegetation parameters</b> | Layer 1         | Layer 2     | Layer 3     |
|------------------------------|-----------------|-------------|-------------|
| Density (-/m <sup>2</sup> )  | 25              | 1           | 1           |
| Diameter (m)                 | 0.05            | 0.1         | 0.1         |
| Drag coefficient (m)         | See Figure 4-13 | Figure 4-13 | Figure 4-13 |
| Vegetation height (m)        | 0.4             | 0.4         | 0.4         |

Table 4-5 Hydraulic conditions

| <b>Hydraulic conditions</b>       |            |
|-----------------------------------|------------|
| Water level (m)                   | 1.5        |
| Bed slope (-)                     | horizontal |
| Significant wave height $H_s$ (m) | 0.4        |
| Peak period $T_p$ (s)             | 6          |

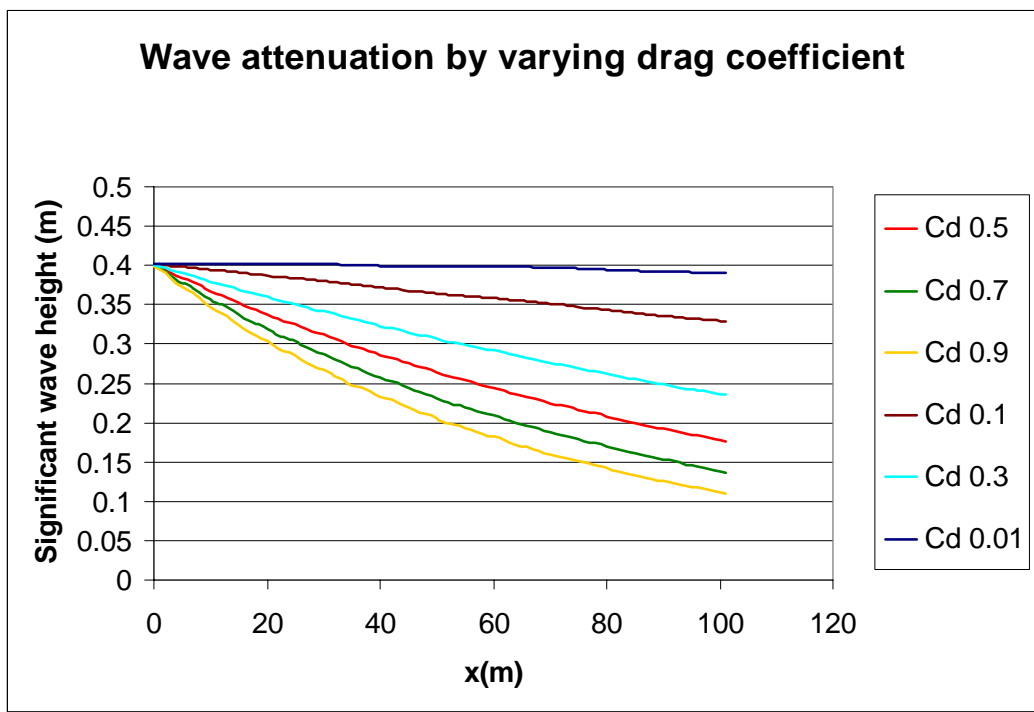


Figure 4-13 Wave attenuation by varying drag coefficient

#### 4.5.4 Hydraulic conditions

Not only vegetation parameters influence the wave attenuation also the hydraulic conditions have their effect. The influence of the wave conditions and water level on the rate of wave attenuation will be discussed in this section.

##### Water level

To analyse the sensitivity of water level on the wave attenuation, two cases A and B are schematised one with homogenous and one with vertical varying vegetation.

##### Case A

The expected influence of the water level on the attenuation is, that with increasing water level the relative effect of the vegetation on the wave attenuation will decrease. With vegetation parameters and hydraulic conditions used according to Table 3-1 and Table 4-7, this effect is shown in Figure 4-14, where the wave reduction  $r$  is defined as:

$$r = \frac{H_{in} - H_{out}}{H_{in}} \quad (0.35)$$

where  $H_{in}$  is the incoming wave height and  $H_{out}$  the transmitted wave height.

What needs notice is the linear section of the curve from a water level of 1.5 m and decreasing. This corresponds to the previous discussed phenomenon in section 4.3.3, the linear relation between energy dissipation and the vegetation height in the vegetation.

Table 4-6 Case A Vegetation parameters

| Vegetation parameters       | Layer 1 | Layer 2 | Layer 3 |
|-----------------------------|---------|---------|---------|
| Density (-/m <sup>2</sup> ) | 25      | 25      | 25      |
| Diameter (m)                | 0.05    | 0.05    | 0.05    |
| Drag coefficient (m)        | 0.2     | 0.2     | 0.2     |
| Vegetation height (m)       | 0.5     | 0.5     | 0.5     |

Table 4-7 Case A Hydraulic conditions

| Hydraulic conditions              |                          |
|-----------------------------------|--------------------------|
| Water level (m)                   | according to Figure 4-14 |
| Bed slope (-)                     | horizontal               |
| Significant wave height $H_s$ (m) | 0.4                      |
| Peak period $T_p$ (s)             | 6                        |

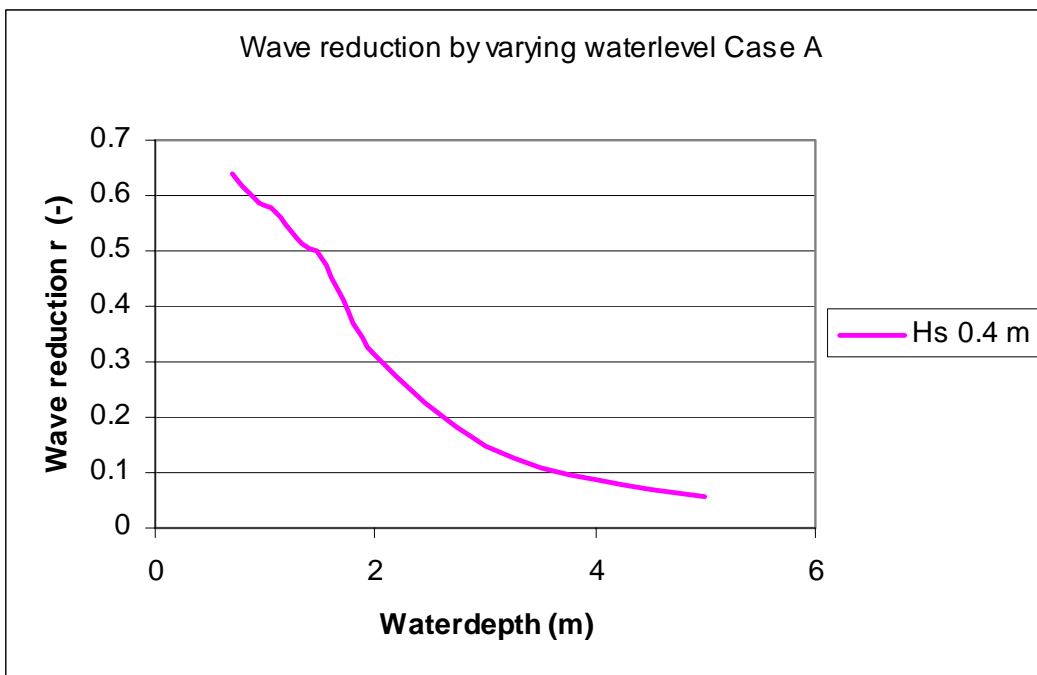


Figure 4-14 Wave reduction by varying water level Case A



**Case B**

For this case a non homogeneous vertical distribution is applied. This vegetation schematisation, shown in Table 4-8 is mangrove tree like, layer 3 representing a high density canopy, layer 2 the trunk section and layer 1 the root system. Varying the water level in the vegetation with this layer configuration, will give rise to a non-evenly attenuation. E.g. layer 3 will induce more friction than layer 1. The result of this can be found in Figure 4-15. When applying a non homogenous layered vegetation system (mangroves), it is illustrated that the contribution of dense layers to wave attenuation are larger. Once the water level drops below the canopy less attenuation can be expected.

Table 4-8 Case B Vegetation parameters

| <b>Vegetation parameters</b> | Layer 1 | Layer 2 | Layer 3 |
|------------------------------|---------|---------|---------|
| Density (-/m <sup>2</sup> )  | 75      | 1       | 1000    |
| Diameter (m)                 | 0.03    | 0.1     | 0.003   |
| Drag coefficient (m)         | 0.1     | 0.1     | 0.1     |
| Vegetation height (m)        | 1.0     | 1.0     | 1.0     |

Table 4-9 Case B Hydraulic conditions

| <b>Hydraulic conditions</b>                |                 |
|--|-----------------|
| Water level (m)                            | See Figure 4-15 |
| Bed slope (-)                              | horizontal      |
| Significant wave height H <sub>s</sub> (m) | 0.4             |
| Peak period T <sub>p</sub> (s)             | 6               |

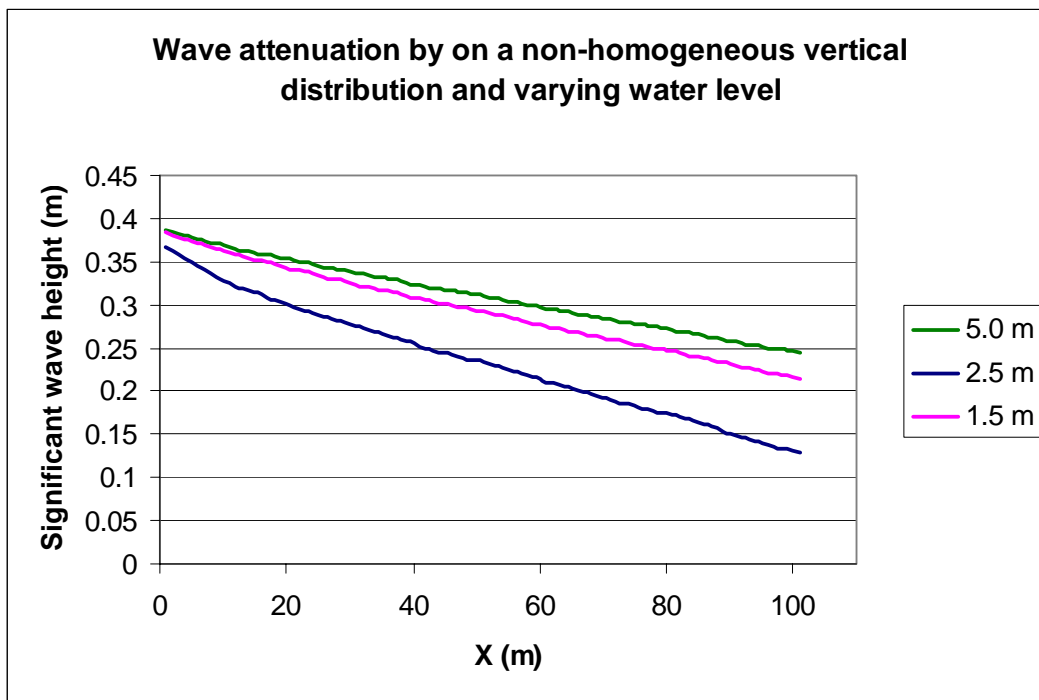


Figure 4-15 Wave attenuation by non homogeneous vertical vegetation and varying water level

## Wave height

Larger significant wave heights will be relatively more attenuated than smaller waves by the by considering the same hydraulic conditions and vegetation parameters. The influence depth on the vegetation is larger with large waves causing this phenomenon, demonstrated in Figure 4-16. This case has been executed with the vegetation parameters and hydraulic conditions found in Table 4-10 and Table 4-11.

Table 4-10 Vegetation parameters

| Vegetation parameters       | Layer 1 | Layer 2 | Layer 3 |
|-----------------------------|---------|---------|---------|
| Density (-/m <sup>2</sup> ) | 25      | 1       | 1       |
| Diameter (m)                | 0.05    | 0.1     | 0.1     |
| Drag coefficient (m)        | 0.2     | 0.2     | 0.2     |
| Vegetation height (m)       | 0.5     | 0.5     | 0.5     |

Table 4-11 Hydraulic conditions

| Hydraulic conditions              |                 |
|-----------------------------------|-----------------|
| Water level (m)                   | 1.5             |
| Bed slope (-)                     | horizontal      |
| Significant wave height $H_s$ (m) | See Figure 4-16 |
| Peak period $T_p$ (s)             | 6               |

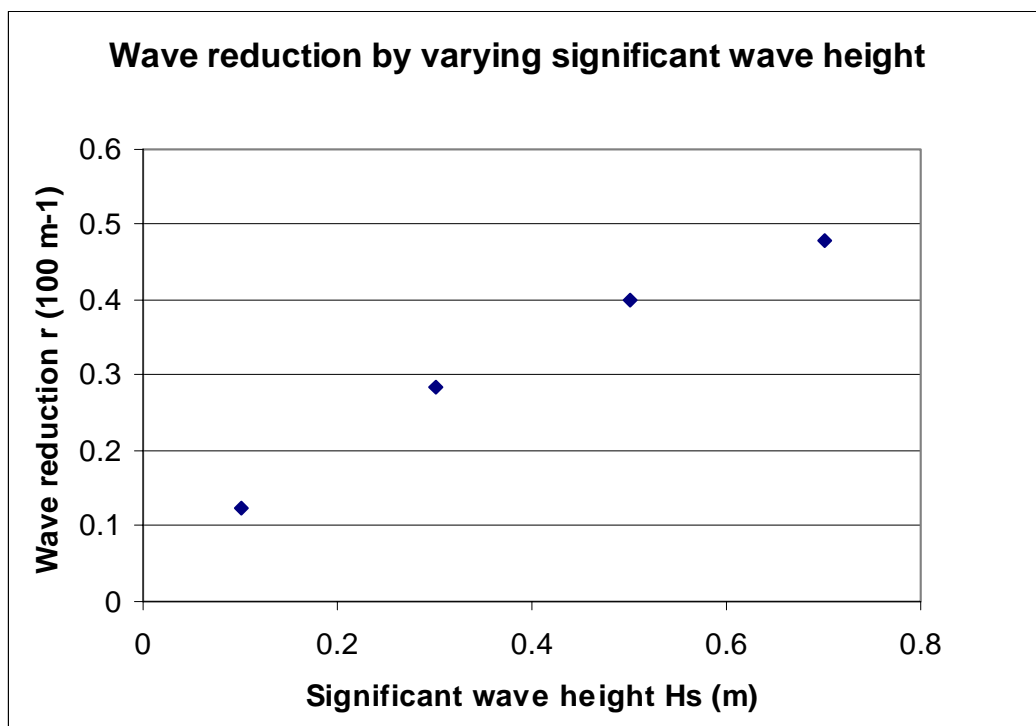


Figure 4-16 Wave reduction by varying significant wave height

### Wave frequency

When a wave spectrum is considered, various waves of different frequencies are dissipated in different manners. From Figure 4-17 it can be seen that a spectrum with a large peak period and a low frequency range (lower peak frequency) dissipates more energy than a spectrum with a range of higher frequencies. In figure x the amount of dissipated energy per frequency is shown for three cases A, B and C:

Table 4-12 Spectral properties Cases A, B and C

|        | Peak period (s) | Spectral boundaries (Hz) |
|--------|-----------------|--------------------------|
| Case A | 6.25            | 0.1 - 0.4                |
| Case B | 2.5             | 0.3 - 0.6                |
| Case C | 2.85            | 0.2 - 0.5                |

The vegetation parameters and hydraulic conditions are shown below in Table 4-13 and Table 4-7.

Table 4-13 Vegetation parameters

| <b>Vegetation parameters</b> | Homogeneous |
|------------------------------|-------------|
| Density (-/m <sup>2</sup> )  | 1000        |
| Diameter (m)                 | 0.004       |
| Drag coefficient (m)         | 1.0         |
| Vegetation height (m)        | 0.25        |

Table 4-14 Hydraulic conditions

| <b>Hydraulic conditions</b>                |                |
|--|----------------|
| Water level (m)                            | 1.0            |
| Bed slope (-)                              | horizontal     |
| Significant wave height H <sub>s</sub> (m) | 0.05 - 0.2     |
| Peak period T <sub>p</sub> (s)             | See Table 4-12 |

As the total amount of energy present in the spectrum is equal to the surface area under the spectral curve it appears that more energy is dissipated for a spectrum with larger peak periods.

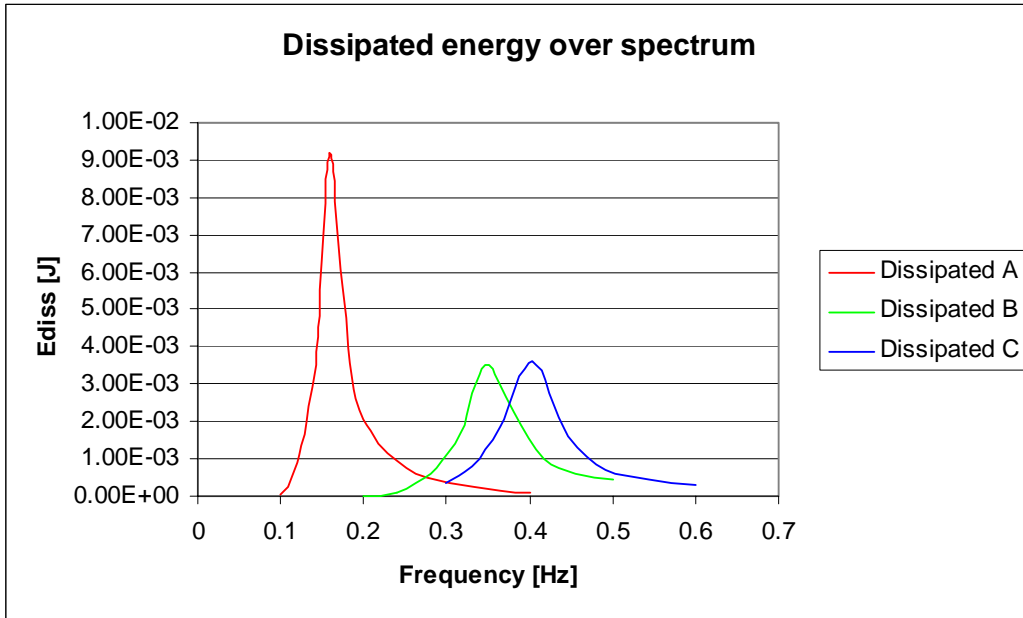


Figure 4-17 Figure x the difference between the incoming spectral energy and the spectral energy behind the vegetation

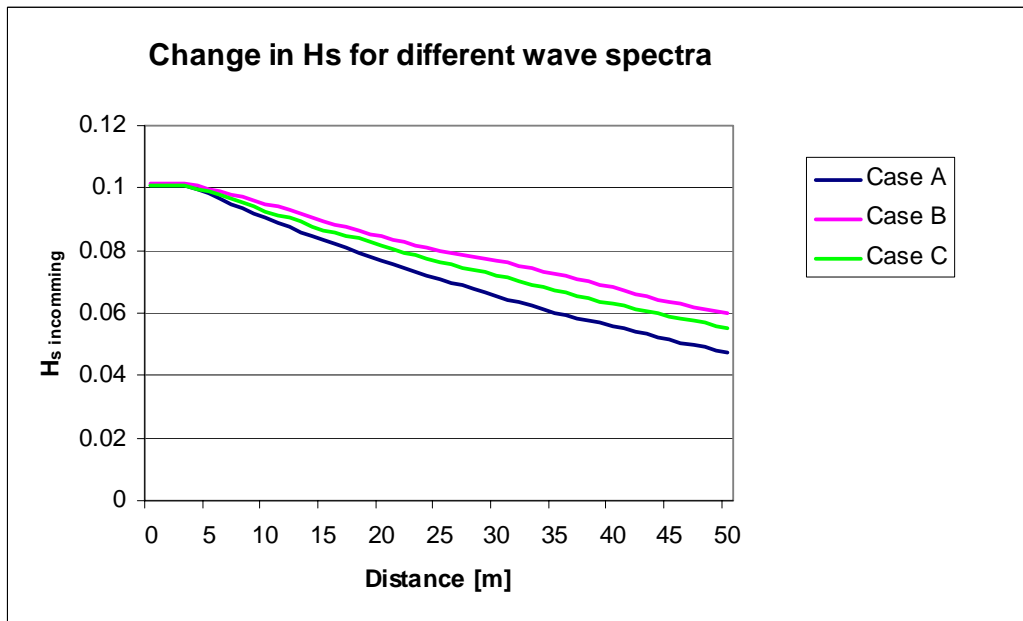


Figure 4-18 Change in  $H_s$  for different wave spectra

From Figure 4-18 can be concluded that wave spectrum A with low peak frequency and a low frequency range contains more energy. Because wave energy is proportional to  $H_s^2$ , in this frequency range the highest waves are present, which will be attenuated more by the vegetation.

As was mentioned in section 3.3, on a scale of one single stem, a wave with a small wave period will cause more energy decrease than a long wave. This is among others dependent on the ration between the obstacle size and the wave length. On a larger scale, as considered in case of a vegetation field, waves with large peak periods contain more energy and have larger wave heights than other waves in the spectrum. Because wave energy is proportional to  $H_s^2$ , around the peak frequency the highest waves are present, which will be attenuated most by the vegetation, leading to the highest decrease in energy density.

What needs to be noted is that in case the factor  $kl \ll 1$  ( $k$ = wave number,  $l$ =length of vegetation field) the scattering of the waves by the field is negligible and the diffraction of the waves around the obstacle is almost 100%, meaning the waves are unaffected. For instance, a wave with length of 2000m in a vegetation field of 50 meters in length will result in a value for  $kl$  of 0.15 and is practically unaffected by the vegetation.

### Horizontal orbital wave motion

The reduction of orbital velocities due to the presence of mangrove vegetation will be shown with two cases. Case A with a sparse root system and Case B with a denser root system, translated by varying layer 1, shown in Table 4-15 and Table 4-16.

Table 4-15 Vegetation parameters Case A

| <b>Vegetation parameters</b> | Layer 1 | Layer 2 | Layer 3 |
|------------------------------|---------|---------|---------|
| Density (-/m <sup>2</sup> )  | 1       | 1       | 1       |
| Diameter (m)                 | 0.05    | 0.1     | 0.1     |
| Drag coefficient (m)         | 0.5     | 1.0     | 1.0     |
| Vegetation height (m)        | 0.5     | 0.5     | 0.5     |

Table 4-16 Case B Vegetation parameters

| <b>Vegetation parameters</b> | Layer 1 | Layer 2 | Layer 3 |
|------------------------------|---------|---------|---------|
| Density (-/m <sup>2</sup> )  | 25      | 1       | 1       |
| Diameter (m)                 | 0.05    | 0.1     | 0.1     |
| Drag coefficient (m)         | 0.5     | 1.0     | 1.0     |
| Vegetation height (m)        | 0.5     | 0.5     | 0.5     |

Table 4-17 Hydraulic conditions Case A and B

| <b>Hydraulic conditions</b>                |             |
|--|-------------|
| Water level (m)                            | 1.5         |
| Bed slope (-)                              | horizontal  |
| Significant wave height H <sub>s</sub> (m) | Figure 4-19 |
| Peak period T <sub>p</sub> (s)             | 6           |

As expected case B influences the orbital velocity more due to more friction of a denser root system. What also must be noted is the larger decrease of the maxima of the horizontal orbital velocity of larger waves after passing the vegetation. This is due to the larger influence depth on the vegetation of larger waves as was mentioned in the part of the sensitivity analysis on the wave height, but could also be a result of wave breaking.

Although this thesis does not focus on morphology, the rate of wave attenuation and with that the reduction of horizontal orbital velocities due to vegetation is of significant importance in morphology in and around mangrove vegetation. In spite of the fact SWAN being depth averaged, the model is able to calculate maximum values of the near bottom horizontal orbital velocity, which is of use to study morphology cases in mangrove forests or vegetation fields in general. Important to assess is the magnitude of these velocities and to what extent they represent the reality. Mentioned in 4.3.3, Figure 4-3 the horizontal orbital velocity profile in SWAN is uniform. Because a uniform profile is not representative for a real time situation with vegetation it is therefore likely that the near bottom values for the velocities are overestimated by SWAN.

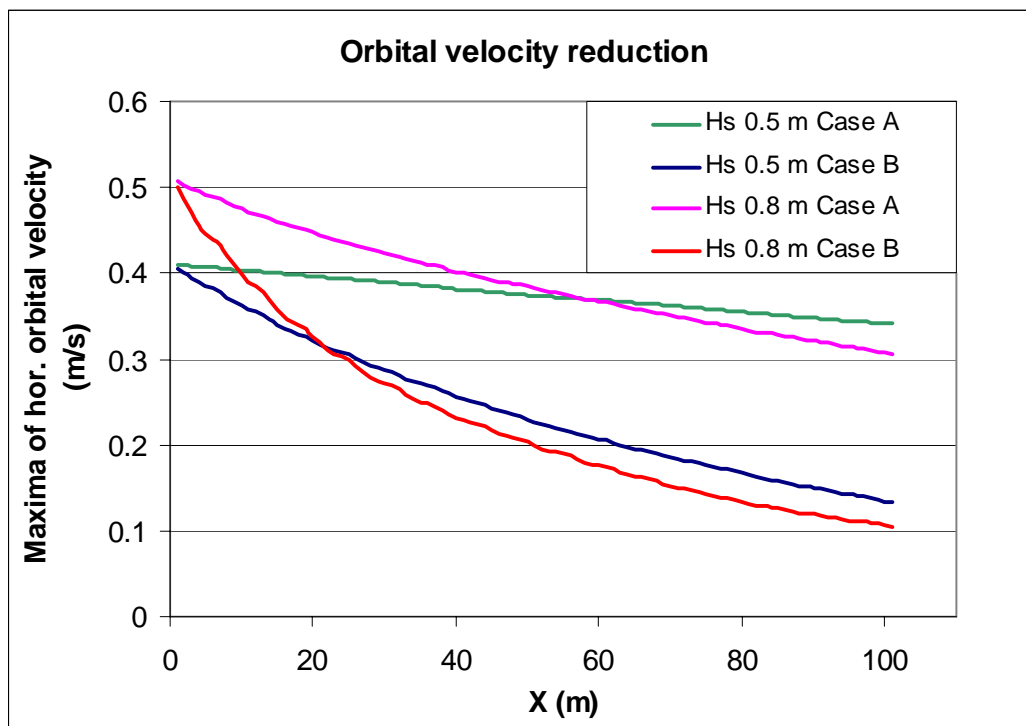


Figure 4-19 Orbital velocity reduction

### Wave breaking on vegetation

As mentioned in the introduction of this sensitivity analysis, wave breaking on the vegetation as shallower bottom effect could be the case. In this section this phenomenon is tested. Again two cases are tested, Case A with wave breaking turned on in the model, and case B where the wave breaking is turned off. These test were done for different densities and diameters and the results where in a cases the same for case A and B. From this it can be concluded that this process is not accounted for in the adapted SWAN model.



## 4.5.5 Conclusions on the sensitivity analysis

Conclusions that can be drawn from the sensitivity analysis are described here.

### Vegetation characteristics

- The layer order of a layered vegetation system is not important.
- With increasing density and diameter, the attenuation will increase as expected.
- With increasing drag coefficient, the attenuation will increase as expected.

### Hydraulic conditions

#### Water level

- The relative influence of the vegetation with increasing water depth becomes less, and therefore the attenuation as well. The wave attenuation in the vegetation (emerged) related to the vegetation height is linear as was expected from paragraph 4.3.3.
- When applying a non homogenous layered vegetation system (mangroves), it is illustrated that the contribution of dense layers to wave attenuation are larger. E.g. once the water level drops below the canopy less attenuation can be expected.

#### Wave height

- Larger waves will be more attenuated than smaller ones, because of the larger influence depth.

#### Wave period

- As the total amount of energy present in the spectrum is equal to the surface area under the spectral curve it appears that more energy is dissipated for a spectrum with larger peak periods.

#### Orbital velocity

- The horizontal orbital velocity decreases with the attenuation of the waves. Because SWAN is a depth averaged model, the results of these near orbital velocities (in the vegetation model) are overestimated by SWAN.

### Bottom friction and wave breaking

- The bottom friction in general, but also in a spectral wave model as SWAN has a significant effect when very mild slopes, shallow water conditions and long distances for the waves (in the order of kilometers) to travel over, are present. Here however because of the small length of the grid no energy was lost due to the bottom friction and therefore did not influence the wave attenuation.
- Wave breaking induced by the vegetation is not present in the model.

#### 4.6 Wave setup induced currents by 'Patchy' vegetation

Gradients in radiation stress that are a result of non-uniformities in the wave motion can induce both a rise in water level and currents in the water wherein the wave motion takes place. Without external forces (viscous damping, bottom shear stress), the sum of the radiation stress and the hydrostatic pressure force is constant as the waves go from deep to shallow water. When waves approach in shallow water, wave radiation stresses decrease due to energy dissipation induced by bottom friction and breaking. This decrease in radiation stress needs to be compensated by an increase in hydrostatic pressure force (conservation of momentum), resulting in a rise in water level towards the shoreline, shown in Figure 4-20.

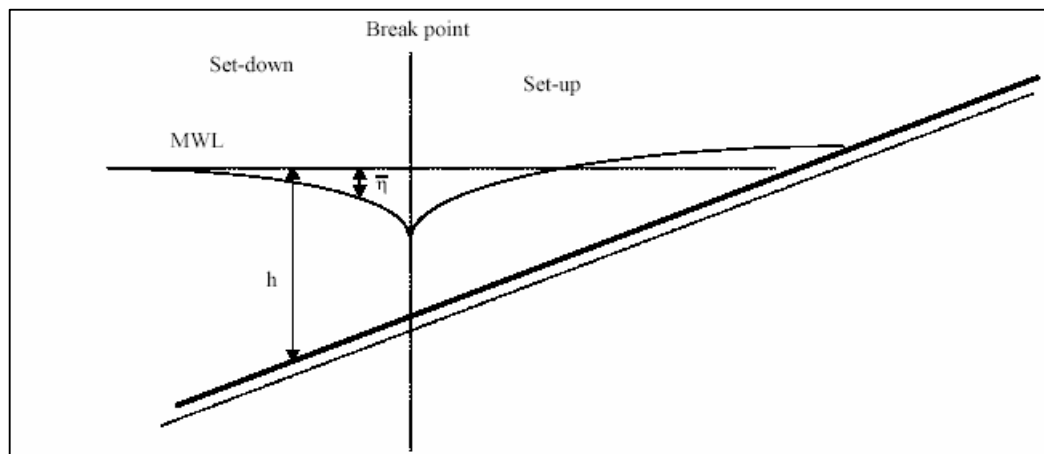


Figure 4-20 Schematisation of wave set down and setup

In the area before the breaker zone wave energy dissipation can be neglected, therefore conservation of wave energy can be considered. When waves approach the breaker zone, on a sloping bottom, wave celerity decreases due to a decrease in water depth. Conservation of energy implies that a decrease in wave celerity causes an increase in wave radiation stress. Analogue to the situation described behind the breaker zone, an increase in radiation stress needs to be compensated by a decrease in pressure gradients (conservation of momentum), resulting in a decrease in water level (set down). What has to be mentioned here is, that the SWAN model uses the linear wave theory to calculate the wave setup effect. However according to Dean and Bender (2005) nonlinear transfer of energy and momentum can also contribute to wave setup, but is not accounted for in the SWAN model.

When vegetation is present, extra energy dissipation due to wave-vegetation interaction causes larger gradients in radiation stress, resulting in wave setup. In patchy vegetation this can lead to a difference in setup between vegetated and non vegetated areas. These setup differences can result in secondary flows.

To visualise this, two cases have been modelled where a part of the grid is vegetated and another part is non-vegetated, see figure x. For both a grid of 125 by 500 meters, with homogenous vegetation with a density of 1000  $-/m^2$ , vegetation diameter of 0.004 m, drag coefficient of 0.5 and a vegetation height of 1.5 m was used. The hydraulic conditions: a constant water level of 2.0 m and a wave spectrum with a  $H_s$  of 0.5m and a  $T_p$  of 6 s.

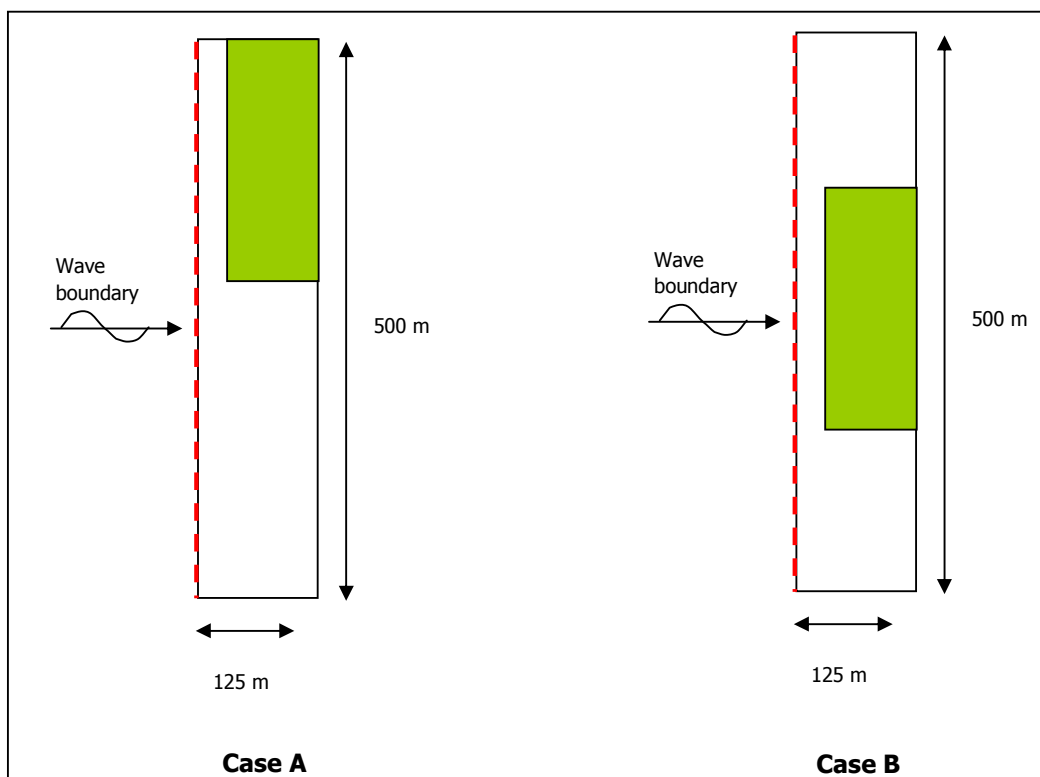


Figure 4-21 Model layout for wave setup cases

Case B will be studied in this section, for more results on case A see appendix E *Wave setup*. As can be seen in Figure 4-22 the wave attenuation in the vegetation causes wave setup in the vegetation and a small a set down in front of the vegetation. Also outside the vegetation wave setup is present, though smaller. As mentioned before currents can originate due to the setup differences. In this case a current out of the vegetation is expected, shown in Figure 4-23. Although beyond the scope of this study, the impacts of these wave setup induced currents are thought to be significantly. Several dynamic processes as progression or degradation of vegetation or sedimentation accumulation can be explained with this phenomenon.

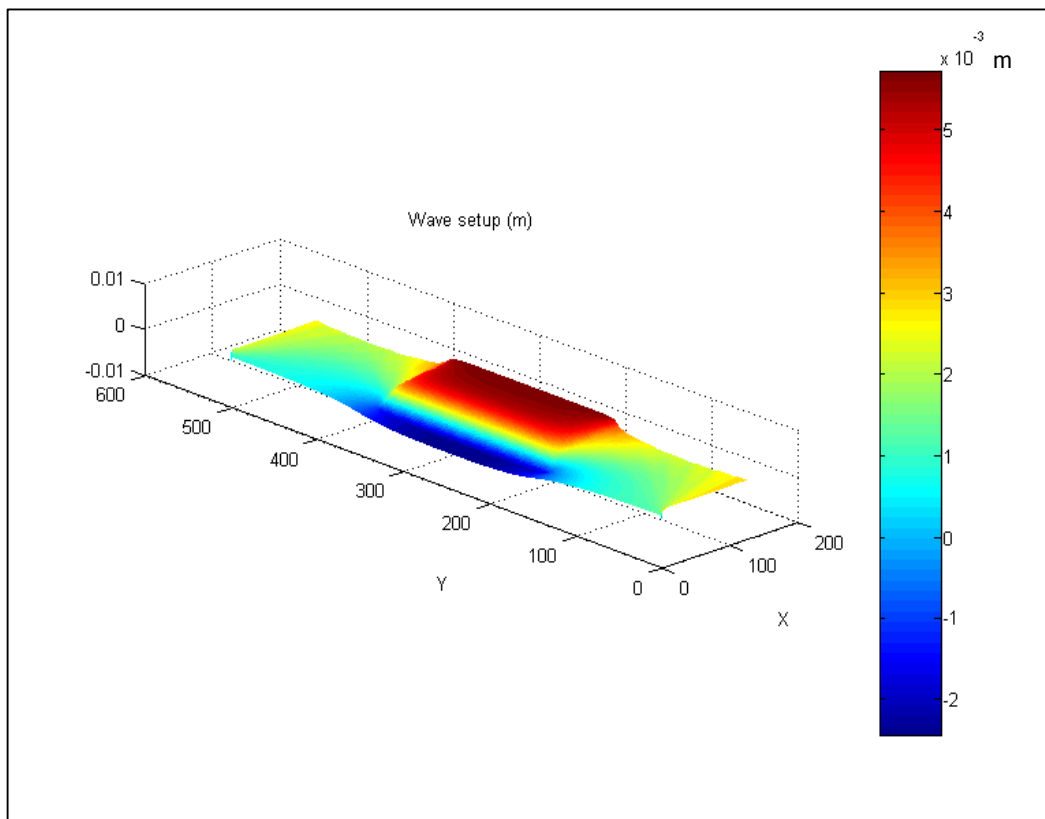


Figure 4-22 3 D view wave setup in case B

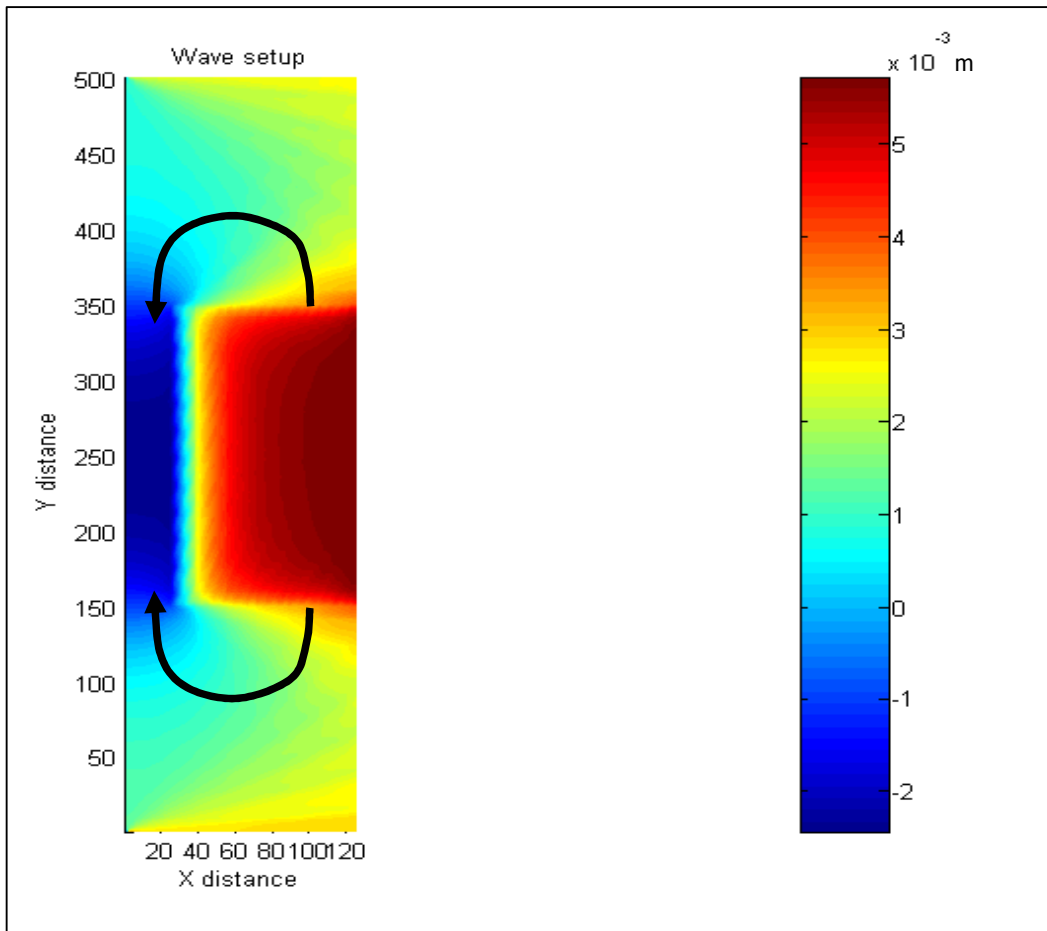


Figure 4-23 Top view wave setup with possible flow pattern Case B

-

## 5 Test cases

In this section the adapted SWAN model is tested for two cases in which wave attenuation is measured in situ. These measurement cases are on wave attenuation in mangrove forest, which both have happened to take place in Vietnam. General, measurement data on vegetation characteristics combined with data on wave attenuation in situ, is very valuable and scarce. The data of the wave attenuation in mangroves is taken from articles, whereas after communication with authors the raw data was not available for this study.

From section 3.3 it has become clear that with varying vegetation characteristics e.g. relative spacing, different values for the drag coefficient are to be use in modelling. For schematising vertical layered vegetation this would imply, applying for each layer a different drag coefficient. Because at this moment such detailed background on the drag coefficient is not available and calibration in this way would be very difficult, here the same drag coefficient is applied for each layer.

As mentioned in the preface of this report Martijn Mijer working parallel to this study on wave attenuation by salt marsh vegetation tested and calibrated the adapted SWAN model for salt marsh vegetation. Which showed the adapted SWAN model is able to simulate other types of vegetation. For this test case, there is referred to thesis report of 'Wave attenuation over salt marsh vegetation'.

## 5.1 Thuy Hai

In this campaign by Madza et al. (1997) the wave reduction was investigated in a mangrove reforestation area, close to aquaculture ponds in the Tong King delta, Vietnam. In front of the coast of Thuy Hai and Thuy Trong, tidal flats with slopes of 1/2000 stretch out approximately 8 km offshore. On these tidal flats a strip of 1.5 km wide (in offshore direction) and 3 km long (along shore), was planted with *Kandelia Candel* mangrove shoots, in three phases. At the time of the measurement campaign the three zones A, B and C, were respectively 1/2, 2-3 and 5-6 years old. See Figure 5-1.

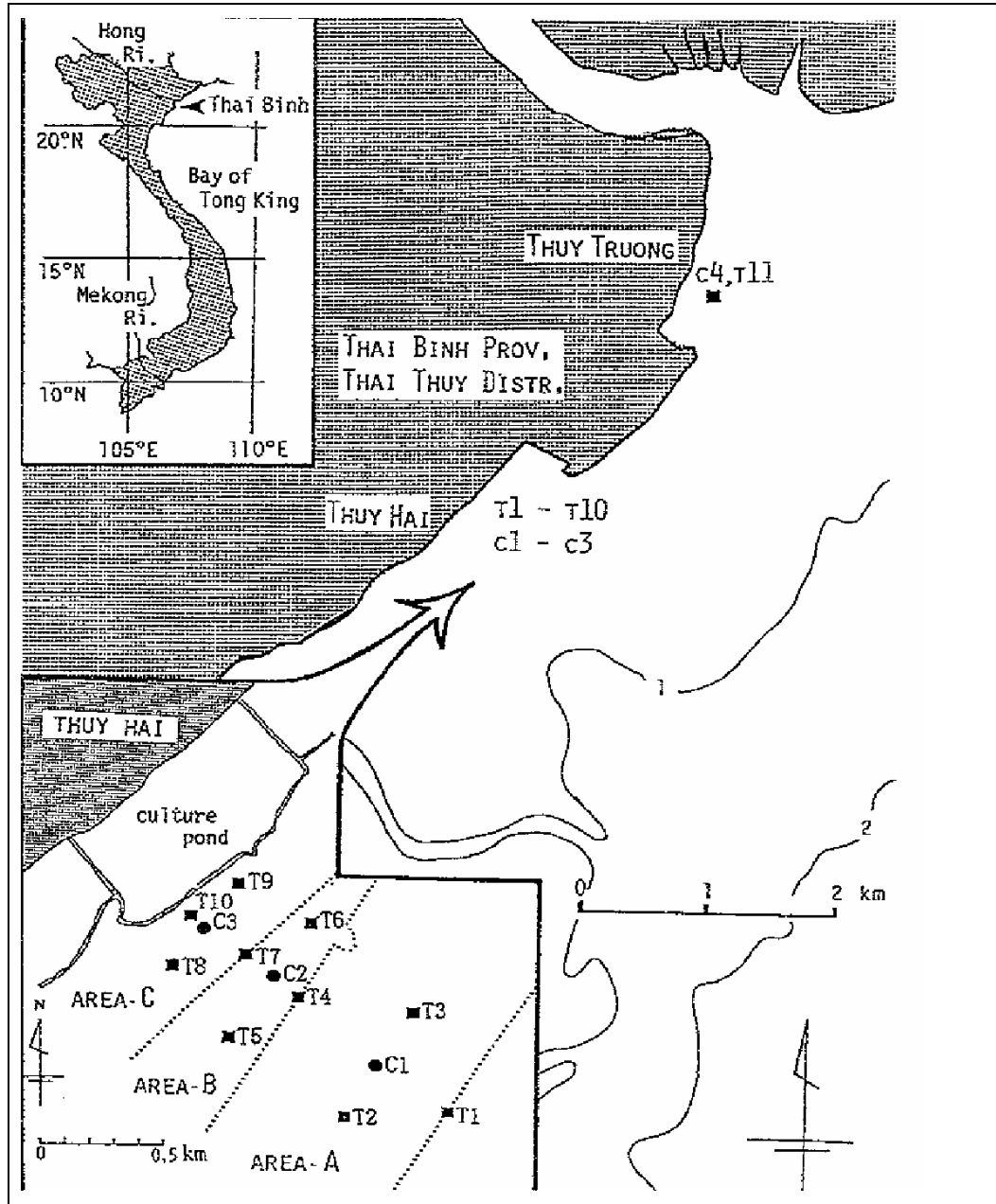


Figure 5-1 Thuy Hai reforestation area, Vietnam



### 5.1.1 Mangrove vegetation

*Kandelia candel* usually appears in pure forests and have several prop roots see . They are famous for their viviparous method of reproduction, which involves germinating the seeds directly on the tree and then waiting until the time is right to either drop the seeds into the mud below or float them on waves until they find a suitable environment for survival. *Kandelia Candel* are good at preventing erosion and thus are useful for protecting coastlines. Consequently, they are often used to help reclaim land from the oceans. The *Kandelia Candel* that was planted in the reforestation area consists of three groups A, B and C of which the characteristic dimensions are presented in Figure 5-1.

Table 5-1 Average mangrove dimensions Thuy Hai area

| Dim (m) | Area A | Area B | Area C |
|---------|--------|--------|--------|
| A       | 0.03   | 0.10   | 0.15   |
| B       | 0.0    | 0.10   | 0.13   |
| C       | 0.02   | 0.05   | 0.08   |
| D       | 0.03   | 0.05   | 0.06   |
| E       | 0.40   | 0.30   | 0.30   |
| F       | 0.30   | 0.50   | 0.75   |
| G       | 0.10   | 0.45   | 0.75   |
| H       | 1.0    | 1.0    | 1.0    |

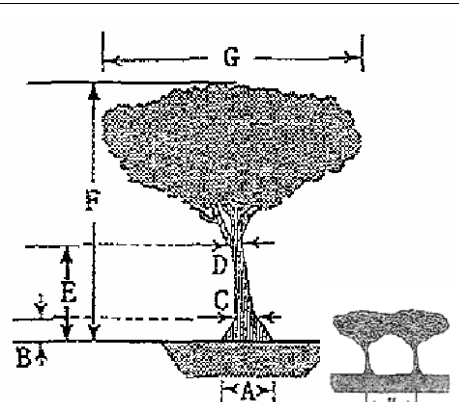
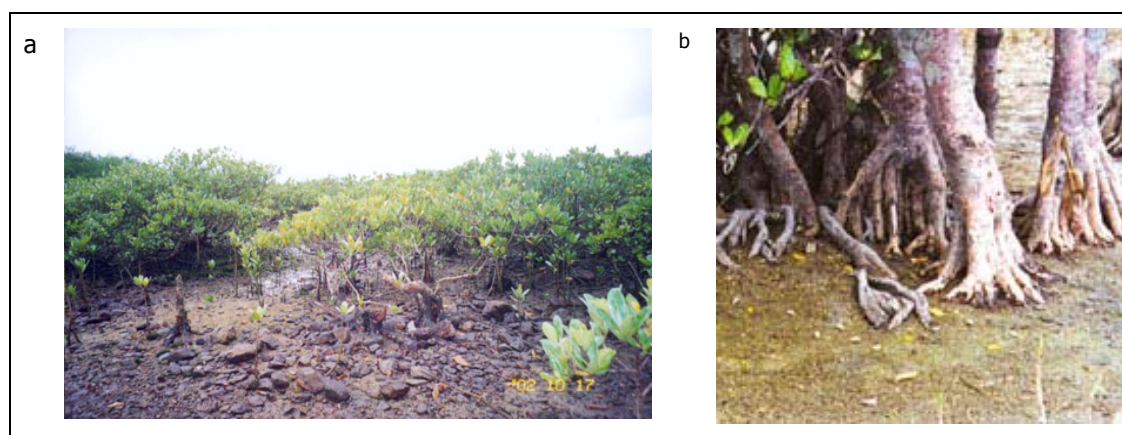



Figure 5-2 Candelia Kandel trees (a) and prop roots (b)

### 5.1.2 Wave conditions

Wave periods varied between 5 and 8 sec. As for the wave heights, in the article relative wave attenuation rates are published.

### 5.1.3 Results of wave reduction

On the site where the young mangrove trees grew (area A) the wave reduction due to the drag force on the trees was hardly effective. On the other sites (area B & C) where mangrove trees were sufficient tall, the rate of wave reduction per 100 m was as large as 20%, shown in Figure 5-3 (b). Along the whole transect vegetation characteristics were measured. Drag coefficients are specified dependent on the depth and per vegetation type. Due to the high density of the vegetation, distributed trough out the whole water depth, the effect of wave reduction was large and even when the depth increased. The effect of wave reduction does not decrease with increasing water depth. Note that the  $C_d$  values in presented in Figure 5-3 (a) cannot be compared with the drag coefficient used for the SWAN adaptation in this study, because Madza (1997) calculates the effect of the flow resistance due to mangrove vegetation as a bottom friction using Bretscheider and Reid (1954).

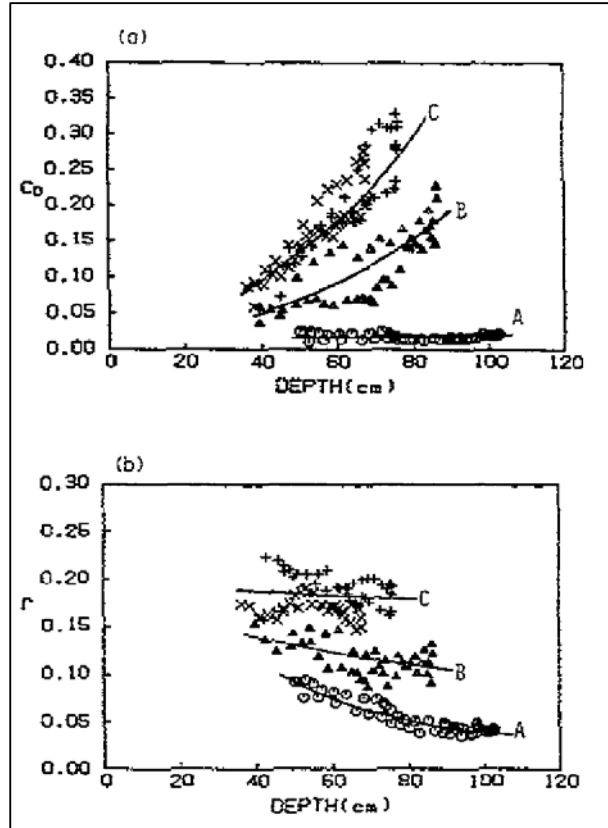


Figure 5-3 (a) Drag force - depth relation (b) Wave reduction - depth relation (from Mazda et 1997)

The reduction rate is defined as:

$$r = \frac{H_{in} - H_{out}}{H_{in}}$$

where  $H_{in}$  is the incoming wave height and  $H_{out}$  the transmitted wave height.

### 5.1.4 Modelling the results

For the modelling only area C is used, because in this area the vegetation is substantially grown, and significant wave attenuation was measured. According to the dimensions of the *Candelia Kandel* measured in area C the vegetation dimensions have been schematised into a three-layer system shown in Table 3-1 in the following manner. For the schematisation of the canopy only outer dimensions are measured, however to be able to include the canopy in the modelling a reasonable density and diameter is assumed.

Because the wave attenuation data is presented by a reduction factor per 100 meter, for the grid setup a transect of 125 m has been used. The first 25 meter of the grid is non-vegetated to exclude boundary disturbances (see appendix D *Layout SWAN model*).

The calibration of the model on this Thuy Hai case is an adjustment of the drag coefficient to match the wave reduction of 20 % of area C, see table XX with the vegetation parameters and hydraulic conditions. Note that layer 1 represents the near bottom layer of vegetation and increasing layer number corresponds with increasing vegetation height.

Table 5-2 Vegetation parameters used in the Calibration of area C

| <b>Vegetation parameters</b> | Layer 1    | Layer 2    | Layer 3    |
|------------------------------|------------|------------|------------|
| Density (-/m <sup>2</sup> )  | 1          | 1          | 100        |
| Diameter (m)                 | 0.15       | 0.07       | 0.003      |
| Drag coefficient (m)         | Calibrated | Calibrated | Calibrated |
| Vegetation height (m)        | 0.13       | 0.17       | 0.5        |

Table 5-3 Hydraulic conditions

| <b>Hydraulic conditions</b>                |                   |
|--|-------------------|
| Water level (m)                            | 0.2 0.5 0.7 0.9   |
| Bed slope (-)                              | 1:2000            |
| Significant wave height H <sub>s</sub> (m) | 0.08 0.15 0.3 0.4 |
| Peak period T <sub>p</sub> (s)             | 6.5               |

Specific wave data on the significant wave heights are not available, therefore various wave conditions and water levels, shown in Table 5-3 have been used.

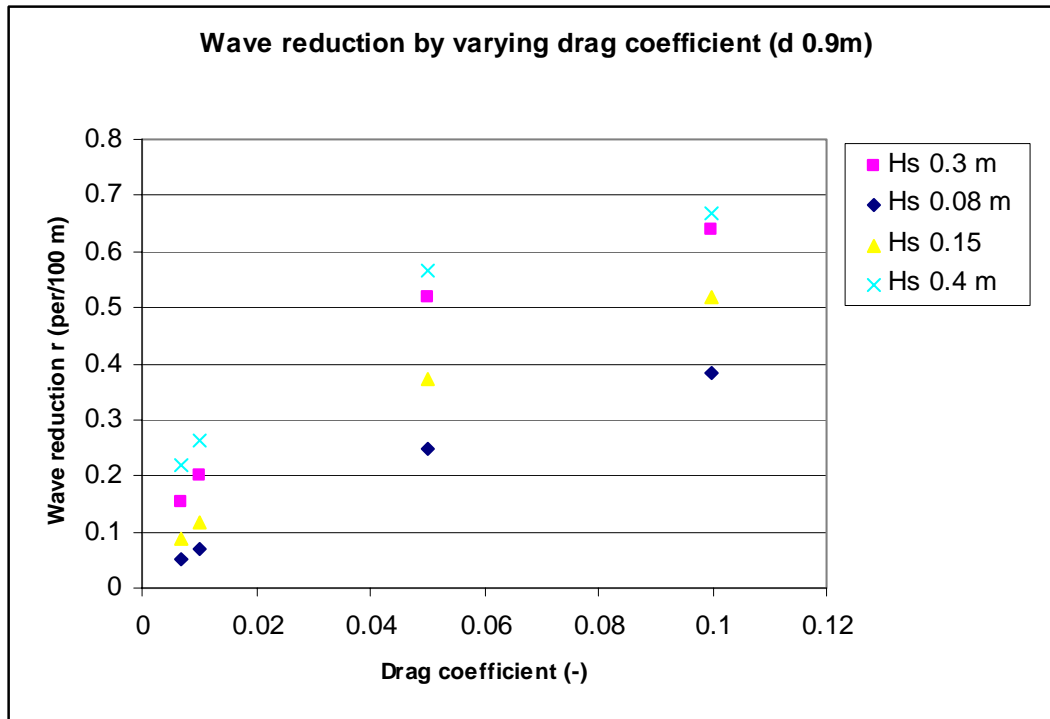


Figure 5-4 Calibration results of Thuy Hai case

As was mentioned in section 3.3, the drag force is dependent of wave parameters as well as vegetation parameters. The calibration here was done with constant vegetation parameters, as mentioned before. However as for the wave parameters and the water level different values are used. Seen from Figure 5-4, it becomes clear that to obtain a reduction rate of 20 %, for each significant wave height a different drag coefficient has to be applied, here only the drag coefficient varied with wave height is shown. The trend seen from the figure, shows for larger waves lower drag coefficient are to be used, corresponding to previous expectations. For each wave height combined with a certain water level, a drag coefficient has to be calibrated. See appendix G *Calibration on Thuy Hai*, for more calibration results of the Thuy Hai case.

## 5.2 Vinh Quang

In this measurement campaign the wave reduction due to one of mangrove species, *Sonneratia* sp., were analyzed, based on a field observation based on a field observation carried out just after a typhoon at the Vinh Quang coast, northern Vietnam. The study site is shown in Figure 5-5. According to Hong and San (1993) and Hong (2004), the coast along the village of Vinh Quang, northern Vietnam, consists of wide mud flats (slope of 1:2000) which stretch out offshore and have been formed by a huge quantity of alluvial sediment brought by the Red River (Song Hong). As seen in fig xx, a part of the coast is protected by a well grown mangrove belt where trees of *Sonneratia* sp. were artificially planted. This belt has a width of ca.100 m.

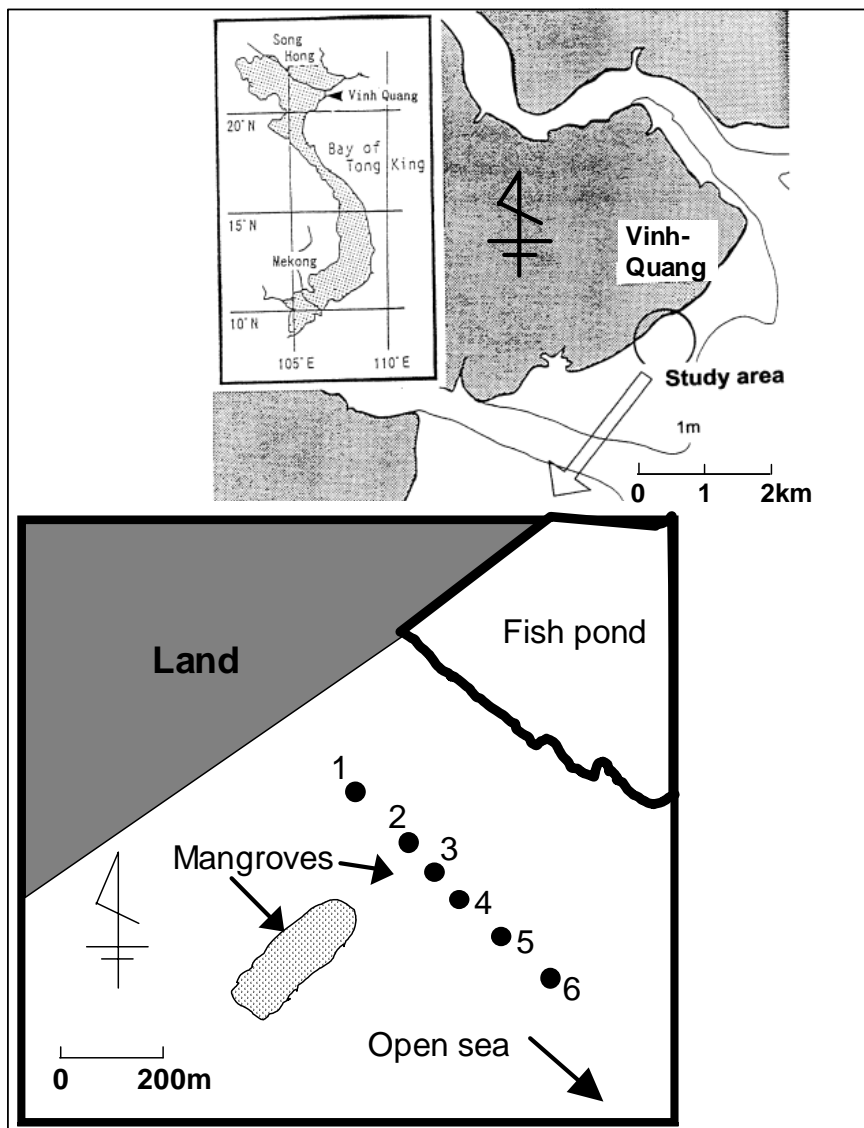


Figure 5-5 Research Area Vinh Quang Vietnam (from Mazda et al)

## 5.2.1 Mangrove vegetation

*Sonneratia* is a mangrove species with vertical erect aerial roots densely emerging around the mother tree. Furthermore a single trunk which forms the base on which on top a canopy in which thick leaves spreads. See Figure 5-6 for an impression.

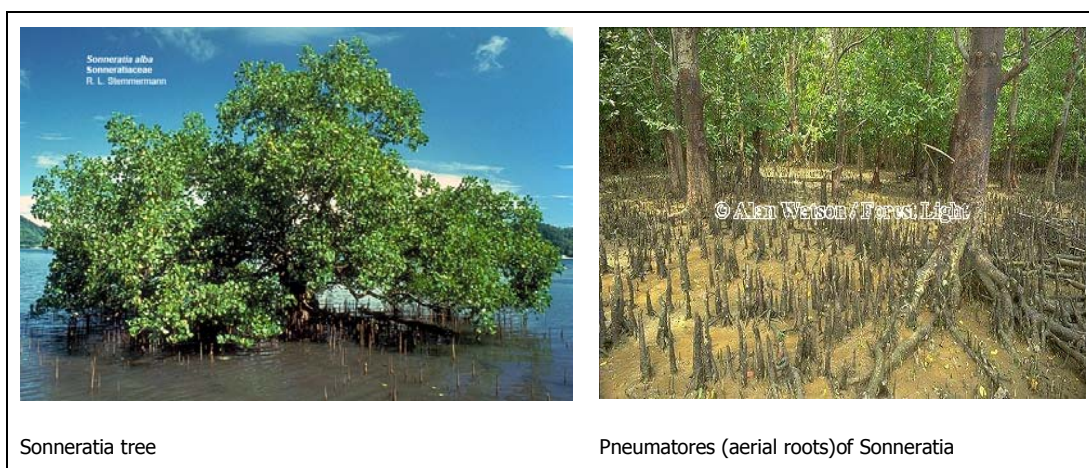


Figure 5-6 Impressions of *Sonneratia* sp. mangrove species

Table 5-4 Average dimensions of *sonneratia* sp.(from Mazda et al)

| Dimensions (m)                    |       |   |
|-----------------------------------|-------|---|
| Density (-/12,5 m <sup>2</sup> )  | 1.0   | <p>The diagram consists of two parts, (a) and (b). Part (a) shows a side view of a tree with a canopy of height <math>H</math>, a trunk of height <math>H_f</math>, and a trunk width <math>W_t</math>. Part (b) shows a cross-section of a root with a height <math>H_r</math> and a width <math>W_r</math>. An arrow points from the trunk in (a) to the root in (b).</p> |
| Wt                                | 0.117 |   |
| Hf                                | 0.82  |   |
| Density roots (-/m <sup>2</sup> ) | 131   |   |
| Wr                                | 0.073 |   |
| Hr                                | 13.8  |   |
|                                   |       |   |

In this table the mean dimensions measured in the Vinh Quang area are presented. The density of the mother tree is 1 per 12,5 m<sup>2</sup>. Assumed is that the area between the separate trees is fully covered with aerial roots of a density of 131 per m<sup>2</sup> as this is not clear from the measurement data.

## 5.2.2 Wave conditions

The wave period varied between 5 and 8 sec, various significant wave heights can be found in Figure 5-7 (a).

## 5.2.3 Results of measured wave reduction

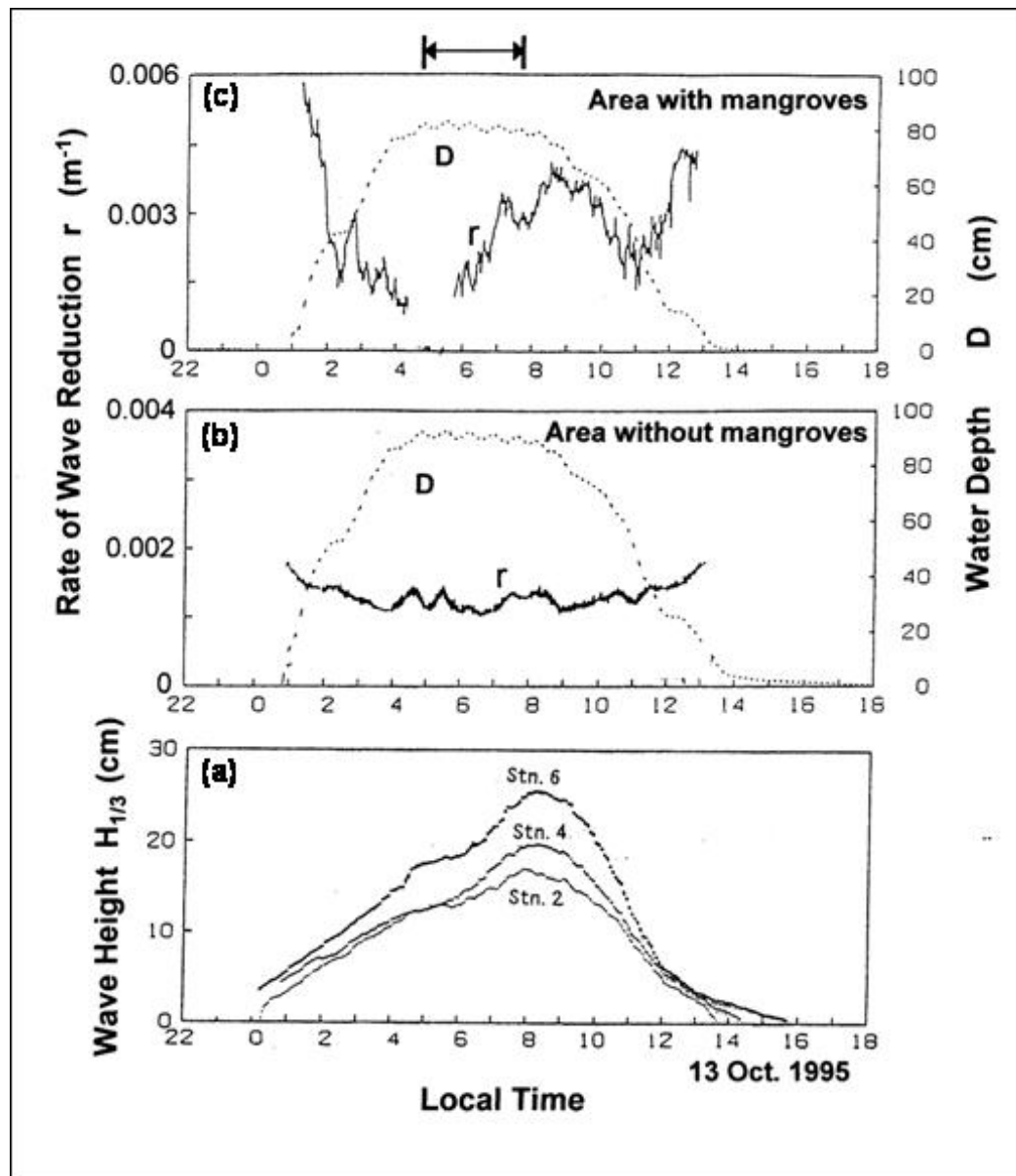


Figure 5-7 Results of measurements in the Vinh Quang case (from Mazda et al)

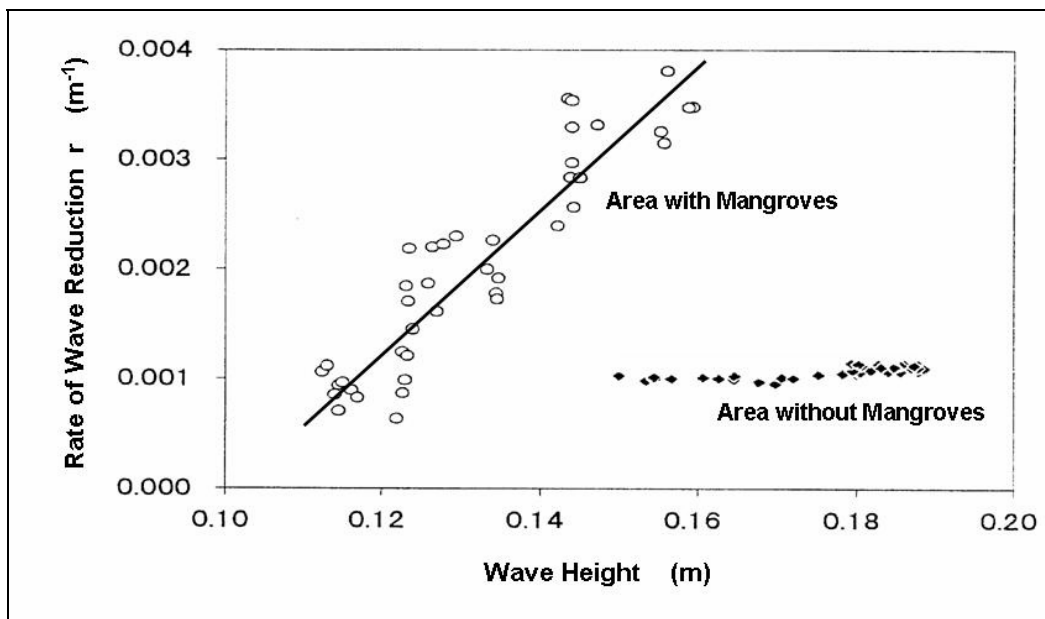


Figure 5-8 Wave reduction for different wave heights and a constant water level 0.8 m (from Mazda et al)

Note that from Figure 5-8 that the wave reduction rate depends linear on the wave height.



## 5.2.4 Modelling the results

Seen from Figure 5-7 between 05:00 and 08:00 hours of the time record the water level was constant. In order to remove the effect of the variation of the water level on the other measured parameters this time period was used to for the analyses by Mazda et al. The results of the wave reduction for this time record is found in Figure 5-8. It has been used for the calibration of the adapted SWAN model on this case. However the wave attenuation data is presented by a reduction factor per meter, for the grid setup is a transect of 125 m has been used. The wave reduction rates converted to rates per meter.

From the measured vegetation characteristics (Table 5-4), a schematisation is made to be used in the SWAN model, presented in Table 5-5. Note that layer 1 represents the aerial roots and layer 2 corresponds with the trunk of the mangrove tree. The canopy is not modelled because no useful measurement data is present to schematise the canopy.

Table 5-5 Vegetation parameters used for the calibration Vinh Quang

| <b>Vegetation parameters</b> | Layer 1    | Layer 2    |
|------------------------------|------------|------------|
| Density (-/m <sup>2</sup> )  | 131        | 0.08       |
| Diameter (m)                 | 0.0073     | 0.117      |
| Drag coefficient (m)         | Calibrated | Calibrated |
| Layer height (m)             | 0.14       | 0.68       |

Table 5-6 Hydraulic conditions for Vinh Quang

| <b>Hydraulic conditions</b>       |             |
|-----------------------------------|-------------|
| Water level (m)                   | 0.8 m       |
| Bed slope (-)                     | 1:2000      |
| Significant wave height $H_s$ (m) | 0.12 – 0.16 |
| Peak period $T_p$ (s)             | 6.5         |

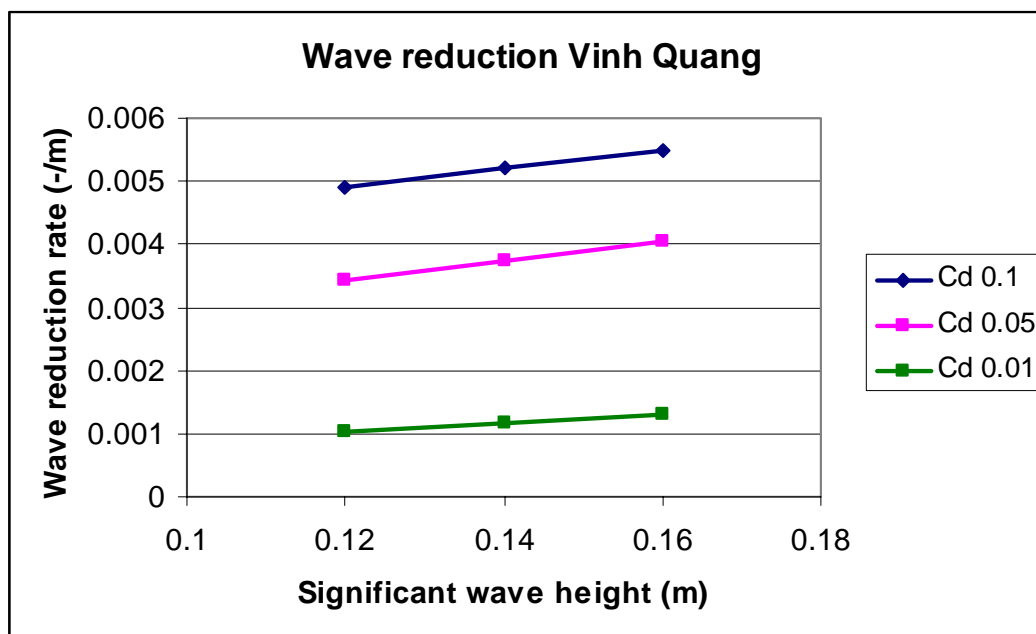


Figure 5-9 Wave reduction rate by varying Drag coefficient calculated with the adapted SWAN model

As can be seen from Figure 5-9 there is not one drag coefficient which fits the wave reduction for all three wave heights 0.12m, 0.14m and 0.16m. Therefore for each hydraulic condition a drag coefficient needs to be calibrated. Striking though is the linear trend of the wave reduction dependent of the wave height which was also found by Mazda et al. In the sensitivity analysis a somewhat more curved trend for the wave reduction related to the wave height was found, this is due to the fact a larger range of the wave height was investigated Figure 4-16.

### **5.3 Conclusions on the test cases**

Both for the Thuy Hai and Vinh Quang case the drag coefficient is successfully calibrated under certain hydraulic conditions. Concluded is that if hydraulic conditions and vegetation parameters are known for a vegetation field, the adapted SWAN model can be calibrated on this case and wave attenuation can be simulated.

The magnitudes of the drag coefficient found in the test cases are in the order of 0.01 to 0.1, which is quite small compared to literature. However what needs to be realised, is that this coefficient is a calibration parameter in which numerous processes are discounted. More important is that general trends, for example an increase of wave reduction with increase of wave height, are correctly shown by model.

The effect of the canopy in relation to wave attenuation is quite important with mangrove forests. Unfortunately dimensions of the canopies in the available measurement data for this study were minimal, which resulted in assumptions on this effect.

### **5.4 Discussion on drag coefficient**

In this discussion a coupling is tried to be made between the theoretical section on the drag coefficient and the sensitivity analysis and the test cases. From section 3.3 (Physical background on the drag coefficient), it became clear that the drag coefficient is influenced by the vegetation characteristics and the hydraulic conditions. Considering the flow regime in mangroves, this is in the order of area  $b$  (Figure 3-6). This would imply that the drag coefficient is in the order of 1 for a single trunk. For higher densities than  $1 \text{ -/m}^2$ , Nepf illustrated that because of the influence the trunks or stems have on each other, the drag coefficient is lower because of turbulence and wake interference. As for the relation between the wave conditions and the drag coefficient Mendez and Losada used the  $K$  number, see section 3.3, to illustrate that the drag coefficient is dependent on the wave parameters. The order of the drag coefficient in the test cases is between 0.01 and 0.1. This is lower than expected from literature. The test cases do not give insight in the above described relations for the drag coefficient drawn from literature. The cause of this is that the provided measurement data in these cases is not constant for either the wave parameters or the vegetation characteristics.

### **5.5 Predictive modelling for Guyana**

Royal Haskoning participates as a consultant in an Integrated Coastal Zone Management project, executed by the government of Guyana. Mangrove areas are part of the sea defence system of Guyana. As mentioned in the introduction of this thesis a lot of mangrove areas are declining because of human action in those mangroves. Therefore there is a need to quantify and model hydraulic and morphologic processes, wave attenuation in particular, in order to predict and simulate the natural hydraulic behaviour and evaluate the consequences of any artificial measure in mangrove forests.

With the implementation of the physical description of vegetation (also layered mangrove vegetation) it has become possible to simulate waves attenuated by a mangrove vegetation field. However to be able to model a whole mangrove coastal system, far more work has to be done concerning the coupling between wave attenuation, tidal currents and morphology.

In this stage the adapted SWAN model is able to handle wave attenuation by mangrove vegetation but not in a predictive sense, because of the relations between the drag coefficient and the wave and vegetation parameters. To do so, first of all vegetation measurements and wave measurements have to be executed in situ. Next the drag coefficient could be calibrated in the area to model the existing situation. Subsequently the model then can be used to do predictions on wave attenuation.

## 6 Conclusions & Recommendations

In this section conclusions and recommendations are presented. The conclusions drawn are in chronological order throughout the report.

### 6.1 Conclusions

- The best numerical approximation of wave attenuation in vegetation, and the most suitable to implement in SWAN, was found to be the Dalrymple (1984) formulation.
- It was found valid to vertically divide the vegetation into segments, and add up the energy dissipation per segment to form the total amount of energy dissipation over the plant height. This method was implemented in the SWAN model; the result was an adapted SWAN model in which vegetation can be horizontally and vertically varied.
- The drag coefficient  $C_d$  is the only parameter in the formulation that cannot directly be determined by measurements; hence it needs to be calibrated on physical model tests or specific field measurements.
- The drag coefficient in oscillating flow appeared not to have a constant value, but to be dependent on the Reynolds number and hence the flow regime. The flow regime for waves through a vegetation field is determined by both wave and vegetation parameters.
- The dependency of the drag coefficient on wave characteristics was determined by the horizontal orbital velocity and the peak period, and can best be described by the relation between the drag coefficient and the Keulegan-Carpenter number.
- The trunk configuration, trunk diameter, relative vegetation height, and relative spacing determine the dependency of the drag coefficient on vegetation characteristics. In sparse vegetation, the drag coefficient approaches the value for flow around one cylinder, with increasing density the drag coefficient decreases due to wake interference and sheltering.
- A number of processes that are not accounted for in the Dalrymple (1984) formulation are discounted in the drag coefficient. Therefore it is not physically correct to refer to the  $C_d$  that is used in the model, as the drag coefficient.
- The adapted SWAN model was validated on flume test results (Mendez and Losada (2004)). The model results and the flume tests matched; therefore the implementation was found successful.
- A sensitivity analyses showed the validity of the expected characteristic relations between the behaviour of the wave attenuation and the varying parameters and hydraulic conditions.
- With the adapted SWAN model, differences in wave setup between areas with and without vegetation (patchy vegetation) can be modelled.
- The adapted SWAN model was applied and calibrated on wave reduction measurements done in two mangrove areas in Vietnam. Drag coefficients between 0.1 and 0.01 were found.
- When mangrove tree canopies are to be modelled, detailed data on diameter and density are needed. Furthermore the flexible effect of the canopies needs to be discounted in the drag coefficient.

## **6.2 Recommendations**

The recommendations are divided in three groups: general recommendations, recommendations with regard to the adapted SWAN model and specific recommendations on the drag coefficient.

### **6.2.1 General**

In order to be able to model and predict the natural hydraulic behaviour and evaluate the consequences of any artificial measure in mangrove forests, more field measurement campaigns on different sorts of vegetated shores should be undertaken. Specifically measurement data on vegetation combined with wave attenuation data should be collected. For mangrove vegetation, the measurements should focus on the wave damping function of the canopies, because of the limited knowledge available.

### **6.2.2 Adapted SWAN model**

A useful extension of the model would be the implementation of the adapted SWAN model in a three dimensional model e.g. D3D of WL | Hydraulics. The combination of tide and currents (D3D-Flow), wave attenuation by vegetation (SWAN) and morphology (D3D MOR / SED) is very suitable to model the often complex mangrove forest and salt marshes. Because SWAN is already included as D3D-Wave, it will be a matter of the exchange of the right parameters, as wave conditions and the vegetation parameters. In D3D-Flow the possibility to schematize vegetation is already present, in a similar way as the vegetation is now schematised in SWAN. The SWAN vegetation model could use this vegetation description to calculate (among other processes) the effect on the wave climate due to vegetation. However the drag coefficient for vegetation to be use in waves is different than for flow. This would need attention.

### 6.2.3 Drag coefficient

More research is needed on the dependency of the drag coefficient on wave and vegetation characteristics. When more is known about these relations, a better first prediction can be made on the value of the drag coefficient in a specific situation. The following relations should be examined:

- The Keulegan-Carpenter number in relation to the drag coefficient in oscillating flow should be determined for different situations. These relations can be used to obtain a good first estimate on the value of the drag coefficient in the field. An elaboration on this recommendation of a physical model test to obtain this relation is given below.
- An inventory should be made on the processes that are not accounted for in the Dalrymple (1984) formulation. The attribution of these processes to the wave attenuation should be known in order to filter any non-drag related phenomena out of the drag coefficient.
- More research is required on detailed hydraulic processes taking place in the vegetation in order to describe and evaluate their contribution to the determination of the value of the drag coefficient. For mangrove vegetation especially the functioning of mangrove tree canopies in waves needs attention.

This research could best be executed in the form of wave flume model tests with homogeneous (artificial) vegetation. The tests should be performed with constant conditions (water level, vegetation characteristics), only varying the wave conditions. The amount of wave damping can be measured and the drag coefficient can be calculated. When repeated for different water levels, a relation between the drag coefficient and the Keulegan-Carpenter number (wave conditions) can be obtained. These experiments can be repeated for different combinations of vegetation density, diameter and relative spacing between the stems. With these results it could be examined if an empirical relation can be found between the drag coefficient and the vegetation characteristics for given wave conditions. An important issue to account for in wave flume test the scaling behaviour of the vegetation combined with wave parameters.

## References

- Airy G.B.**, 1845, 'Tides and waves', Encycl. Metrop., London
- Baptist M.J.**, 2005, Modelling floodplain biogeomorphology, Delft University Press, pp. 49-54
- Battjes J.A.**, 1999, Vloeistofmechanica, CTme2100, Collegediktaat
- Battjes J.A.**, 2001, Stroming in Waterlopen CTwa3310, Collegediktaat
- Battjes J.A.**, 2001, Korte Golven CTwa4320, Collegediktaat
- Booij, N., R.C. Ris and L.H. Holthuijsen**, 1999, A third-generation wave model for coastal regions, Part I, Model description and validation, *J. Geoph. Research*, 104, C4, 7649-7666
- Chapman V.J.**, 1984, V.J., Mangrove biography, Hydrobiology of the Mangal (Por, F.D. and Dor, I e.d.), pp 15-24, 1984
- Dalrymple R.A., Kirby J.T. Hwang P.A.**, 1984, Wave diffraction due to areas of energy dissipation. J. Waterway Port Coastal Ocean Engineering 110, 67-79
- Dean R.G., Bender C.J.**, Static wave setup with emphasis on damping effects by vegetation and bottom friction, Coastal Engineering (In press)
- Groen R.A.**, 1993, Mangroven als kustverdediging, Afstudeerverslag, Technische Universiteit Delft
- Hasselmann K., T.P. Barnett E. Bouws H. Carlson D.E. Cartwright K. Enke J.A. Ewing H. Gienapp D.E. Hasselmann P. Kruseman A. Meerburg P. Müller D.J. Olbers K. Richter W. Sell and H. Walden** 1973, Measurements of wind-wave growth and swell decay during the Joint North Sea Wave Project (JONSWAP), *Dtsch. Hydrogr. Z. Suppl.*, 12, A8
- Heideman J.C. and Sarpkaya T.**, 1985, Hydrodynamic forces on dense arrays of cylinders, 17th Offshore Technology Conference
- Komen, G.J., Cavaleri, L., Donelan, M., Hasselmann, K., Hasselmann, S. and P.A.E.M. Janssen**, 1994: *Dynamics and Modelling of Ocean Waves*, Cambridge University Press, 532 p.
- Massel S.R. et al**, 1999, Surface wave propagation in mangrove forests , Fluid Dynamics Research, no. 24, p. 219-249
- Mazda Y. et al.**, 1997, Mangroves as a coastal protection from waves in the Tong King delta, Vietnam, Mangroves and Salt marshes 1: p 127-135
- Mazda Y., Wolanski E., King B., Sase A., Ohtsuka D., Magi M.**, 1997, Drag force due to vegetation in mangrove swamps, Mangroves and Salt Marshes ,P(3), 193-199
- Mendez F.M., Losada I.J.**, 2004, An emperical model to estimate the propagation of random breaing and nonbreaking waves over vegetation fields, Coastal Engineering 51 (2004) p 103-118.
- Morison J.R.M., O'Brien M.P., Johnson J.W., Schaaf S.A.**, 1950, The force exerted by surface waves on piles. Petrol. Trans., AWME, Vol 189
- Nepf H.M.**, 1999, Drag, turbulence and diffusion in flow trough emergent vegetation, Water Resources Research, Vol 35, no. 2, p. 479-489
- Schiereck G.J.**, 2001, G.J. Introduction to bed bank and shore protection, Delft University Press
- Suhayda J.N.**, 1977, Surface waves and bottom sediment response: in Richards, A. F., (ed.), Marine slope stability, Marine Geotechnology, no. 2, p. 135-146.
- Teas H.J.**, May 1976, Mangrove swamp creation, Rehabilitation and Creation of Selected Coastal Habitats: Proceedings of a workshop, Sapelo island, Georgia, p16-20
- Tomlinson P.B.**, 1986, P.B. The botany of mangroves, Cambridge University Press
- Vos W.J.**, 2004, Wave attenuation in mangrove wetlands, Red river delta Vietnam, Master thesis TUDelft, Hydraulic Engineering
- Vries de, M.B. and Roelvink D**, 2004, Delft Hydraulics, Vegetation friction factor algorithm (unpublished)
- WAMDI group**, 1988: The WAM model - a third generation ocean wave prediction model, J.

*Phys.Oceanogr.*, **18**, 1775-1810

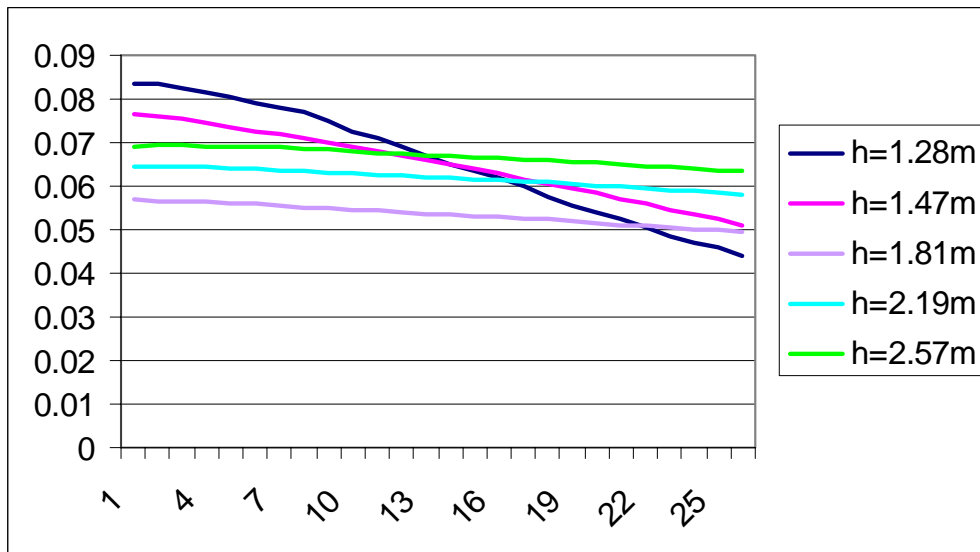
**Whitham, G.B., 1974**, *Linear and nonlinear waves*, Wiley, New York, 636 p.

**Young I.R.**, 1999, *Wind Generated Ocean Waves*, Ocean Engineering Book Series, Vol.2

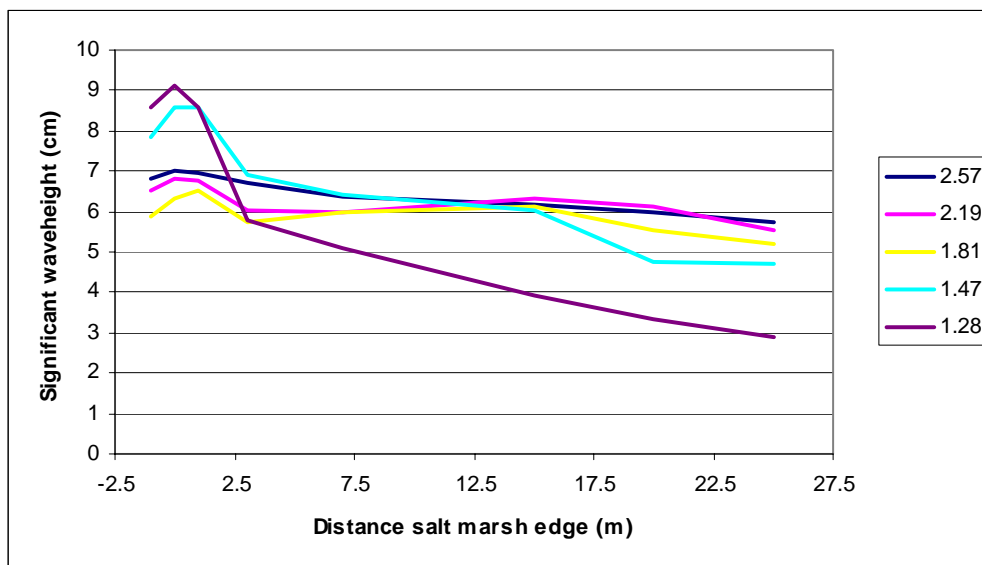


# Appendices

## Appendix A Results of test calculations Dalrymple formulation



Calculated wave attenuation with Dalrymple 1984



Measured wave attenuation results Paulina Marsh

## Appendix B Implemented code

### General description SWAN source code

SWAN has been released under public domain (<http://fluidmechanics.tudelft.nl/SWAN>) and is integrated in WL | Delft Hydraulics DELFT3D modelling package (DELFT3D-WAVE module). SWAN is an open source code program, anyone may make adaptations for own use. SWAN source code is written in fixed form Fortran 90. To adapt SWAN a Fortran 90 compiler is necessary. The source code comprises different so-called subroutines. In the main program (*swanmain*) these subroutines are called upon. The most important subroutine used in this implementation is *swancom2*. This subroutine contains some dissipation formula's e.g. bottom friction, wave breaking and whitecapping.

### Working with SWAN

All routines are compiled with a Fortran 90 compiler and linked to form the executable *swan.exe*. This executable reads an input file that contains the user defined information. In the input file physical processes as e.g. bottom friction, white capping and breaking can be activated or deactivated, wave and wind spectra parameters as well as the desired output parameters (e.g.  $H_s$ ,  $T_p$  etc.) can be defined. In the input file a reference is made to several other files. The information about the bathymetry is read from a bottom file (*\*.bot*), whereas for the output a file contains the output locations (*\*.loc file*). The output is stored in a table, spectra or block format. A computational grid can be defined in the input file or the grid can be read from an external grid (*\*.grd*) file.

## **Input of parameters**

To input vegetation four input parameters must be set, these are the drag coefficient, density, diameter and vegetation height.

Three 3 types of spatial configuration of the vegetation are possible.

- horizontal and vertical homogeneous
- horizontal heterogeneous and vertical homogeneous
- horizontal heterogeneous and vertical heterogeneous

This input is handled by the subroutine INPVEG

```
SUBROUTINE INPVEG (ILMAX, LAYH, VEGDRGL, VEGDIL, VEGDEL, IX, IY)
```

```
INTEGER ILMAX
```

```
REAL LAYH(ILMAX), VEGDRGL(ILMAX), VEGDIL(ILMAX), VEGDEL(ILMAX)
```

```
IF (IX.LT.25) THEN
```

```
LAYH = (/0.14,0.68/)
```

```
VEGDRGL = (/0,0/)
```

```
VEGDIL = (/0,0/)
```

```
VEGDEL = (/0,0/)
```

```
ELSE
```

```
LAYH = (/0.14,0.68/)
```

```
VEGDRGL = (/1.13,1.13/)
```

```
VEGDIL = (/0.0073,0.117/)
```

```
VEGDEL = (/131.0,0.08/)
```

```
ENDIF
```

```
RETURN
```

```
END
```

## Vertical averaging of parameters

To obtain the contribution of each vegetation layer the input parameters per are multiplied in the subroutine PARVE.

```

! d = waterdepth
! Nlayer = number of layers in grid point
!
! Per layer is known:
!
! LAYH (thickness of the layer),
! VEGDRAG (drag coeff.),
! VEGDIA (vegetation diameter),
! VEGDEN (density)
!
! *****
!
!
! ----- n
!
! ----- 2
!   _ d
! --|----- 1
!   |
! --|----- 0
!
!
! *****
!
! LAY, Cd, BV, DEN are vectors with the size of the numbers of layers inputted.
! The vegetation parameters of the different layers are averaged throughout the water column.
! With these avaraged parameters the dissipation due to vertical varying vegetation can be ! calculated. This
Subroutine checks in which layer the water level is pesent. Subsequently
! the vegetation parameters up to the layer where the waterlevel is in, are used to calculate a ! weighed average.
! Whith this average the dissipation due to the vegetation can be calculated.
!
!
!!IL = layer counter
!!ILMAX = Number of layers
!
      SUBROUTINE PARVE (ILMAX, LAYH, VEGDRGL, VEGDIL, VEGDEL, VEGDRAG ,
&      VEGDIA, VEGH, VEGDEN, DEP2, LAYPART)
      USE SWCOMM3
!
      INTEGER ILMAX

```

```

REAL LAYH(ILMAX), VEGDRGL(ILMAX), VEGDIL(ILMAX), VEGDEL(ILMAX)
REAL VEGDRAG(MCGRD),VEGDIA(MCGRD), VEGH(MCGRD), VEGDEN(MCGRD),
& DEP2(MCGRD)

INTEGER IL, IK, IM
REAL SUMLAYH, SUMLAYH1, SUMLAYH2, VEGDRAGAV, VEGDIAAV, VEGDENAV,
& LAYPART

SUMLAYH = 0.
SUMLAYH1 = 0.
SUMLAYH2 = 0.
VEGDRAGAV = 0.
VEGDIAAV = 0.
VEGDENAV = 0.
LAYPART = 0.

DO IL = 1, ILMAX
  SUMLAYH = SUMLAYH + LAYH(IL)
ENDDO
!
IF (DEP2(KCGRD(1)).GT.SUMLAYH) THEN
DO IL = 1, ILMAX
  VEGDRAGAV = VEGDRAGAV + (VEGDRGL(IL) * LAYH(IL))
  VEGDIAAV = VEGDIAAV + (VEGDIL(IL) * LAYH(IL))
  VEGDENAV = VEGDENAV + (VEGDEL(IL) * LAYH(IL))
ENDDO
VEGDRAG(KCGRD(1)) = VEGDRAGAV / SUMLAYH
VEGDIA(KCGRD(1)) = VEGDIAAV / SUMLAYH
VEGDEN(KCGRD(1)) = VEGDENAV / SUMLAYH
VEGH(KCGRD(1)) = SUMLAYH

ELSE IF (DEP2(KCGRD(1)).LT.LAYH(1)) THEN
  VEGDRAG(KCGRD(1)) = VEGDRGL(1)
  VEGDIA(KCGRD(1)) = VEGDIL(1)
  VEGDEN(KCGRD(1)) = VEGDEL(1)
  VEGH(KCGRD(1)) = DEP2(KCGRD(1))

ELSE
DO IL = 1, ILMAX
  SUMLAYH1 = SUMLAYH1 + LAYH(IL)
IF (DEP2(KCGRD(1)).LE.SUMLAYH1) THEN
DO IM = 1, IL-1

```

```
SUMLAYH2 = SUMLAYH2 + LAYH(IM)
ENDDO
LAYPART = DEP2(KCGRD(1)) - SUMLAYH2
DO IK = 1, IL-1
VEGDRAGAV = VEGDRAGAV + (VEGDRGL(IK) * LAYH(IK))
VEGDIAAV = VEGDIAAV + (VEGDIL(IK) * LAYH(IK))
VEGDENAV = VEGDENAV + (VEGDEL(IK) * LAYH(IK))
ENDDO
VEGDRAG(KCGRD(1)) = (LAYPART * VEGDRGL(IL) + VEGDRAGAV)
& / DEP2(KCGRD(1))
VEGDIA(KCGRD(1)) = (LAYPART * VEGDIL(IL) + VEGDIAAV)
& / DEP2(KCGRD(1))
VEGDEN(KCGRD(1)) = (LAYPART * VEGDEL(IL) + VEGDENAV)
& / DEP2(KCGRD(1))
VEGH(KCGRD(1)) = DEP2(KCGRD(1))
EXIT
END IF
ENDDO
ENDIF
RETURN
END
```



**SVEG**

The actual energy dissipation of the vegetation is calculated by the subroutine SVEG.

```

!*****
!
SUBROUTINE SVEG (DEP2 ,AC2 ,
&      IMATDA ,KWAVE ,SPCSIG ,
&      IDCMIN ,IDCMAX ,
&      ISSTOP ,DISSC1 ,VEGDRA ,VEGDIA ,
&      VEGH ,VEGDEN )
!
!*****
!
USE SWCOMM3
USE SWCOMM4
USE OCPCOMM4
!
!-----|
! | Delft University of Technology          |
! | Faculty of Civil Engineering          |
! | Environmental Fluid Mechanics Section  |
! | P.O. Box 5048, 2600 GA Delft, The Netherlands |
! |                                     |
! | Programmers: R.C. Ris, N. Booij,      |
! |      I.J.G. Haagsma, A.T.M.M. Kieftenburg, |
! |      M. Zijlema, E.E. Kriezi,         |
! |      R. Padilla-Hernandez, L.H. Holthuisen |
! |-----|
!
!
! SWAN (Simulating WAVes Nearshore); a third generation wave model
! Copyright (C) 2005 Delft University of Technology
!
! This program is free software; you can redistribute it and/or
! modify it under the terms of the GNU General Public License as
! published by the Free Software Foundation; either version 2 of
! the License, or (at your option) any later version.
!
! This program is distributed in the hope that it will be useful,
! but WITHOUT ANY WARRANTY; without even the implied warranty of
! MERCHANTABILITY or FITNESS FOR A PARTICULAR PURPOSE. See the
! GNU General Public License for more details.
!
! A copy of the GNU General Public License is available at

```

```

! http://www.gnu.org/copyleft/gpl.html#SEC3
! or by writing to the Free Software Foundation, Inc.,
! 59 Temple Place, Suite 330, Boston, MA 02111-1307 USA
!
!
! 0. Authors
!
! 40.55: Bastiaan Burger, Martijn Meijer
!
! 1. Updates
!
! 40.55, May. 05: implementation of vegetation friction formula
!
! 2. Purpose
!
! Computation of the source terms due to vegetation friction
!
! 3. Method
!
! The energy dissipation due to vegetation is described by a
! Morrison type equation, modeling the plants as vertical,
! noncompliant cylinders, neglecting swaying motions induced by
! waves. Vegetation characteristics that are used as input are:
! drag coefficient, vegetation height, plant density and diameter.
!
!
! SVEGEO = (1/(2*SQRT(PI))) * RHO * VEGDRAG * VEGDEN * VEGDIA *((KWAVE*GRAV)/SPCSIG)**3 * ((A +
B)/C) * HRMS**3
!
! with
!
! HRMS = HSIG*SQRT(2)
! A = (SINH(K*VEGH))**3
!
! B = 3*SINH(K*VEGH)
! C = 3*K*((COSH(KD))**3)
!
!
! 4. Argument variables
!
! SPCSIG: Relative frequencies in computational domain in sigma-space 30.72
!
! REAL SPCSIG(MSC)                                30.72
!
! INTEGERS :
```

```

! -----
!
! IX    Counter of gridpoints in x-direction
! IY    Counter of gridpoints in y-direction
! IS    Counter of relative frequency band
! ID    Counter of the spectral direction
!
! ITER  Number of iteration i.e. number of full sweeps
!
!
! MXC   Maximum counter of gridppoints in x-direction
! MYC   Maximum counter of gridppoints in y-direction
! MSC   Maximum counter of relative frequency
! MDC   Maximum counter of directional distribution
! ISSTOP Maximum counter of wave component in frequency
!       space that is propagated
!
! REALS:
! -----
!
! DD    Spectral direction band width
! DS    Width of the frequency band
! GRAV  Gravitational acceleration
! KD    Wavenumber * Depth
! SVEGEO Sourceterm for the vetatationfriction to be stored in the array IMATDA
!
! one and more dimensional arrays:
! -----
!
! DEP2  2D  Depth
! ESIN  1D  Sin per spectral direction (id)
! ECOS  1D  Cos per spectral direction (id)
! IMATDA 2D  Coefficients of diagonal of matrix
! KWAVE 2D  Wavenumber function of frequency and IC
! DISSC1 2D  Dissipation coefficient, function of sigma and theta
! VEGDRAG 2D  Spatially variable drag coefficient
! VEGDEN 2D  Spatially variable vegetation density
! VEGDIA 2D  Spatially variable vegetation diameter
! VEGH   2D  Spatially variable vegetation height
!
! 7. Common blocks used
!
!
! 8. Subroutines used
!

```

```

! ---
!
! 9. Subroutines calling
!
! SOURCE
!
! 10. Error Messages
!
! ---
!
! 11. Remarks
!
! ---
!
! 12. Structure
!
! -----
!
! -----
!
! 13. Source text
!

      REAL :: VEGDRAG(MCGRD), VEGDIA(MCGRD), VEGH(MCGRD),
&          VEGDEN(MCGRD)
!
      INTEGER ID ,IS ,ISSTOP
      REAL KD ,KVEGH ,SVEGEO, ADUM, BDUM, CDUM
!
      REAL DEP2(MCGRD) ,
&          AC2(MCGRD,MDC,MSC) ,
&          IMATDA(MDC,MSC) ,
&          DISSC1(MDC,MSC) ,
&          KWAVE(MSC,ICMAX)
!
      INTEGER IDCMIN(MSC) ,
&          IDCMAX(MSC)
!
      SAVE IENT
      DATA IENT/0/
      IF (LTRACE) CALL STRACE (IENT,'SVEG')

      DO IS = 1, ISSTOP
         KD = KWAVE(IS,1) * DEP2(KCGRD(1))

```

```

KVEGH = KWAVE(IS,1) * VEGH(KCGRD(1))
ADUM = (SINH(KVEGH))**3
BDUM = 3*SINH(KVEGH)
CDUM = 3*KWAVE(IS,1)*(COSH(KD))**3

SVEGEO1 = (1/(2*SQRT(PI))) * VEGDRAG(KCGRD(1)) *
& (VEGDEN(KCGRD(1))) * VEGDIA(KCGRD(1)) *
& ((KWAVE(IS,1)*GRAV)/(2*SPCSIG(IS))**3*
& ((ADUM + BDUM)/CDUM)

DO IDDUM = IDCMIN(IS) , IDCMAX(IS)
  ID = MOD ( IDDUM - 1 + MDC , MDC ) + 1

  SVEGEO = SVEGEO1 *
& SQRT(SPCSIG(IS)*AC2(KCGRD(1),ID,IS))

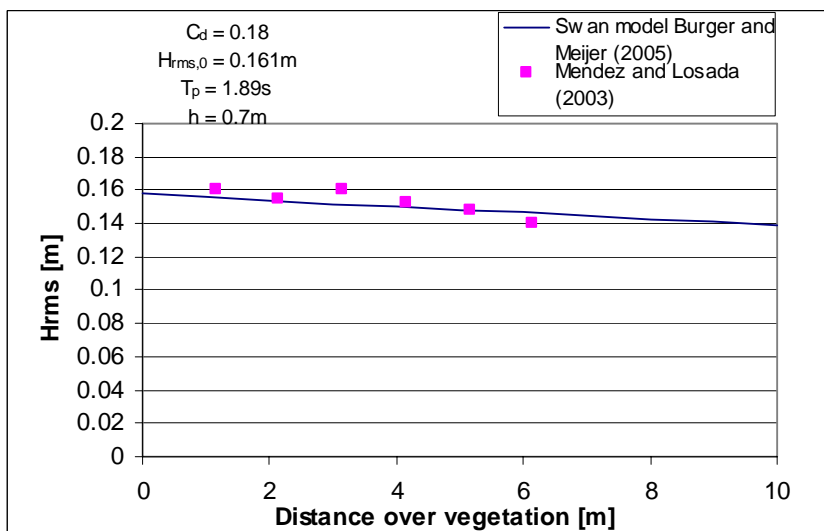
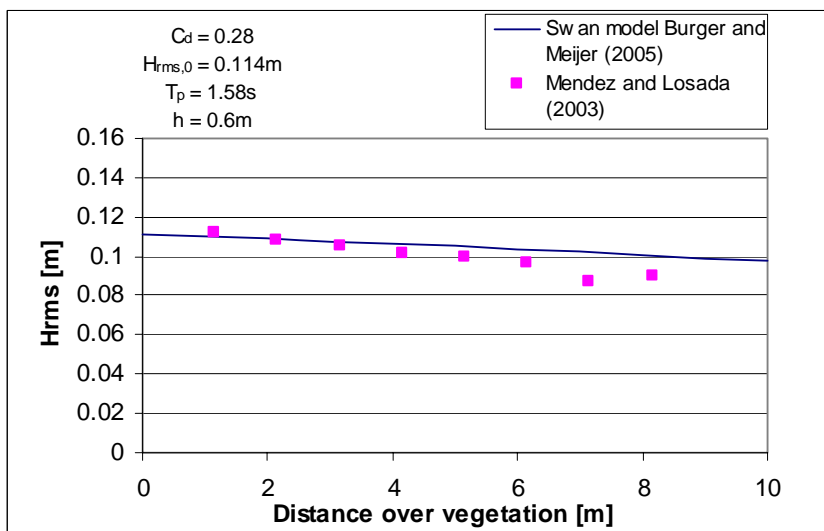
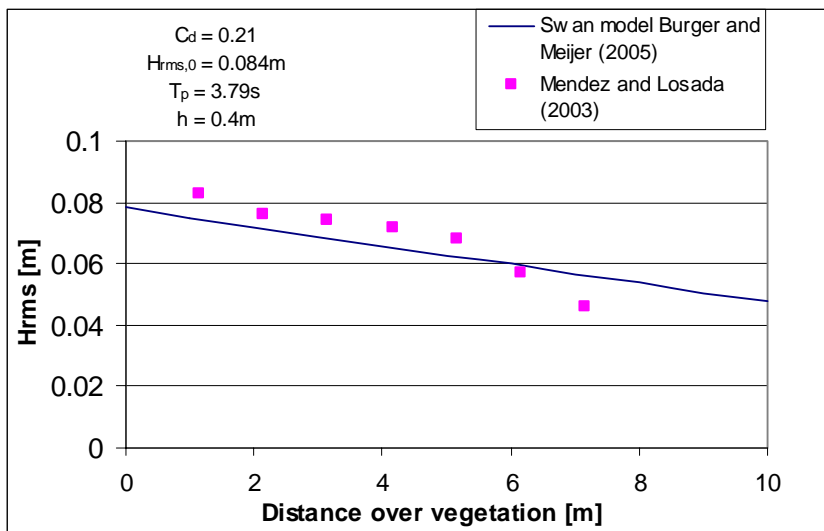
!   *** store the results in the array IMATDA ***
!
  IMATDA(ID,IS) = IMATDA(ID,IS) + SVEGEO
  DISSC1(ID,IS) = DISSC1(ID,IS) + SVEGEO

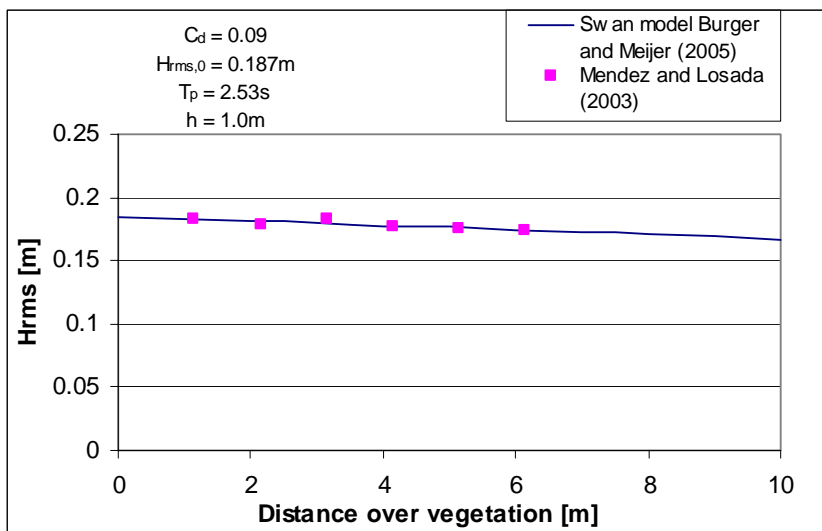
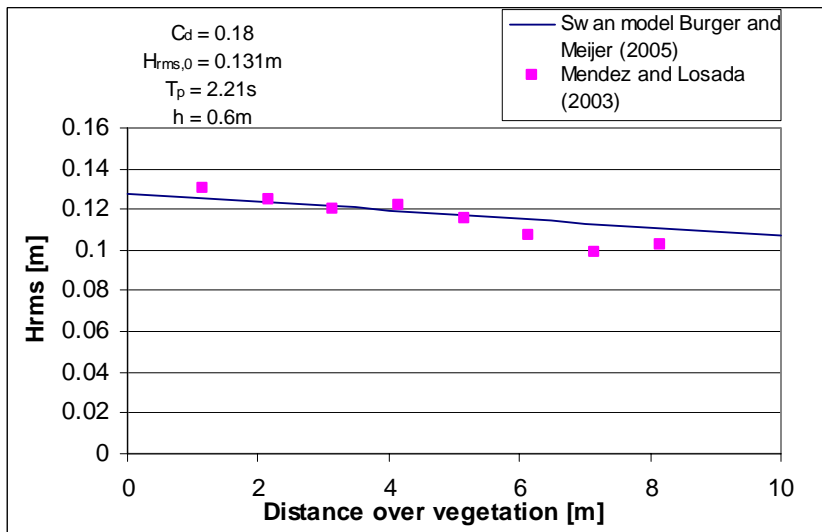
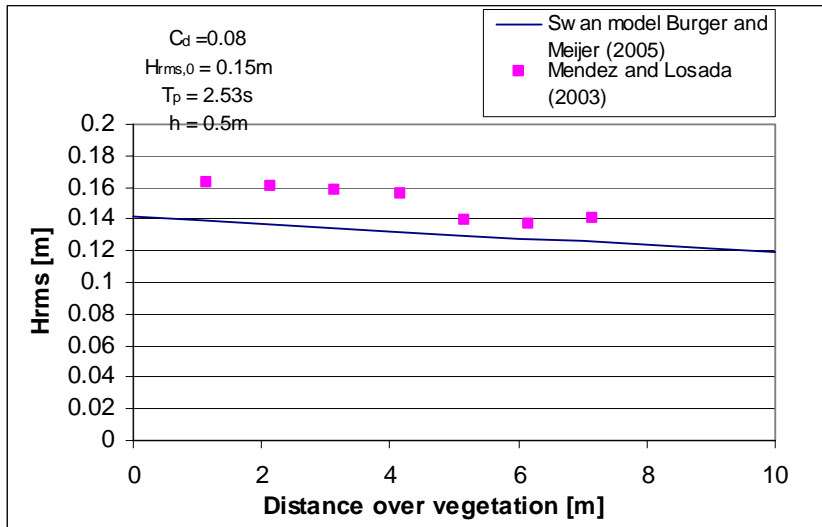
END DO
CONTINUE
END DO

! End of subroutine SVEG
RETURN
END

```

### Appendix C Validation on flume experiments





## Appendix D Layout SWAN model

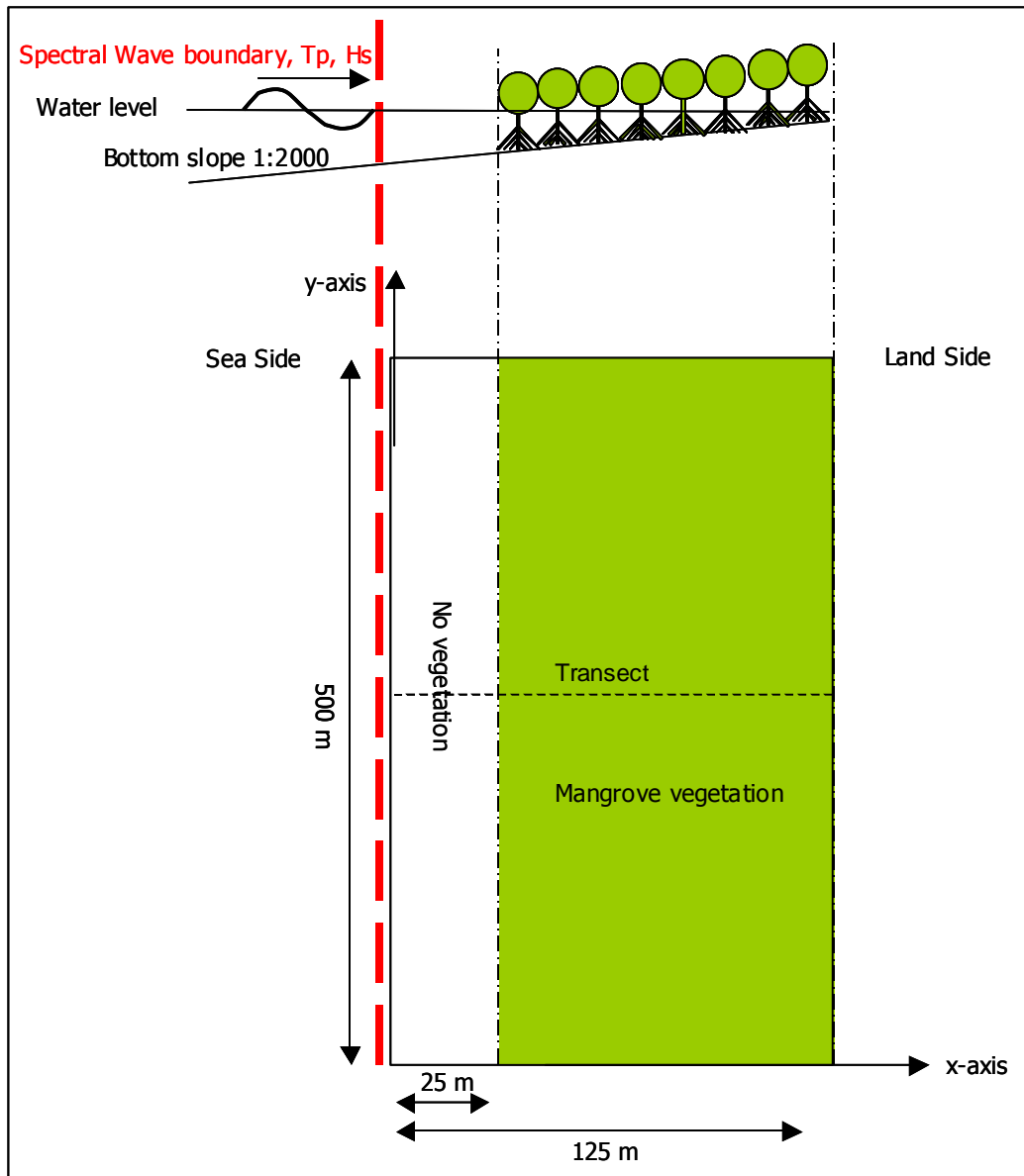
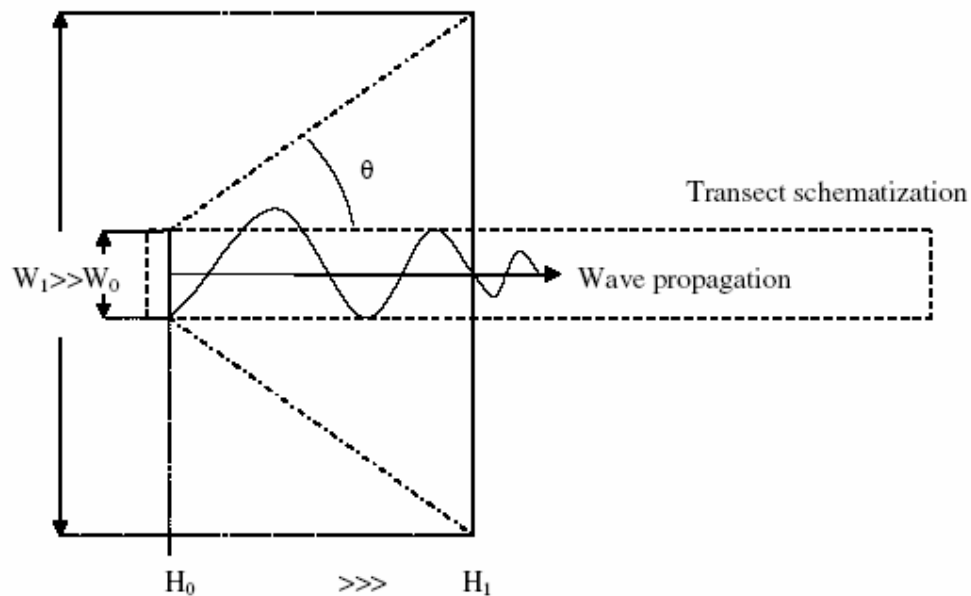


Figure Model layout

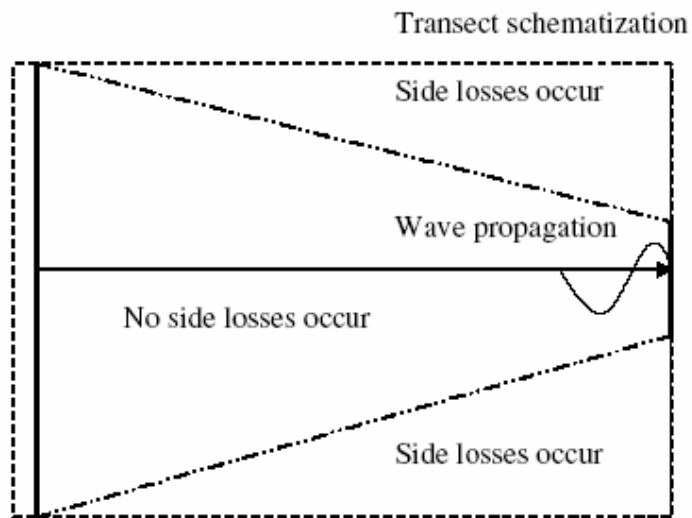
The 2D model layout is such that it can be used as 1D model. Calculations are executed for the whole of the grid, but for a 1D case only the results along the transect shown in the figure above are considered. As for the configuration of the vegetation, the first 25 m there is none, to exclude the possible influence of the wave boundary on the vegetation present in the y-axis of the model.



Another problem with 1D schematizations is that wave energy flows out via the long sides of the model. This is because SWAN does not 'feel' borders along the sides of the model. So a wave will propagate in the wave direction, but at the same time, the wave energy will spread over the side borders of the model, causing a strong decrease in wave height. Figure X illustrates this problem. The figure shows a wave at the boundary (left side of schematization) with wave height  $H_0$  and wave width  $W_0$ . After some time, the wave width has increased to  $W_1$  because of the spreading of the wave under an angle  $\theta$ . The result of this is a decrease in wave height to  $H_1$ . The solution to this problem is to choose a very large schematization width, so that  $W \gg L$ , in which  $L$  is the schematization length. In this case, the wave will still spread out over the side borders, but the middle line of the section (the measurement transect) will not have been effected by this phenomenon yet when the wave has traveled a distance  $L$ .

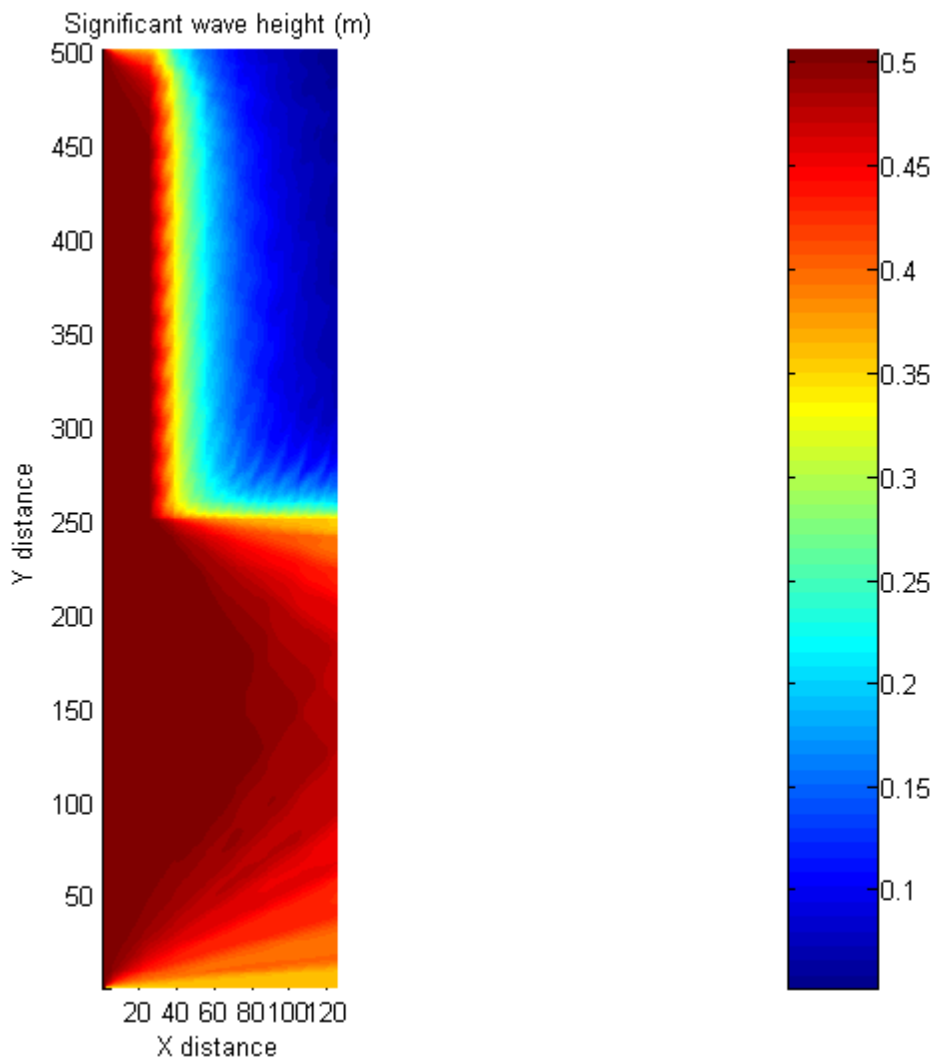


In order to make a correct model, the width of the model will have to be chosen several times larger than the length. The figure shows the area where waves are affected by energy losses through the long sides and the area that is not yet affected by this energy loss. So, the analysis of the results of SWAN should be done using the wave height at the middle line of this schematization, representing the measurement transect.

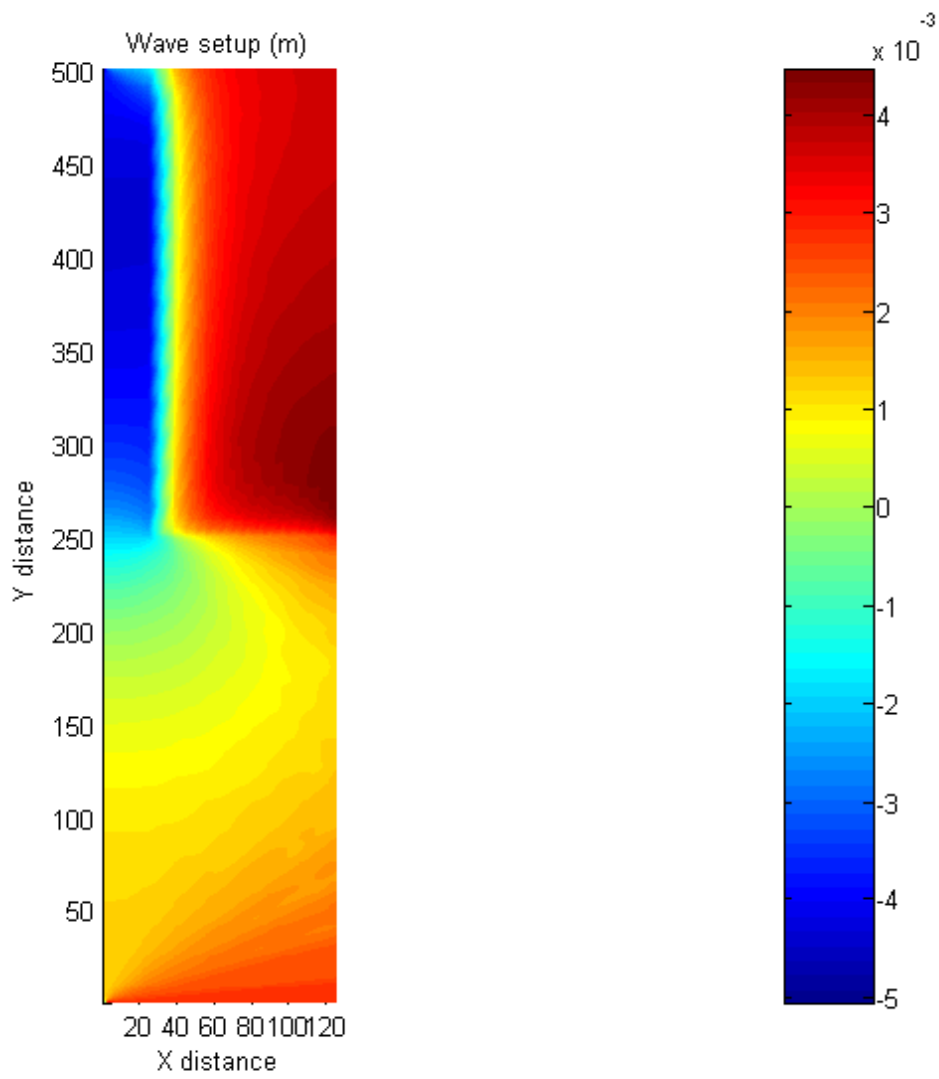


From: Mol, A. WL Delft Hydraulics (2003)

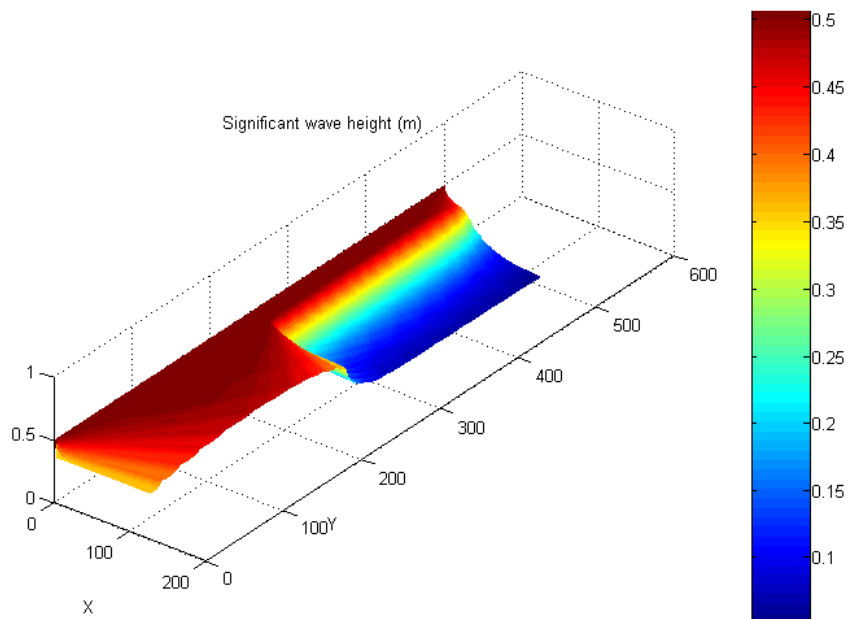
## Appendix E Wave setup



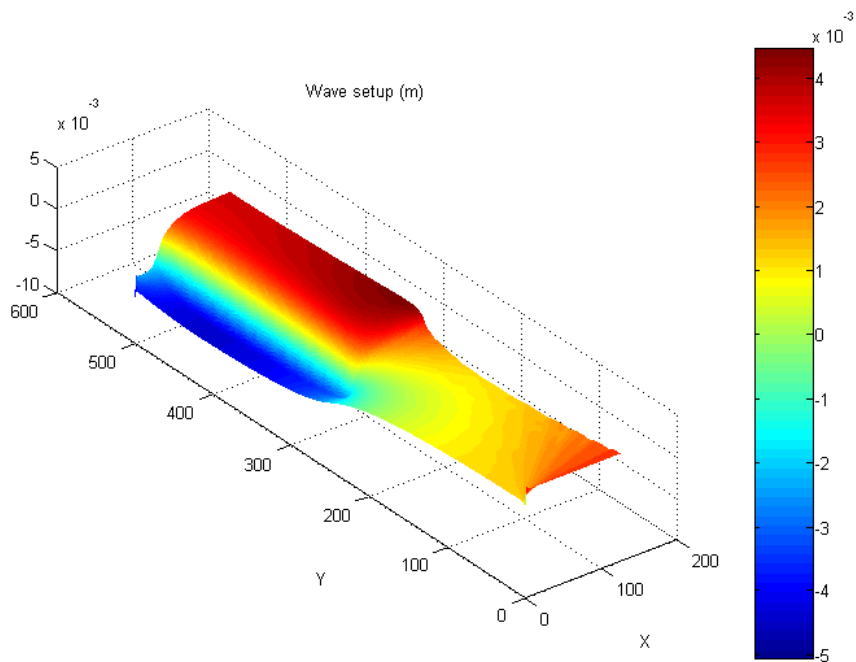
Top view significant wave height Case A



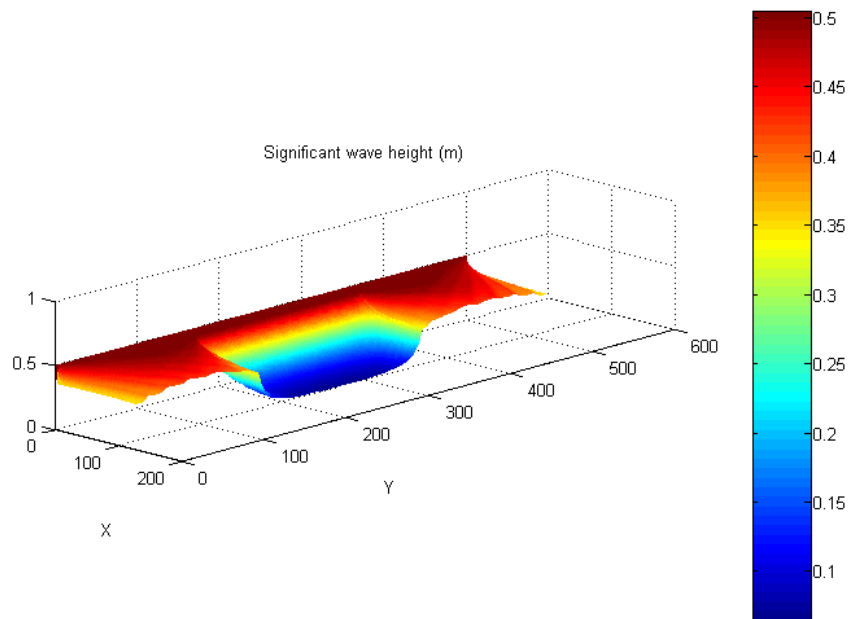
Top view wave setup Case A



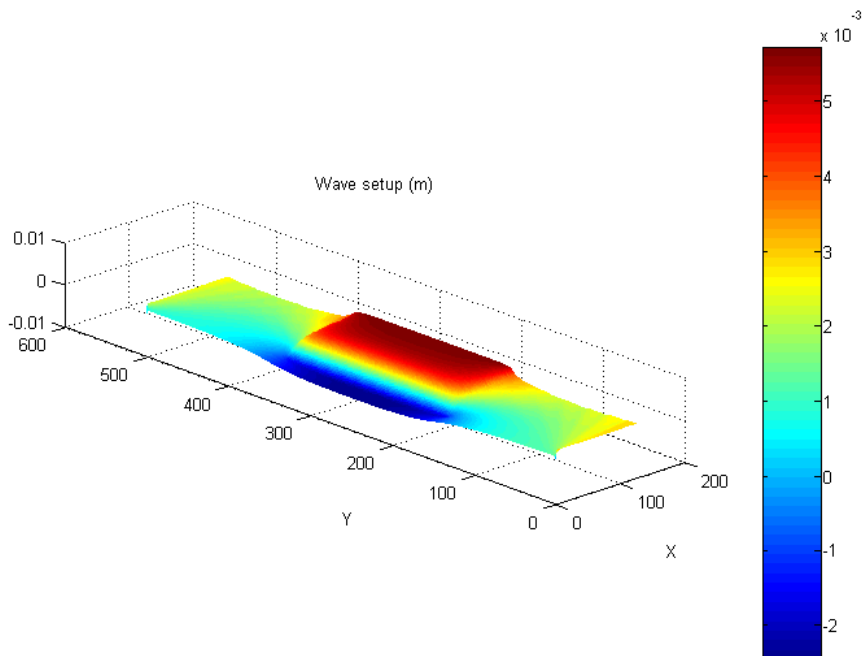
Significant wave height Case A



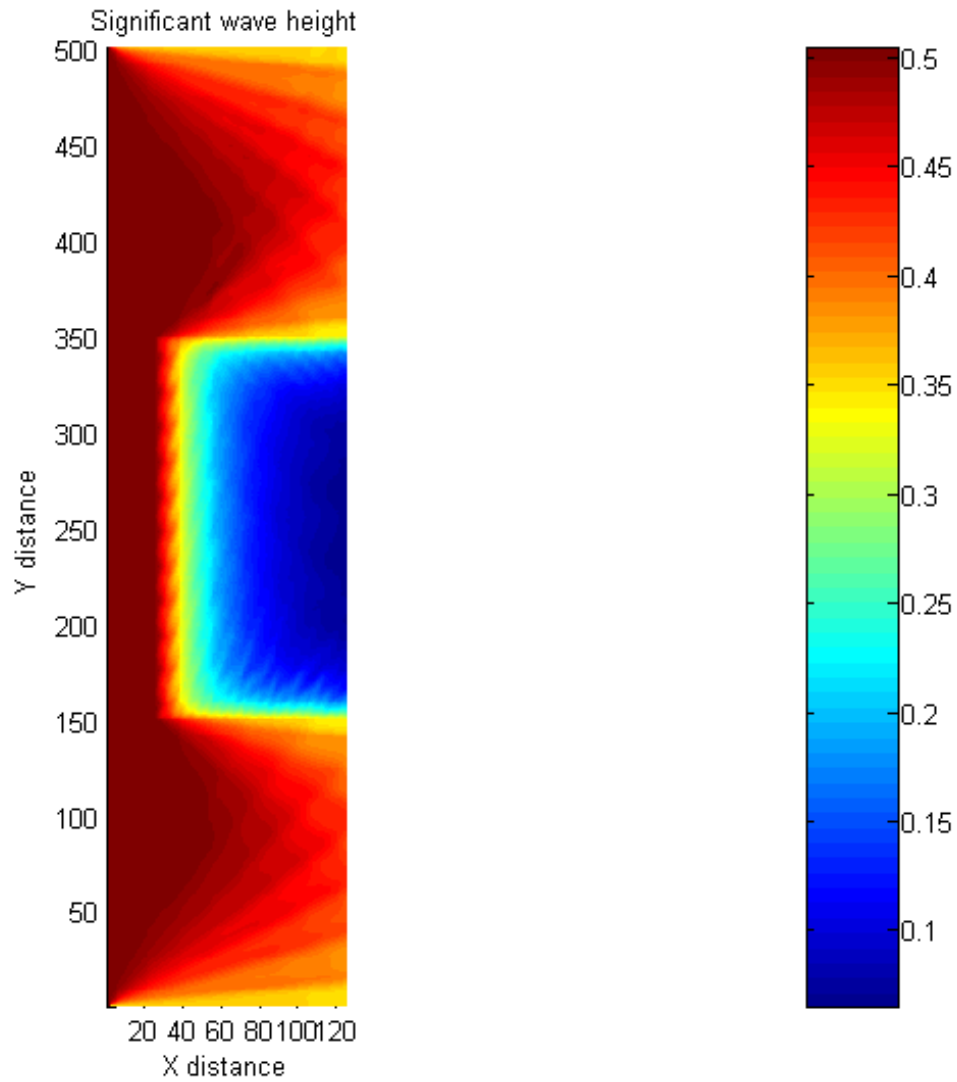
Wave setup Case A



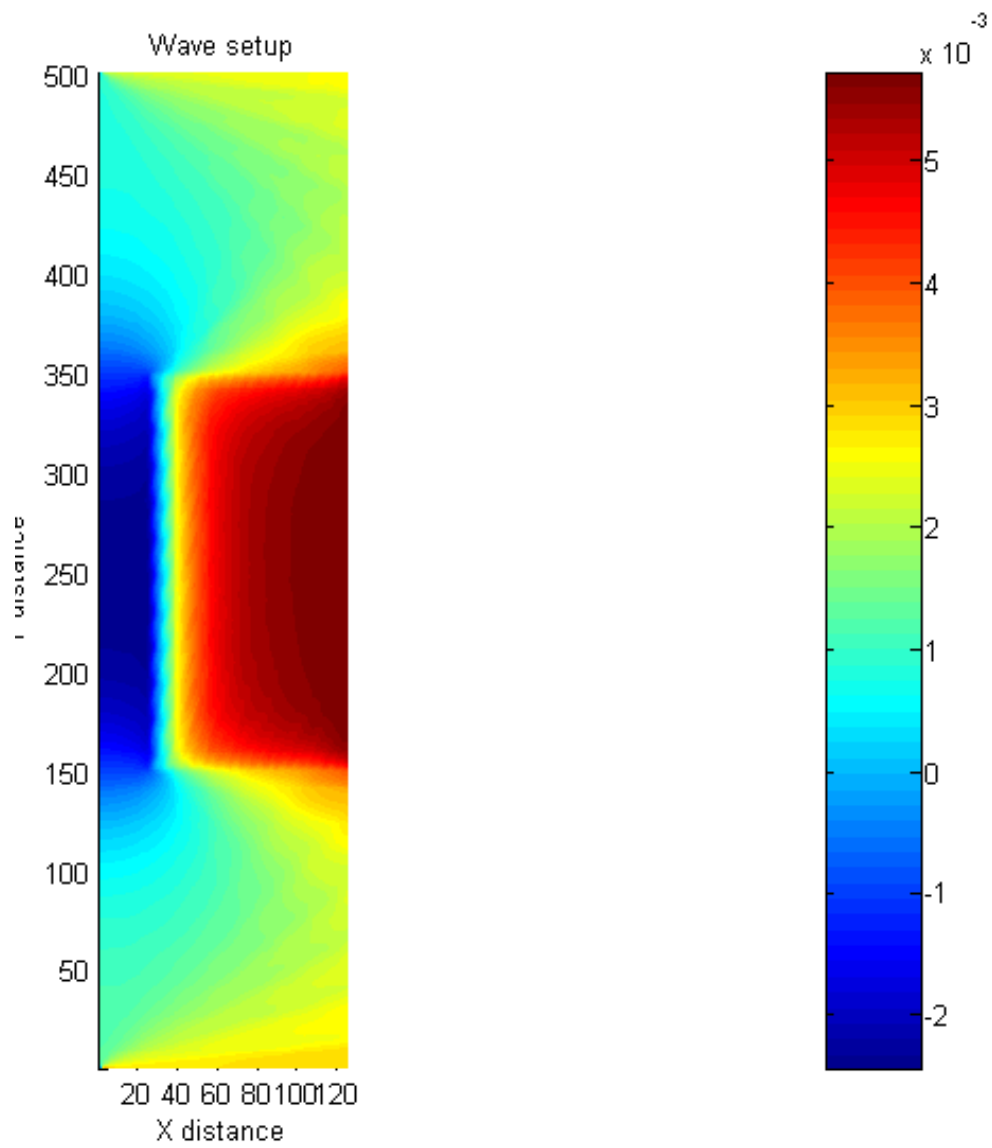
Significant wave height Case B



Wave setup Case B



Top view significant wave height Case B



Top view wave setup Case B



## Appendix G Calibration on Thuy Hai

